Université de Liège
Faculté des Sciences
Centre d'ingénierie des Protéines
Laboratoire de Biochimie

# Adaptations structurales et fonctionnelles aux températures extrêmes au sein de la famille des alpha-amylases chlorure-dépendantes.

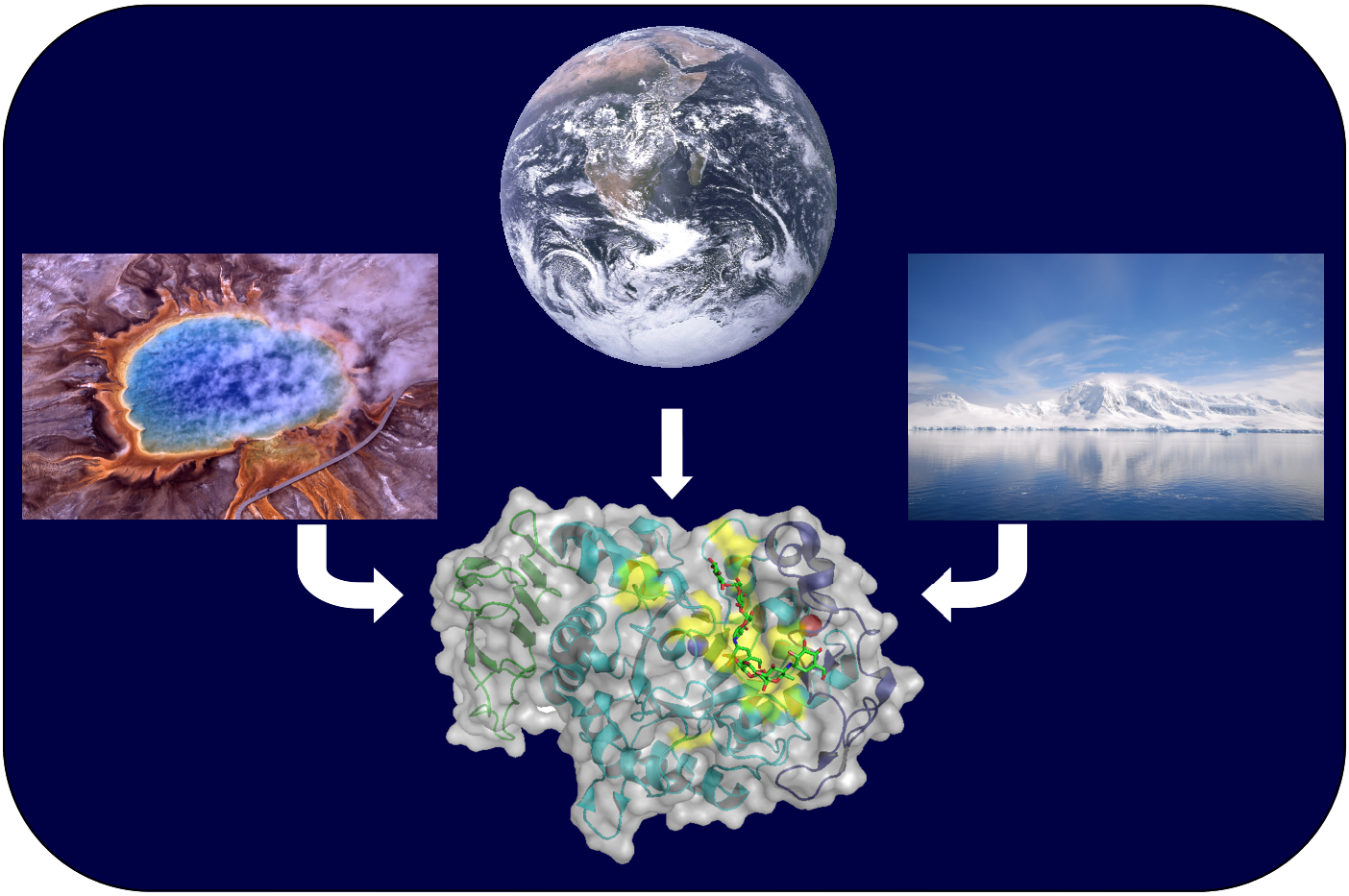

Thèse présentée par Alexandre Cipolla
en vue de l'obtention du titre de Docteur en Sciences
Année académique 2012-2013

Qui aurait cru qu'encore un autre « Zoolo », comme on aime nous appeler, finirait au bout de quatre ans et des grosses poussières par présenter une thèse dans le laboratoire de Biochimie ?

Et bien il est un homme qui n'a pas hésité à faire confiance à ce « Zoolo » et qui l'a guidé, soutenu et orienté tout au long de ces quatre années. C'est pourquoi je réserve mon premier et plus profond remerciement au **Dr Georges Feller**. Sa clairvoyance, sa maitrise du sujet et son expérience dans nos chères alpha-amylases m'ont permis de réaliser le travail dont vous êtes témoin.

Merci aussi à celui qui a initié l'étude de l'adaptation des protéines aux basses températures, à savoir le professeur **Charles Gerday**, sans qui je ne me serai peut-être pas passionné pour le sujet. Je le remercie aussi pour m'avoir accepté dans son bureau durant ces deux dernières années, de sa bonne humeur et de son franc parler.

Un grand merci à nos trois mousquetaires, **Florence Piette**, **Amandine Godin** et **Caroline Struvay**, (et oui sur la fin, Georges et moi étions les seuls représentant de la gent masculine !) pour leurs bons humeurs et leurs sourires, nos échanges de points de vues (rarement houleux) et d'expériences. Mais je n'oublie pas mes deux collègues masculins de début de thèse, **Frédéric Roulling**, qui m'a merveilleusement encadré durant mon mémoire et **Salvino D'Amico**, qui est un peu mon père spirituelle puisqu'une partie de mon travail découle du sien.

N'oublions pas notre bienveillante **Fabienne** pour son soutien administratif mais surtout sa joie de vivre, ses anecdotes à la pause-café, ainsi que tous ces mots de vocabulaires découverts dans ce vieux Larousse du siècle dernier (« potron-minet »).

Un remerciement particulier au groupe du professeur **André Matagne** et à lui-même pour m'avoir formé et informé sur l'utilisation de leur appareil : **Roya** (un tout grand merci), **Alex**, **Julie**, **Chloé**, **Natacha**, **Jessica**…

En parlant de la pause-café, je remercie aussi tous mes compatriotes caféinophiles (ou caféinomanes pour certains) de notre petite cafeteria, **Etienne**, **Jean-Marie**, **Giorgios**, **DéDé**, **Sapu, René** (les lundis), et j'en passe… dont ceux précédemment cités. Avec un remerciement particulier à **Olivier** pour son agréable compagnie aux congrès de Stockholm dont j'espère te fournir les photos avant notre pension.

Merci à tous ceux qui ont fait de ces quatre années un souvenir inoubliable : **Sébastien** (pour ton amitié, nos bourses aux insectes, et la préparation d'un enterrement de vie de garçon dont on se souviendra !), **Marylène**, **Jean-Sébastien**, **Renaud** alias Mr Antipatosse, **la grande Sophie**, **Maude**, **Fred de Lemos**, **Matthias**, **Julie**, **Iris**, **Anne-Marie**, **Caroline** et j'en oublie en rédigeant ces lignes toutes mes excuses…

A ceux du labo d'en face, les cyano, je vous remercie de votre agréable compagnie au quotidien : **Yannick**, **Zorigto**, **Marie-José**, **Pedro**, …

Et enfin un remerciement particulier à ma famille : mon épouse, mes parents et beaux-parents et plus récemment notre petite Camille. Sans votre soutien journalier, dans les bons ou les mauvais moments, ce projet n'aurait pu aboutir et faire de moi celui que je suis aujourd'hui.

Merci à toutes les personnes, qui de près ou de loin ont contribué à cette thèse et que je n'aurais pas citées dans ces lignes.

Alexandre

# Table des matières

# Contenu

# Chapitre 1 : Introduction

## *Section I: Les Glycoside Hydrolases et la famille 13 des GHs.*

# 1.1. L'Amidon

## 1.1.1. Définition

L'amidon est, avec le glycogène, le plus important polysaccharide de réserve d'énergie sur terre. Il est le composant de stockage de base chez les plantes supérieures. C'est sous la forme de granules semi-cristallins et insolubles que l'on retrouve préférentiellement l'amidon lorsqu'il sert de stockage dans les graines, les tubercules et les racines. On le retrouve également, en moindre quantité, dans la plupart des tissus végétaux. Il est composé de deux types de polymères, l'amylose et l'amylopectine (Figure 1), eux-mêmes des polymères de D-glucose ou plus précisément de D-anhydroglucopyranose (AGU). Ces deux polymères représentent 98 à 99% du poids sec de l'amidon. Les molécules d'amidon sont hautement hydratées car elles exposent un grand nombre de groupements hydroxyles capables d'établir des ponts hydrogène avec des molécules d'eau. Cependant, sous forme de granules, l'amidon présente une faible solubilité dans l'eau à cause de sa grande taille et de sa structure. Les granules peuvent varier en taille, de 1 à 100µm de diamètre, et de forme (polygonale, sphérique, lenticulaire). Les proportions d'amylose et d'amylopectine, l'architecture des branchements et le degré de cristallisation sont responsables de la forte variabilité de structure et de propriétés physico-chimiques de l'amidon. (Nelson *et al.,* 2005; Buléon *et al*., 1998; Copeland *et al*., 2009)

a)

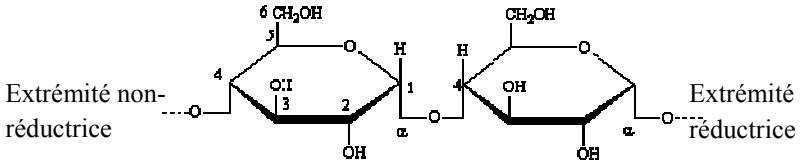


b)

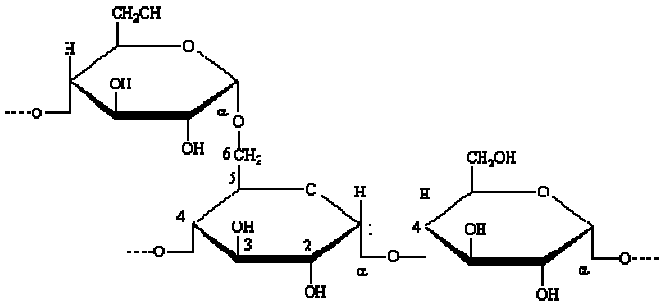

**Fig. 1.** Amylose et amylopectine, les polysaccharides composant l'amidon. Structure chimique d'un court segment d'amylose (a) et d'amylopectine (b).

## 1.1.2. Structure de l'Amidon

L'amidon est constitué de deux homopolymères de D-glucose, l'amylose et l'amylopectine. La structure principale de l'amylose est constituée d'une longue chaine d'unités D-glucose connectées entre elles via une liaison α 1-4. Le poids moléculaire de cette chaine peut varier de quelques milliers à plusieurs millions d'unités avec un degré de polymérisation (DP) de 1000 à 10.000 unités de D-glucose (exemple : DP 1000-6000 pour le maïs contre un DP de 200-1200 pour le blé. Van der Maarel

*et al.,* 2002). Moins de 0,5% de ce glucose possède une liaison α 1-6, dont il résulte un très faible degré de branchement pour des structures de 3 à 11 chaines constituées de 200 à 700 résidus glucose par molécule. A cause de son faible degré de branchement, l'amylose en solution a tendance à former des agrégats de semi-cristaux insolubles. L'amylopectine est un polymère plus grand, avec un poids moléculaire de $10^8$ et un degré de polymérisation supérieur à un million. La plupart des types d'amidons contiennent entre 60 et 90% d'amylopectine bien qu'il existe de l'amidon constitué de seulement 30% d'amylopectine (Amidon à haute teneur en amylose). Dans l'amylopectine, on retrouve jusqu'à 5% des unités D-glucose avec une liaison α 1-6 rendant sa structure hautement ramifiée. Il existe trois types d'amylopectine en fonction de la substitution : les chaines A sont non ramifiées, les chaines B sont ramifiées et les chaines C portent l'extrémité réductrice (Figure 2).

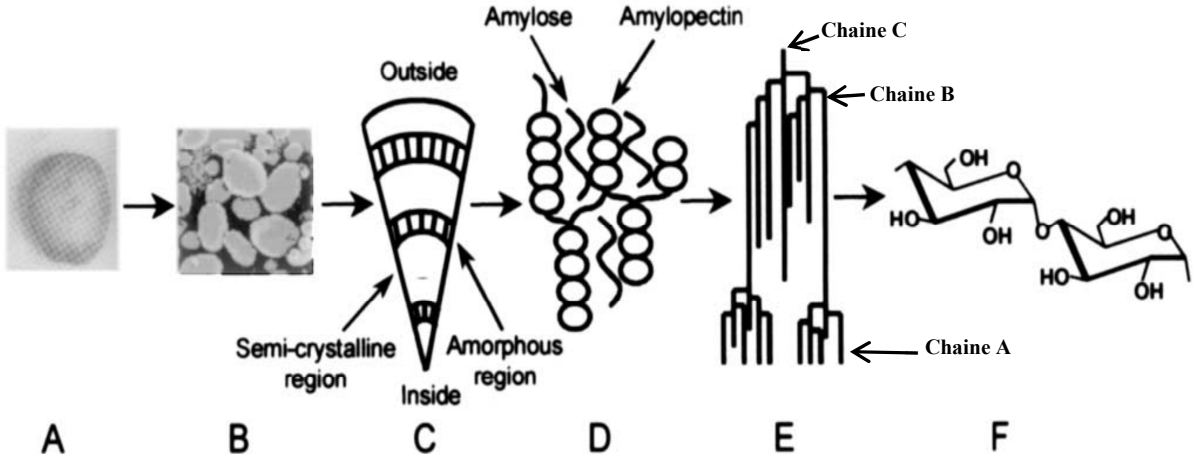


**Fig. 2.** Représentation schématique de l'amidon du tubercule de pommes de terre, de la macro structure à la structure moléculaire. A, tubercule ; B, image au microscope des granules d'amidon ; C, coupe d'un granule montrant les anneaux de croissance constitués de régions semi-cristallines et amorphes ; D, détail de la région semi-cristalline ; E, organisation arborescente de la molécule d'amylopectine ; F, dimère de glucose liés par une liaison glycosidique α 1-4.

## 1.2. Les Glycoside Hydrolases

Les carbohydrates, qu'ils soient sous forme de mono-, di-, oligo- ou polysaccharides, jouent un rôle capital dans la nature. Le nombre de combinaisons possibles pour un simple oligosaccharide est astronomique et il en résulte une diversité de structures et de fonctions plus grandes que celles des peptides ou des acides nucléiques de taille comparable. D'un point de vue purement mathématique, on pourrait construire près de $10^{12}$ isomères à partir d'un seul hexasaccharide. Les oligo- et les polysaccharides jouent donc un rôle primordial dans une grande variété de processus biologiques tels que la formation de structure, le stockage alimentaire ou la signalisation cellulaire. Les enzymes hydrolysant ces polysaccharides, appelées les « Glycoside Hydrolases » ou « GHs », sont donc aussi impliquées dans une grande gamme de processus biologiques et pathologiques tels que des déficiences

héréditaires (intolérance au lactose ou mucopolysaccharidose). Avec les progrès du séquençage et l'amélioration des techniques de prospection, ainsi que la robotisation des techniques de cristallisation, des quantités énormes de séquences et de structures sont disponibles et fournissent un grand nombre de nouvelles GHs potentielles. C'est pourquoi il était nécessaire de mettre au point une classification permettant de prendre en compte la structure 3D, la spécificité de substrat et le mécanisme de réaction. (Henrissat, 1991 ; Henrissat & Davies, 1995)

### 1.2.1. Classification basée sur la similarité des séquences en acides aminés

La classification d'origine des GHs était celle basée sur la spécificité de substrat recommandée par l'IUBMB (International Union of Biochemistry and Molecular Biology) exprimée par le numéro EC (ex: EC 3.2.1.x, x représentant la spécificité de substrat). Simple, elle ne prend cependant pas en compte les enzymes à substrats multiples ni les homologies des structures 3D des enzymes. Elle nécessite en plus la connaissance du substrat impliquant un travail de laboratoire pour chaque enzyme, travail rendu difficile à cause de l'abondance des gènes qui découlent du séquençage des génomes et autres banques métagénomiques. De même, certaines notions comme le mode d'action du mécanisme catalytique, à savoir par rétention ou inversion de la configuration anomérique du carbone 1 du sucre, ainsi que la capacité d'attaquer le substrat en mode « *endo* », à l'intérieur du polysaccharide, ou en mode « *exo* », via une extrémité de la chaine polysaccharidique, n'étaient, elles non plus, pas prises en compte dans la classification de l'IUBMB et présentent pourtant un intérêt essentiel.

Pour pallier à ces défauts, Henrissat proposa en 1991, une classification basée sur la similarité de séquences en acides aminés. Puisque structure et séquence sont liées, cette dernière peut apporter des informations sur le mécanisme d'action et la structure uniquement à partir de la structure primaire. (Henrissat, 1991 ; Henrissat & Bairoch, 1993)

La base de données CAZy pour Carbohydrate Active Enzymes (http://www.cazy.org/Home.html) est constituée de 125 familles de GHs divisées en 14 clans structuraux. De plus elle inclut d'autres types d'enzymes telles que les Glycosyl Transferase (GTs), les Polysaccharide Liases (PLs) et les Carbohydrate Esterases (CEs) mais aussi des modules de fixation du substrat accompagnant souvent les carbohydrate enzymes appelés CBM pour « Carbohydrate-binding modules ».

### 1.2.2. Topologie du site actif

Bien que les GHs soient divisées en 125 familles basées sur leur similarité de séquence en acides aminés et qu'elles présentent une grande variabilité de structure 3D, la topologie du site actif peut-être divisée en 3 grands groupes (Henrissat & Davies, 1997):

- La topologie en « **cratère** » ou en « **poche** ». Cette topologie est optimale pour la reconnaissance d'extrémité saccharidique non réductrice et se retrouve chez les monosaccharidases

comme les β-galactosidases, β-glucosidases, sialidases et les neuraminidases, ou encore les exopolysaccharidases telles que les glucoamylases et les β-amylases. Ces exopolysaccharidases sont adaptées à des substrats présentant un grand nombre d'extrémités de chaine, tels que les granules d'amidon natif, dont les structures radiales exposent toutes les extrémités non réductrices en surface (Figure 3a).

❖ La topologie en « **clef** » ou en « gouttière ». Cette structure 'ouverte' permet la liaison de plusieurs unités saccharidiques d'un substrat polymérique et est communément présente chez les endo-enzymes telles que les lysozymes, les endocellulases, les chitinases, les α-amylases et les β-1,3-glucanases (Figure 3b).

❖ La topologie en « **tunnel** ». Cette topologie est une évolution de la précédente car elle présente une longue boucle qui vient couvrir une partie de la gouttière. Le tunnel permet ainsi le passage de longues chaines polysaccharidiques. Cette structure est spécifique aux cellobiohydrolases. (Figure 3c)

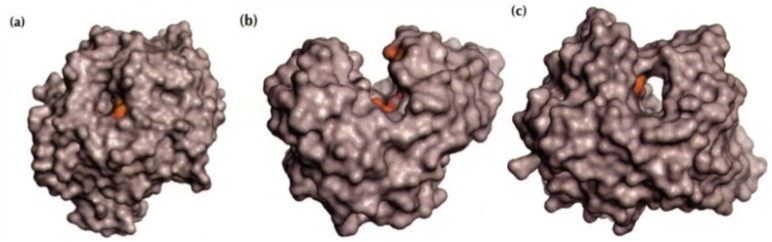


**Fig. 3.** Les trois types de topologies du site actif existant chez les GHs. **(a)** La « poche » (ex : glucoamylase). **(b)** la « clef » (ex : α-amylase). **(c)** Le « tunnel » (ex : cellobiohydrolase). Les résidus catalytiques sont colorés en rouge. (MOLVIEWER program.)

### 1.2.3. Nomenclature des sites de fixations des GHs

Les sous-unités du site catalytique fixant le substrat sont numérotées de $-n$ à $+n$, avec $-n$ à l'extrémité non réductrice et $+n$ à l'extrémité réductrice. La zone de clivage est toujours située entre le site -1 et +1. Cette nomenclature à l'avantage d'être applicable à toutes les classes d'enzymes et permet une comparaison de tous les sites actifs en respectant le point de clivage. (Davies, 1997) (Figure 4)

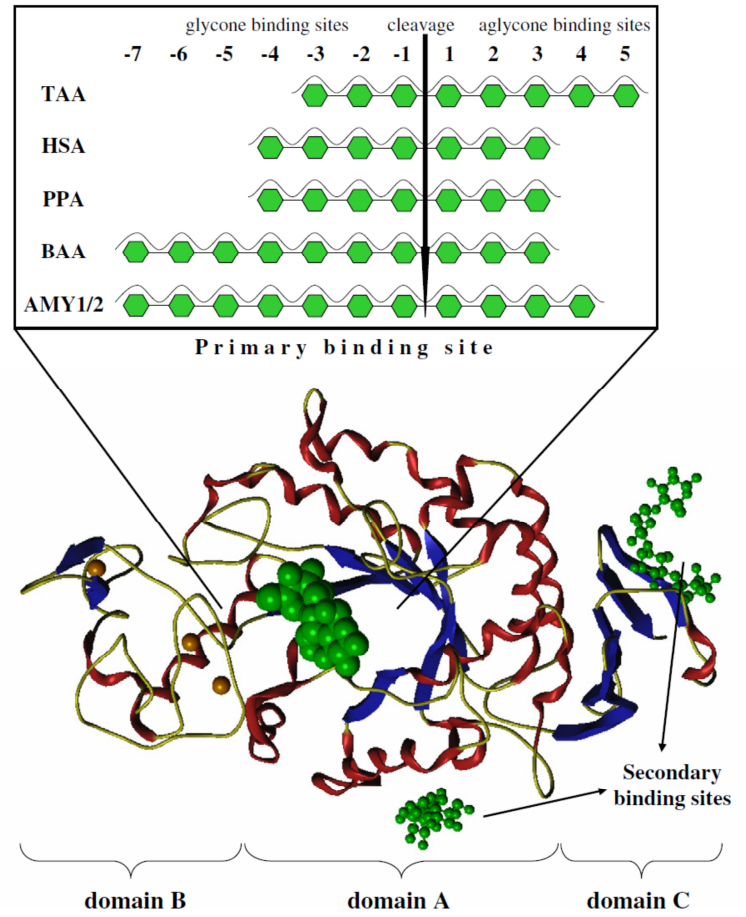


**Fig. 4.** Représentation schématique des sous-unités catalytiques de plusieurs α-amylases (une endo-enzyme type) et localisation sur la structure cristallographique (D'après Motyan *et al.,* 2011).

## 1.2.4. Mécanismes catalytiques des GHs

L'hydrolyse enzymatique des liaisons glycosidiques a lieu via une catalyse acide qui requiert deux résidus : un donneur de proton ou acide et une base/nucléophile. Cette hydrolyse se déroule selon deux mécanismes majeurs donnant soit une « rétention » soit une « inversion » de la configuration anomérique du carbone 1. Dans les deux cas, la position du donneur de proton est identique. Chez les enzymes de type « rétention », la base est très proche du carbone anomérique alors que pour celle de type « inversion » elle est plus éloignée car une molécule d'$H_2O$ doit être accommodée entre la base et le sucre. De cette différence résulte une distance moyenne entre les deux résidus catalytiques qui est de 5.5Å pour la « rétention » contre 10Å pour le type « inversion ». (Henrissat & Davies, 1995 ; Koshland, 1953)

*Le mécanisme de rétention* : Dans ce mécanisme, l'oxygène de la liaison glycosidique est protoné par le résidu catalytique acide (donneur de proton). En même temps, le résidu basique réalise une attaque nucléophile sur cette même liaison provoquant la formation d'un intermédiaire de type « glycosyl-enzyme ». Ensuite, le résidu acide joue alors le rôle de base en réalisant une attaque nucléophile sur

une molécule d'$H_2O$ permettant l'hydrolyse de l'intermédiaire. La seconde substitution nucléophile du carbone anomérique génère un produit présentant la même stéréochimie que la molécule de substrat initiale. (Figure 5)

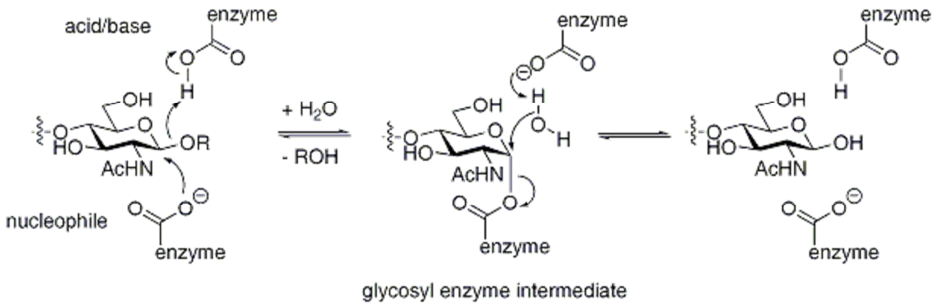


**Fig. 5.** Représentation du mécanisme catalytique de type « rétention ».

*Le mécanisme d'inversion* : Ici, La protonation de l'oxygène de la liaison glycosidique est accompagnée par l'attaque d'une molécule d'$H_2O$ activée par le résidu basique. Cette substitution nucléophile simple conduit à un produit présentant une stéréochimie opposée à celle du substrat de départ. (Figure 6)

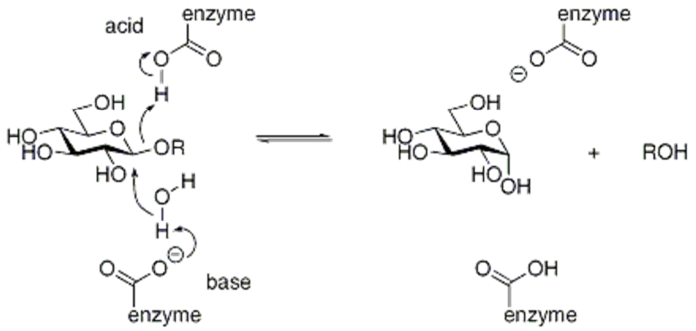


**Fig. 6.** Représentation du mécanisme catalytique de type « inversion ».

## 1.3. La famille des α-amylases (GH 13)

Comme défini dans la partie 1.1, l'amidon est un polymère complexe d'unités D-glucose reliées entre elles via des liaisons O-glycosidiques de types α-1,4. De par la complexité de sa structure, sa métabolisation nécessite diverses enzymes dont notamment celles de la famille 13 appelées « alpha-amylases ». La première α-amylase découverte fut celle du malt ou diastase, en 1833 par Anselme Payen et Jean-François Persoz (Payen & Persoz, 1833). Ces α-amylases sont dites endo-glycosidases car elles hydrolysent la liaison O-glycosidique uniquement à l'intérieur de la chaine polysaccharidique. D'autre part, elles conservent la configuration anomérique du carbone 1 via le mécanisme dit de « rétention ». D'autres enzymes hydrolysant l'amidon, par exemple les β-amylases (GH-14) ou les glucoamylases (GH-15), utilisent l'autre mode d'action et sont donc appelées des exo-glycosidases car elles attaquent la chaine polysaccharidique via son extrémité. De plus, ces deux types

d'enzymes sont caractérisés par un mécanisme d'« inversion » car le produit résultant de l'attaque hydrolytique présente un carbone 1 de configuration inversée.

D'après la dernière mise à jour de la base de données CAZy de juin 2011, la famille 13 des GHs serait composée de 22 types de spécificités différentes auxquelles viennent s'ajouter des transporteurs d'acides aminés (Tableau 1). Non seulement ces enzymes partagent un mécanismes catalytiques de type « rétention », mais surtout elles appartiennent toutes à la sous-famille structurale des GH-H présentant un repliement en tonneau $(\beta/\alpha)_8$.

**Tableau 1 :** Spécificités actuelles des différentes enzymes de la famille GH-13

| | |
|---|---|
| α-amylase (EC 3.2.1.1) | isoamylase (EC 3.2.1.68) |
| pullulanase (EC 3.2.1.41) | glucodextranase (EC 3.2.1.70) |
| isomaltulose synthase (EC 5.4.99.11) | maltohexaose-forming α-amylase (EC 3.2.1.98) |
| cyclomaltodextrinase (EC 3.2.1.54) | maltotriose-forming α-amylase (EC 3.2.1.116) |
| trehalose-6-phosphate hydrolase (EC 3.2.1.93) | branching enzyme (EC 2.4.1.18) |
| oligo-α-glucosidase (EC 3.2.1.10) | trehalose synthase (EC 5.4.99.16) |
| maltogenic amylase (EC 3.2.1.133) | 4-α-glucanotransferase (EC 2.4.1.25) |
| neopullulanase (EC 3.2.1.135) | maltopentaose-forming α-amylase (EC 3.2.1.-) |
| α-glucosidase (EC 3.2.1.20) | amylosucrase (EC 2.4.1.4) |
| maltotetraose-forming α-amylase (EC 3.2.1.60) | sucrose phosphorylase (EC 2.4.1.7) |
| malto-oligosyltrehalose trehalohydrolase (EC 3.2.1.141) | cyclomaltodextrin glucanotransferase (EC 2.4.1.19) |

### 1.3.1. Le tonneau $(\beta/\alpha)_8$ et le sillon catalytique

Ce tonneau $(\beta/\alpha)_8$ (Figure 8) est l'une des caractéristiques de la famille 13 des GHs qui appartiennent au clan des GH-H. Elles partagent cependant ce mode de repliement avec les familles 70 et 77 des GHs, respectivement des sucrases et des amylomaltases. Ce tonneau, appelé domaine A, contient l'extrémité N-terminale de la protéine et est composé de 400 à 600 acides aminés. Comme son nom l'indique, il se caractérise par la succession de 8 formations composées d'un brin β suivit d'une hélice α. Le domaine B est inséré entre le feuillet $\beta_3$ et l'hélice $\alpha_3$ et forme, avec une partie du domaine A, le site catalytique de type « gouttière ». Les résidus du site actifs sont situés sur les extrémités C-terminales des brins β et sont constitués, pour l'ensemble de la famille 13 des glycosides hydrolases, de trois résidus acides, Asp 174, Glu 200 et Asp 264 selon la numérotation de l'α-amylase AHA. Asp 174 et Glu 200 jouent, respectivement, le rôle de nucléophile et d'acide/base lors de la réaction enzymatique alors que le résidu Asp264 serait impliqué dans la stabilisation de l'intermédiaire covalent glycosyl-enzyme. (Uitdehaag *et al.,* 1999 ; Hasegawa *et al.,* 1999)

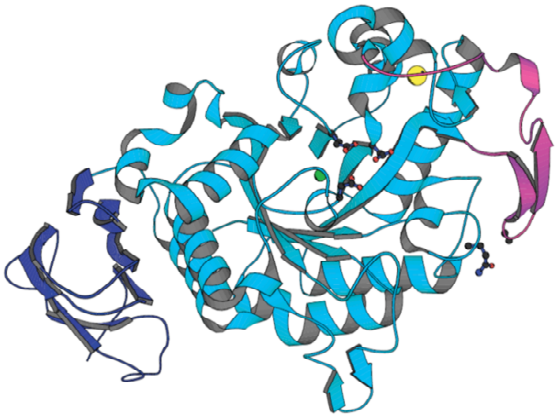

**Fig. 8.** Structure de l'α-amylase psychrophile AHA de *Pseudoalteromonas haloplanktis* (code PDB 1AQM). Vue faciale du tonneau ou domaine A en cyan, le domaine B en rose est à droite et le domaine C en bleu foncé replié en clef grecque est à gauche. Les trois résidus catalytiques sont montrés à proximité de l'ion chlorure en vert, l'ion calcium étant en jaune. (D'après Aghajari *et al.,* 1998)

### 1.3.2. Le domaine B

Le domaine B est inséré entre le brin β 3 et l'hélice α 3 du tonneau $(\beta/\alpha)_8$. Cette boucle présente une structure irrégulière qui varie d'une amylase à l'autre tant par la forme que la composition en acides aminés si bien que dans d'autres familles d'enzymes du clan des GH-H il peut être considéré soit comme un domaine à part entière soit intégré au domaine A comme une simple boucle (MacGregor *et al.,* 2001). Il est constitué de courts brins β et d'une ou plusieurs petites hélices α. Le domaine est essentiel à la catalyse puisque, relié au domaine A, il forme le sillon catalytique. De plus, grâce à sa variabilité, il est responsable de la spécificité de l'activité enzymatique. Il joue aussi un rôle dans la stabilité de la structure protéique via ses interactions avec le domaine A.

### 1.3.3. Les domaines C-terminaux

Enfin, du côté C-terminal de la structure protéique, on retrouve le domaine C qui suit le tonneau principal. Il est constitué de brins β agencés suivant un motif dit de 'clef grecque' (Figure 12). Il présente peu d'interactions avec le reste de la structure protéique et sa fonction reste inconnue. Cependant, un rôle éventuel fut proposé lors de l'étude des sites de fixation de carbohydrates sur la structure cristallographique de PPA (Qian *et al*., 1995). En effet, au sein du cristal, les feuillets β composant le motif en clef grecque du domaine C se situent entre le deuxième site de fixation d'une molécule et le site actif de la molécule suivante, le long d'un axe de la structure cristalline. Cet arrangement pourrait indiquer un rôle potentiel pour le domaine C dans la fixation de la chaine de polysaccharides sur la molécule.

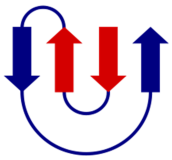

**Fig. 12.** Représentation schématique d'un motif en clef grecque.

## 1.3.4. Site de fixation des cofacteurs ioniques

### 1.3.4.1. L'ion calcium

L'une des propriétés générales de toutes les α-amylases est la présence d'au moins un site de fixation strictement conservé pour un ion calcium. Ce site de fixation est localisé entre le domaine A et le domaine B. Il joue un rôle purement structural en reliant les deux domaines maintenant ainsi l'intégrité du site actif. Chez les α-amylases des vertébrés et de *Tenebrio molitor*, le cation est coordonné par huit ligands strictement conservés à l'exception de Arg 158 (fixation via son groupement carbonyle) qui est remplacé par un Gln chez les α-amylases bactériennes et de drosophile. (D'Amico *et al.,* 2000)

Certaines d'entre elles présentent des sites de fixation supplémentaires pour l'ion calcium jouant le rôle d'inhibiteur à forte concentration en $Ca^{2+}$ (Tanaka & Hoshino, 2003 ; Kadziola *et al.,* 1994). D'autre part, l'α-amylase de *B.licheniformis* (BLA), contient trois sites de fixation dont deux sont impliqués dans une triade métallique $Ca^{2+}$-$Na^{+}$-$Ca^{2+}$ responsable de la cohésion entre les domaines A et B (Machius *et al.,* 1998) (Figure 10).

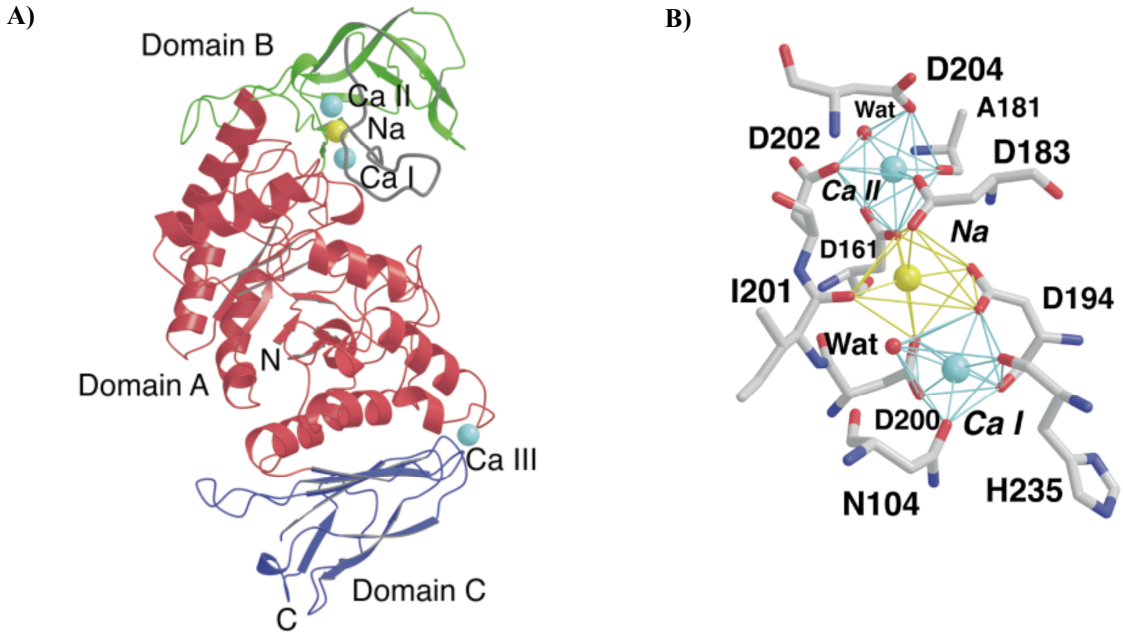


**Fig. 10. A)** Représentation schématique de la structure de la forme *holo* de BLA. Le domaine A est représenté en rouge, le B en vert et le C en bleu. Les ions calcium sont représentés par des sphères bleu clair et l'ion sodium (Na) est en jaune. **B)** Vue détaillée de la géométrie de coordination de la triade Ca-Na-Ca et de ses ligands.

### 1.3.4.2. L'ion chlorure

Certaines amylases présentent, en plus de l'ion calcium, un site de fixation pour un ion chlorure. Ce site se situe au centre du tonneau $(\beta/\alpha)_8$ à proximité du site actif et du site de fixation du l'ion calcium. Historiquement, la capacité à fixer un ion $Cl^-$ était typique des α-amylases animales des mammifères tels que l'homme et le porc (Levinsky & Steer, 1974). Grâce aux séquences de génomes et à l'amélioration des algorithmes d'alignement de séquences, D'amico *et al.*(2000) élargit la notion d'α-amylases chlorure-dépendantes à des organismes tels que les bactéries et les insectes (Long *et al.,* 1987 ; D'amico *et al.*, 2000 ; Da Lage *et al.,* 2004). Chez les vertébrés, et *Tenebrio molitor*, l'ion $Cl^-$ est coordonné par six ligands : Asn298 (ND2) ; Arg195 (NH2 et NE) ; Arg337 (NH1 et NH2) et une molécule d'$H_2O$. Chez les amylases bactériennes chlorure-dépendantes, Arg337 est remplacée par Lys337 qui assure un mode de coordination unidenté via sa chaine latérale (NZ). Les deux autres résidus sont adjacents aux résidus catalytiques principaux, à savoir Asp197 et Asp300, et sont donc conservés dans presque toutes les α-amylases (D'Amico *et al.,* 2000). De par sa proximité avec les résidus catalytiques, la fixation de l'ion chlorure conduit à deux avantages : (1) le déplacement du $pK_a$ des résidus catalytiques et du pH optimum vers des valeurs proche de l'environnement physiologique et (2) une augmentation drastique de l'activité spécifique chez les α-amylases chlorure-dépendantes. (Feller *et al*, 1996) (Figure 11)

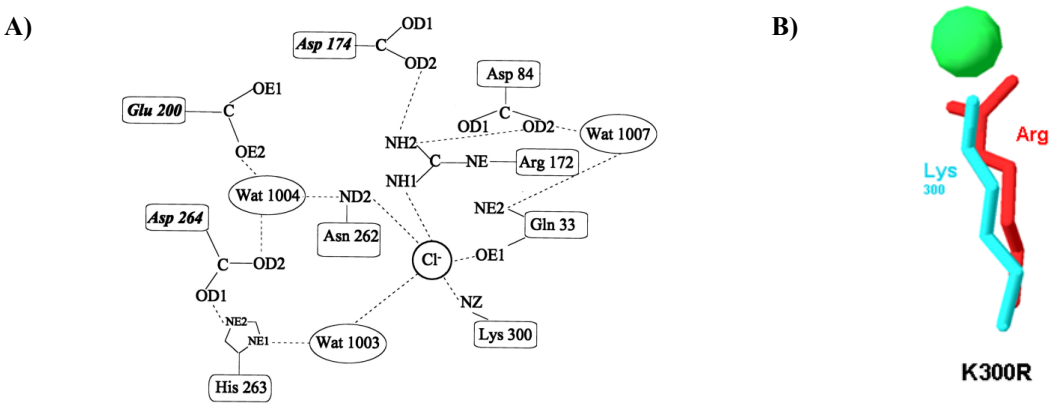


**Fig. 11. A)** Représentation schématique du site de fixation du chlore et de l'interaction avec les résidus du site catalytique. Les résidus principaux sont en italique. Les sites de fixation du chlore sont Lys 300(337), Arg 172(195), Asn 262(298), et $H_2O$ 1003(525) ; les résidus catalytiques sont Glu 200(233), Asp 174(197) et Asp264(300). Numérotation issue de l'α-amylase de *P.haloplanktis,* les nombres entre parenthèses réfèrent à la numérotation de PPA (D'après Aghajari *et al.,* 2002). **B)** Représentation schématique du mode bidenté ou unidenté du site de fixation de Arg/Lys 300(337).

## 1.3.5. La boucle « mobile »

Diverses structures cristallographiques de PPA (Quian *et al.,* 1995) et d'autres α-amylases, ont permis de mettre en évidence une boucle particulière appelée « flexible loop » constituée des résidus 304 à 309. Cette dernière est essentielle dans le mécanisme catalytique puisqu'elle forme une partie du

sillon catalytique et subit une modification lors de la fixation d'acarbose sur PPA. Une boucle similaire riche en glycine a aussi été identifiée chez les α-amylases pancréatique et salivaire humaine (Ramasubbu *et al.,* 1996 et Brayer *et al.,* 1995) ainsi que chez AHA (Aghajari *et al.,* 1998) mais pas chez l'α-amylase de *Tenebrio molitor* TMA (Strobl *et al.,* 1998). Son rôle est encore obscur mais deux hypothèses ont été avancées : elle pourrait maintenir des résidus impliqués dans la catalyse dans une orientation appropriée (Quian *et al.,* 1994 et Uitdehaag *et al.,* 1999) ou induire un mécanisme de capture et relargage du substrat et du produit (Ramasubbu *et al.,* 1996). (Figure 15)

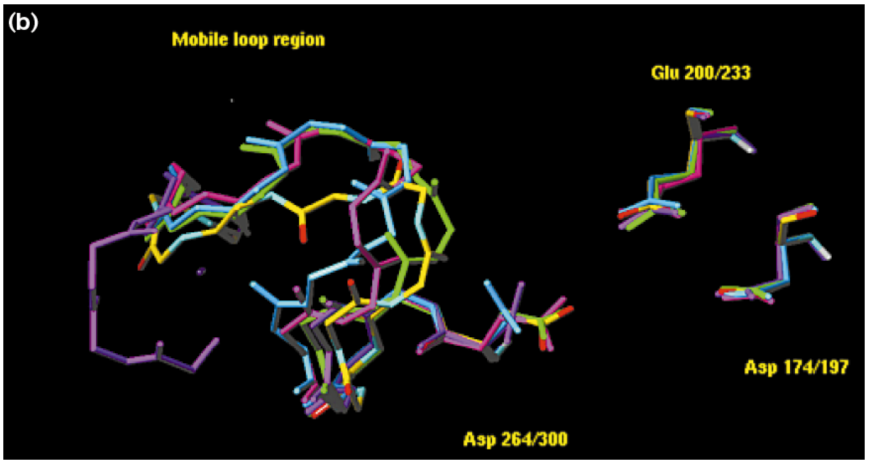


**Fig. 15.** Vue détaillée de la superposition de la région de la « Flexible loop », résidus 268-273 suivant la numérotation d'AHA (304-310 suivant la numérotation des α-amylases de mammifères MMA) et des résidus catalytiques Asp174, Glu200 et Asp264 (Asp197, Glu233 et Asp300). Les couleurs correspondent à AHA wild-type en jaune, AHA recombinant en mauve, PPA en bleu, HPA en rose et HSA en vert. (Adapté de Aghajari *et al.,* 1998)

### 1.3.6. Evolution et régions conservées des α-amylases

Bien que l'ensemble des α-amylases ne présentent que 10% d'identité de séquence, cinq motifs ont été identifiés et sont apparus comme étant conservés et quatre autres présentent de fortes similarités (MacGregor, 1988 ; Janecek, 1992 ; Janecek, 1994). Ces régions ont été identifiées grâce à la conservation stricte de certains résidus entourant d'autres résidus à substitution semi-conservatives. L'une des observations les plus importantes, est que ces régions se situent toujours soit dans des feuillets β soit dans des boucles, jamais dans les hélices du tonneau $(\beta/\alpha)_8$. Ceci reflète que les feuillets β internes au tonneau ont une capacité de variation moindre que les hélices α qui sont, elles, positionnées sur la face extérieure du tonneau.

Le repliement en tonneau $(\beta/\alpha)_8$ est connu depuis longtemps et chez près de 40 enzymes de spécificités différentes, des arguments soutenant une divergence ou une convergence évolutive ont été mis en évidence. L'étude du domaine B pose l'hypothèse de l'existence d'un ancêtre commun. L'insertion du domaine B est conservée au sein de la topologie type du tonneau $(\beta/\alpha)_8$ et l'existence

d'une corrélation entre la chaine lourde de l'antigène de surface 4F2 et une portion typique du domaine B (équivalent à un feuillet β) soutient l'hypothèse de l'ancêtre commun. Il semblerait d'ailleurs que l'insertion du domaine B chez les enzymes de la famille des α-amylases soit un évènement précoce précédant la spécialisation de l'enzyme. La Figure 17 représente les évènements possibles de l'évolution chez les GH-13. (Janecek, 1997)

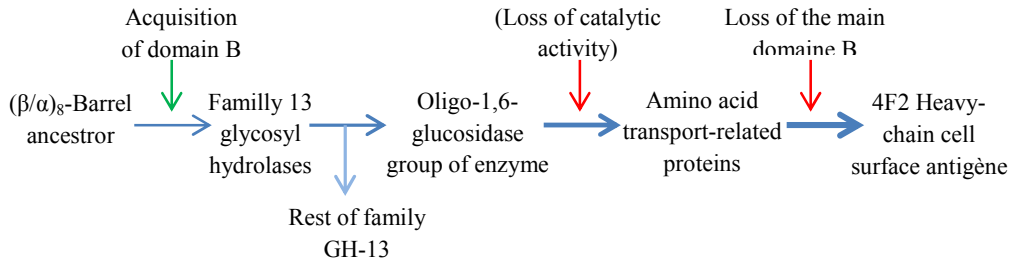


**Fig. 17.** Evènements possibles de l'évolution des enzymes de la famille GH-13.

## 1.3.7. Applications industrielles

L'amidon est l'un des produits majeurs de stockage de nombreux végétaux d'importance économique tels que le blé, le riz, le maïs, le tapioca et les pommes de terre. D'après le département des sciences des plantes et du sol de l'Université d'Oklahoma, la production mondiale en 2009 du maïs se serait élevée à près de 800 millions de Mt et celle du blé et du riz à presque 700 millions de Mt chacun. C'est en 1811 que le scientifique allemand Kirchhoff découvrit l'hydrolyse de l'amidon par traitement acide, technique à partir de laquelle une grande gamme de procédés a émergé. Durant les dix dernières années, on a pu remarquer un shift de l'utilisation des procédés industriels allant de l'hydrolyse acide de l'amidon à l'utilisation d'enzymes de conversion d'amidon dans la production de maltodextrine, d'amidons modifiés, ou encore de sirop de fructose et de glucose. Actuellement, ces enzymes correspondent à plus de 30 % de la production mondiale d'enzymes. Outre l'hydrolyse de l'amidon, ces enzymes sont aussi utilisées dans d'autres procédés industriels (Tableau 2) tels que la lessive et les détergents ou encore comme agents contre le rancissement du pain en boulangerie. Une majorité de ces enzymes appartiennent à une seule et même famille : la famille des α-amylases ou famille 13 des Glycoside hydrolases.

De manière à convertir complètement l'amidon en sirop de glucose par réaction enzymatique, il est nécessaire d'utiliser plusieurs sortes d'enzymes. La première étape consiste à liquéfier l'amidon en courtes chaines de dextrines solubles. Il s'ensuit un traitement enzymatique à l'aide d'α-amylase à une température proche de 100°C durant 90 minutes. Ceci implique l'utilisation d'une amylase thermostable c'est-à-dire conservant ses propriétés enzymatiques à haute température. On retrouve ce type d'amylase chez *Bacillus amyloliquefaciens, B. stearothermophilus ou B. licheniformis*. L'étape suivante est la saccharification de l'hydrolysat d'amidon en un sirop de glucose présentant une teneur

en glucose de 95%. Ceci est possible grâce à l'utilisation d'une glucoamylase qui hydrolyse les liaisons α 1-4 depuis l'extrémité non-réductrice de la chaine (cfr Fig. 7). Ce type d'enzyme se retrouve chez *Aspergillus niger* et les espèces proches. Cependant, cette étape impose l'utilisation d'une troisième enzyme. En effet, la glucoamylase ne peut que lentement hydrolyser les liaisons α 1-6 présentes dans les maltodextrines formées, résultant en l'accumulation d'isomaltose. C'est à l'aide de la pullulanase spécialisée dans l'hydrolyse de ce type de liaison que le problème peut être résolu. La troisième étape consiste alors en la conversion du sirop de glucose en sirop de fructose qui présente un pouvoir sucrant deux fois plus important. Cette conversion est réalisée grâce à l'enzyme D-xylose-cetol isomérase (EC 5.3.1.5) ou encore glucose isomérase.

L'industrie agro-alimentaire et plus précisément l'industrie de travail du grain et des produits amylacés (malt, farine, boulangerie…) est une grande consommatrice d'amidon et d'enzymes. Dans la fabrication du pain et la fermentation de la pâte, les amylases sont ajoutées pour découper les fragments d'amidon en dextrines utilisables par les levures pour provoquer, par fermentation, la montée de la pâte. D'autre part, pour diminuer la capacité naturelle du pain à rassir à cause de l'excès d'amylopectine, améliorer le goût et le volume des produits boulangers, on ajoute des additifs tels que des combinaisons de sucres de petites tailles et d'enzymes tels que les α-amylases, les branching- et debranching-enzymes, les amylases maltogéniques, les β-amylases et les amyloglucosidases et les xylanases. (Van der Maarel, 2002 ; Collins, 2002)

**Tableau 2**

Différents champs d'application des enzymes de la famille des α-amylases

| Application | Enzyme |
|---|---|
| Liquéfaction de l'amidon | α-Amylase |
| Saccharification de l'amidon | Amyloglucosidase, pullulanase, maltogenic α-amylase, α-amylase, isoamylase |
| Détergent et nettoyant de blanchisserie ; Clarification des jus de fruits ; Faciliter la digestion des aliments pour animaux ; Décollement des fibres et du coton ; Traitement des eaux usées ; Amélioration de la panification ; Bières basse calorie… | α-Amylase |
| Production de cyclodextrines | Cyclodextrine glycosyltransférase |
| Formation de gels d'amidon thermoréversible | Amylomaltase |
| Cycloamylose | Amylomaltase, enzyme de branchement, cyclodextrines glycosyltranférase |

Adapté de Van der Maarel, 2002 et Kirk, 2002.

## 1.4. Présentation des α-amylases chlorure-dépendantes étudiées

L'α-amylase psychrophile AHA est originaire de la bactérie à Gram négatif aérobie *Pseudoalteromonas haloplanktis* (souche TAB23) isolée à partir d'un échantillon d'eau de mer de la base antarctique française Dumont d'Urville. AHA est jusqu'à présent l'enzyme psychrophile la plus étudiée (Feller *et al.,* 1992 ; Feller *et al.,* 1994 ; Feller *et al.,* 1999 ; D'Amico *et al,* 2001 ; D'Amico *et al.,* 2002 ; D'Amico *et al.,* 2003a ; D'Amico *et al.,* 2003b).

L'α-amylase mésophile PPA a été extraite du pancréas du porc (*Sus scrofa*). Elle est une enzyme modèle pour la compréhension tant de la structure 3D des GHs de la famille 13 (Buisson *et al.,* 1987) que pour le mécanisme catalytique (Qian *et al.,* 1994). Le porc est un homéotherme (organisme maintenant sa température corporelle par lui-même) dont la température moyenne interne est de 39°C (Baxter, 1984) et ces enzymes, dont l'α-amylase (PPA), sont caractéristiques des enzymes mésophiles.

AmyD, l'α-amylase de *Drosophila melanogaster* (ou Drome), est une chlorure–dépendante, sur base d'alignement de séquence (Da Lage *et al,* 2004). Elle présente la particularité de n'être produite que lors de l'état larvaire de la drosophile (Maczkowiak & Da Lage, 2006). La drosophile est un insecte vivant dans les régions tempérées du globe mais aussi un organisme ectotherme (dont la température corporelle est fonction de la température de l'environnement). Son amylase nous donne donc la possibilité d'étudier une α-amylase chlorure-dépendante mésophile ectotherme.

Enfin, TFA est l'α-amylase de *Thermobifida fusca souche XY*, un actinomycète thermophile vivant dans le compost à des températures de 55-60°C (Bonamore *et al.,* 2005). Sur base des alignements de séquence (Da Lage *et al,* 2004), elle serait aussi chlorure-dépendante.

Grâce à ces quatre enzymes, nous avons en notre possession des α-amylases adaptées à une très large gamme de températures provenant de psychrophile, mésophile ectotherme et homéotherme ainsi que pour la première fois, une α-amylase chlorure-dépendante thermophile.

# Chapitre 1 : Introduction

## *Section II: Psychrophilic Enzymes: Cool Responses to Chilly Problems.*

**(in Extremophiles Handbook. Horikoshi, K. et al., Ed. Springer Verlag, 1ère Ed., 2011)**

# Psychrophilic Enzymes: Cool Responses to Chilly Problems

Frédéric Roulling, Florence Piette, **Alexandre Cipolla**, Caroline Struvay and Georges Feller

Institute of Chemistry B6, University of Liège, Liège-Sart Tilman,
Belgium

In: Koki Horikoshi (ed.), Extremophiles Handbook, DOI 10.1007/978-4-431-53898-1_6.7, Springer 2011

## 1.5 Introduction

Most of the biotopes on Earth are permanently exposed to low temperatures. This includes the Antarctic continent, the Arctic ice floe, the permafrost, the mountain and glacier regions, and the deep-sea waters, the latter covering 70% of the planet surface. If a psychrophile is defined as an organism living permanently at temperatures close to the freezing point of water, in thermal equilibrium with the medium, this definition encompasses a large range of species from Bacteria, Archaea, and Eukaryotes. This aspect underlines that psychrophiles are numerous, taxonomically diverse, and have a widespread distribution. In these organisms, low temperatures are essential for sustained cell metabolism. Some psychrophilic bacteria grown at 4°C have doubling times close to that of Escherichia coli at 37°C. Such deep adaptation of course requires a vast array of metabolic and structural adjustments at nearly all organization levels of the cell, which begins to be understood thanks to the availability of genome sequences and of proteomic approaches. Overviews on these various aspects have been recently published (D'Amico *et al.* 2006a; Gerday and Glansdorff 2007; Margesin *et al*. 2008; Casanueva *et al.* 2010).

This chapter focuses on protein structure and mainly on enzyme function at low temperatures. As a general picture, psychrophilic enzymes are all faced to a main constraint, to be active at low temperatures, but the ways to reach this goal are quite diverse. Previous reviews can also be consulted for a complete coverage of this topic (Smalas *et al*. 2000; Feller and Gerday 2003; Siddiqui and Cavicchioli 2006).

## 1.6 Biocatalysis in the Cold: A Thermodynamic Challenge

The activity of enzymes is strongly dependent on the surrounding temperature. The catalytic constant $k_{cat}$ corresponds to the maximum number of substrate molecules converted to product per active site per unit of time, and the temperature dependence of the catalytic rate constant is given by the relation:

$$k_{cat} = \kappa \frac{k_B T}{h} e^{-\Delta G^{\#}/RT} \qquad (1)$$

In this equation, κ is the transmission coefficient generally close to 1, $k_B$ is the Bolzmann constant ($1.38 \times 10^{-23}$ J $K^{-1}$), $h$ the Planck constant ($6.63 \times 10^{-34}$ J s), R the universal gas constant (8.31 J $K^{-1}$ $mol^{-1}$), and $\Delta G^{\#}$ the free energy of activation or the variation of the Gibbs energy between the activated enzyme-substrate complex ES* and the ground state ES (see Fig. 25.).

Accordingly, the activity $k_{cat}$ is exponentially dependent on the temperature. As a rule of thumb, for a biochemical reaction catalyzed by an enzyme from a mesophile (a bacterium or a warm-blooded vertebrate), a drop in temperature from 37°C to 0°C results in a 20–80 times lower activity. This is the main factor preventing the growth of non-adapted organisms at low temperatures.

The effect of temperature on the activity of psychrophilic and mesophilic enzymes is illustrated in Fig. 18 Equation 1 is only valid for the exponential rise of activity with temperature on the left limb of the curves. This figure reveals at least three basic features of cold adaptation. (1) In order to compensate for the slow reaction rates at low temperatures, psychrophiles synthesize enzymes having an up to tenfold higher specific activity in this temperature range. This is in fact the main physiological adaptation to cold at the enzyme level. (2) The temperature for apparent maximal activity for cold-active enzymes is shifted toward low temperatures, reflecting the weak stability of these proteins and their unfolding and inactivation at moderate temperatures. (3) Finally, the adaptation to cold is not perfect. It can be seen in Fig. 18 that the specific activity of the psychrophilic enzymes at low temperatures, although very high, remains generally lower than that of the mesophilic enzymes at 37°C.

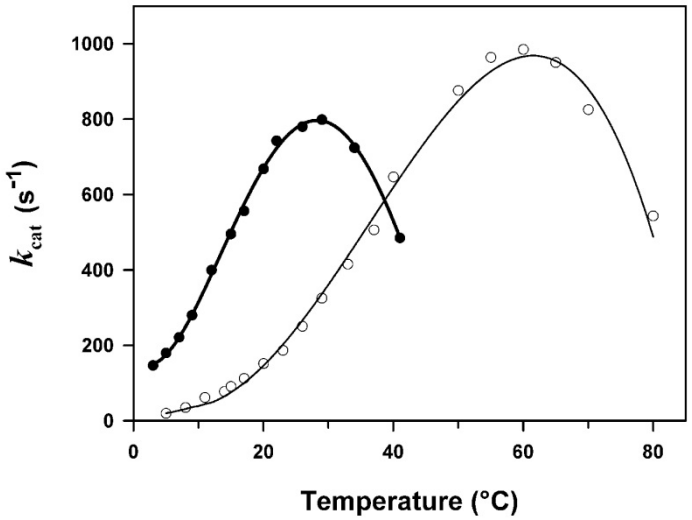


**Fig. 18.** Temperature dependence of the activity. The activity of psychrophilic (filled symbols, heavy line) and mesophilic (open symbols) enzymes recorded at various temperatures illustrates the main properties of cold-active enzymes (see text for details)

## 1.7 'Flexibility' and 'Corresponding States' Hypotheses

Such activity curves have suggested relationships between the activity of the enzyme, the flexibility of the protein, and its stability. Indeed, the high activity at low temperatures seems to arise from an increased flexibility of the protein structure, especially at temperatures that strongly slow down molecular motions, but the consequence of this improved mobility of the protein structure is of course a weak stability. Fluorescence quenching of extremophilic enzymes was used to probe this "flexibility" hypothesis (Fig. 19). It was found that the structure of psychrophilic proteins has an improved propensity to be penetrated by a small quencher molecule, when compared to mesophilic and thermophilic proteins, and therefore revealing a less compact conformation undergoing frequent micro-unfolding events (D'Amico *et al*. 2003b; Collins *et al*. 2003; Georlette *et al*. 2003). The

"flexibility" hypothesis has received further support by the quantification of macromolecular dynamics in the whole protein content of psychrophilic, mesophilic, thermophilic, and hyperthermophilic bacteria by neutron scattering (Tehei *et al*. 2004). This unique tool to study thermal atomic motions has indeed revealed that the resilience (equivalent to macromolecular rigidity in term of a force constant) increases with physiological temperatures. Furthermore, it was also shown that the atomic fluctuation amplitudes (equivalent to macromolecular flexibility) were similar for each microorganism at its physiological temperature. This is in full agreement with Somero's 'corresponding state' concept (Somero 1995) postulating that enzyme homologues exhibit comparable flexibilities to perform catalysis at their physiologically relevant temperatures.

However, the "flexibility" hypothesis has been challenged from an evolutionary point of view. As a matter of fact, directed evolution (Wintrode and Arnold 2000) and protein engineering (Bae and Phillips 2006) of enzymes have demonstrated that activity and stability are not physically linked in protein. Accordingly, it has been proposed that the low stability of cold-active enzymes is the result of a genetic drift related to the lack of selective pressure for stable proteins (Wintrode and Arnold 2000). Nevertheless, several lines of evidences indicate that the situation is more subtle. For instance, in multi-domain psychrophilic enzymes containing a catalytic and a non-catalytic domain, the catalytic domain is always heat-labile (Fig. 20) whereas the non-catalytic domain can be as stable as mesophilic proteins (Lonhienne *et al*. 2001; Claverie *et al.* 2003; Suzuki *et al.* 2005). It is therefore unlikely that a genetic drift only affects the catalytic domain without modifying other regions of the protein. Furthermore, several directed evolution experiments have shown that when libraries of randomly mutated enzymes are only screened for improved activity at low temperatures without any other constraints, the best candidates invariably display the canonical properties of psychrophilic enzymes (see D'Amico *et al.* 2002a for discussion) whereas random mutations improving both activity and stability are rare (Giver *et al*. 1998; Cherry *et al*. 1999). It follows that improvement of activity at low temperatures associated with loss of stability appears to be the most frequent and accessible event. In conclusion, the current view suggests that the strong evolutionary pressure on psychrophilic enzymes to increase their activity at low temperatures can be accommodated for by the lack of selection for stability and represents the simplest adaptive strategy for enzyme catalysis in the cold.

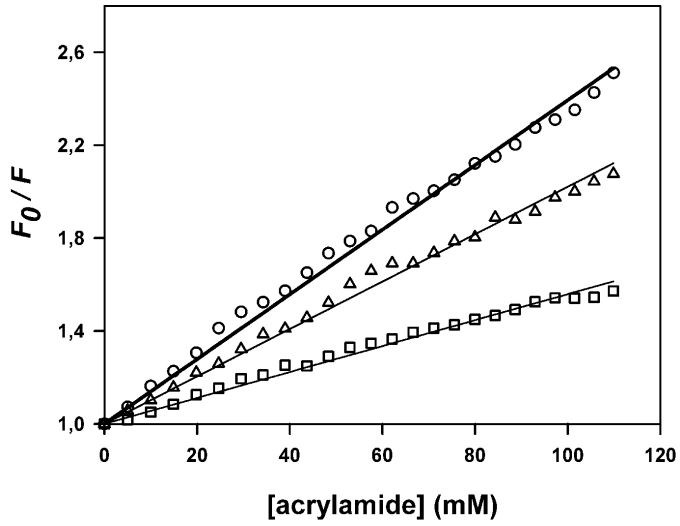


**Fig. 19.** Permeability of the protein structure. Fluorescence quenching experiments on psychrophilic (circles, heavy line), mesophilic (triangles), and heat-stable (squares) enzymes. The steep slope recorded for the psychrophilic enzyme indicates that its structure is easily penetrated by a small quencher molecule (acrylamide), resulting in a larger attenuation of the intrinsic fluorescence ($F_0/F$). This graph shows a clear correlation between this permeability index and the stability of the proteins. Adapted from (D'Amico et al. 2003b)

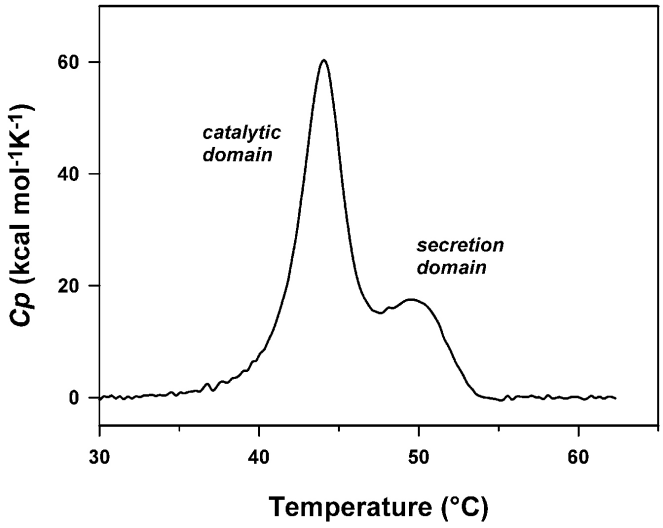


**Fig. 20.** Stability of domains in the α-amylase precursor. The precursor is composed by a catalytic domain and a secretion helper. In this thermogram, the top of the transitions corresponds to the melting points and the area under the transitions is roughly proportional to the domain sizes. Assuming that the low stability of psychrophilic enzymes is simply the result of a genetic drift (lack of selection for stable proteins), it is surprising that the more stable non-catalytic domain has not been subjected to the same extent to this drift. Adapted from (Claverie et al. 2003)

## 1.8 Flexibility and Structural Adaptations at the Active Site

Psychrophilic enzymes all share at least one property: a heat-labile activity, irrespective of the protein structural stability. Furthermore, the active site appears to be the most heat-labile structural element of these proteins (Collins *et al*. 2003; D'Amico *et al*. 2003b; Georlette *et al*.2003). Figure 21 illustrates this significant difference between the stability of the activity and the stability of the structure. The lower panel shows the stability of the structure as recorded by fluorescence. As expected, the structure of the cold-active enzyme is less stable than the mesophilic one. In the upper panel, the activity is recorded under the same experimental conditions and it can be seen that the mesophilic enzyme is inactivated when the protein unfolds. By contrast, activity of the cold-active enzyme is lost before the protein unfolds. This means that the active site is even more heat-labile than the whole protein structure. It was also shown that the active site of the psychrophilic α-amylase is the first structural element that unfolds in transverse urea gradient gel electrophoresis (Siddiqui *et al*.2005). All these aspects point to a very unstable and flexible active site and illustrate a central concept in cold adaptation: localized increases in flexibility at the active site are responsible for the high but heat-labile activity (Fields and Somero 1998), whereas other regions of the enzyme might or might not be characterized by low stability when not involved in catalysis (Chiuri *et al*. 2009).

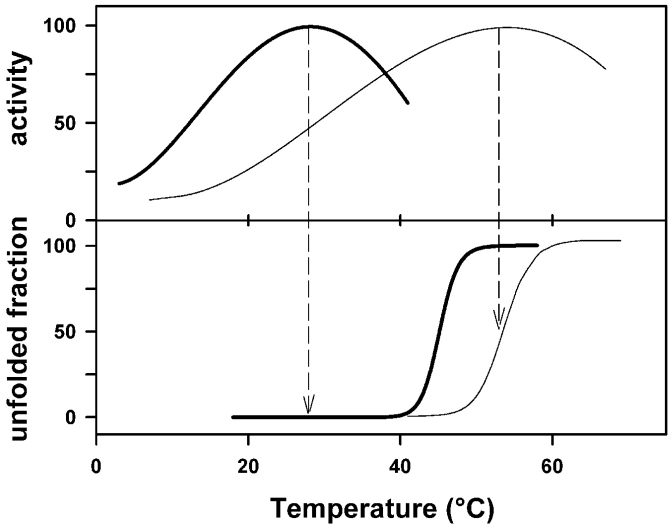


**Fig. 21.** Inactivation and unfolding of psychrophilic enzymes. The activity of psychrophilic enzymes (upper panel, heavy line) is inactivated by temperature before unfolding of the protein structure (lower panel, heavy line) illustrating the pronounced heat-lability of the active site. By contrast, inactivation of mesophilic (thin lines) or thermophilic enzymes closely corresponds to the loss of the protein conformation. Adapted from (D'Amico et al. 2003b)

Crystal structures of psychrophilic enzymes were of course of prime importance to investigate the properties of these heat-labile and cold-active catalytic centers. The first basic observation is that all side chains involved in the catalytic mechanism are strictly conserved. Indeed, comparison of the first X-ray structure of a psychrophilic enzyme, the cold-active α-amylase (Aghajari *et al.* 1998a, b), and of

its closest structural homologue from pig both in complex with acarbose, a pseudosaccharide inhibitor mimicking the transition state intermediate (Aghajari *et al*. 2002; Qian *et al*. 1994), has shown that all 24 residues forming the catalytic cleft are strictly conserved in the cold-active α-amylase (Fig. 22). This outstanding example of active site identity demonstrates that the specific properties of psychrophilic enzymes can be reached without any amino acid substitution in the reaction center. As a consequence, changes occurring elsewhere in the molecule are responsible for the optimization of the catalytic parameters.

Nevertheless, significant structural adjustments at the active site of psychrophilic enzymes have been frequently reported. In many cases, a larger opening of the catalytic cleft is observed and achieved by various ways, including replacement of bulky side chains for smaller groups, distinct conformation of the loops bordering the active site, or small deletions in these loops, as illustrated by a cold-active citrate synthase (Russell *et al*. 1998). In the case of a $Ca^{2+}$, $Zn^{2+}$-protease from a psychrophilic Pseudomonas species, an additional bound $Ca^{2+}$ ion pull the backbone forming the entrance of the site and markedly increases its accessibility when compared with the mesophilic homologue (Aghajari *et al*. 2003). As a result of such a better accessibility, cold-active enzymes can accommodate substrates at lower energy cost, as far as the conformational changes are concerned, and therefore reduce the activation energy required for the formation of the enzyme-substrate complex. The larger active site may also facilitate easier release and exit of products and thus may alleviate the effect of a rate limiting step on the reaction rate. It was also shown that an opening of the active site takes place upon binding of substrate or product in a cold-active xylanase whereas similar large scale movements are not observed in mesophilic or thermophilic structural homologues (De Vos et al. 2006). This can be tentatively related to higher active site mobility in the psychrophilic enzyme.

In addition, differences in electrostatic potentials in and around the active site of psychrophilic enzymes appear to be a crucial parameter for activity at low temperatures. Electrostatic surface potentials generated by charged and polar groups are an essential component of the catalytic mechanism at various stages: as the potential extends out into the medium, a substrate can be oriented and attracted before any contact between enzyme and substrate occurs. Interestingly, the cold-active citrate synthase (Russell et al. 1998), malate dehydrogenase (Kim et al. 1999), uracyl-DNA glycosylase (Leiros et al. 2003), and trypsin (Smalas et al. 2000; Gorfe et al. 2000; Brandsdal et al. 2001) are characterized by marked differences in electrostatic potentials near the active site region compared to their mesophilic or thermophilic counterparts that may facilitate interaction with ligand. In all cases, the differences were caused by discrete substitutions in non-conserved charged residues resulting in local electrostatic potential differing in both sign and magnitude.

Finally, two last examples illustrate the unsuspected diversity of strategies used to improve the activity in psychrophilic enzymes. With few exceptions, b-galactosidases are homotetrameric enzymes bearing four active sites.

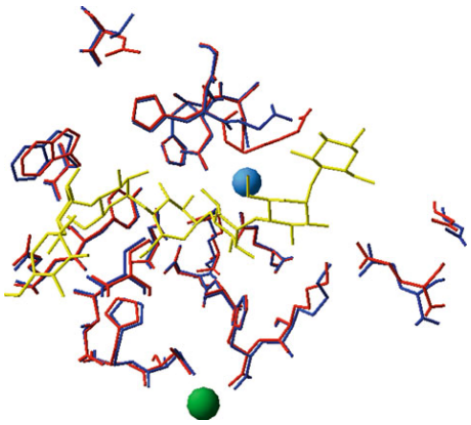

**Fig. 22.** Structure of the active site. Superimposition of the active site residues in psychrophilic (blue) and mesophilic (red) α-amylases. The chloride and calcium ions are shown as blue and green spheres, respectively. The 24 residues performing direct or water-mediated interactions with the substrate analog derived from acarbose (yellow) are identical and superimpose perfectly within the resolution of the structures, demonstrating a structural identity in these psychrophilic and mesophilic enzymes.

However, the crystal structure of a cold- active β-galactosidase revealed that it is a homohexamer, therefore possessing six active sites certainly contributing to improve the activity at low temperatures (Skalova et al. 2005). Cellulases are microbial enzymes displaying a modular organization made of a globular catalytic domain connected by a linker to a cellulose-binding domain. Psychrophilic cellulases were found to possess unusually long linkers about five times longer than in mesophilic cellulases (Garsoux et al. 2004; Violot et al. 2005). The long linker adopts a large number of conformations, and considering the cellulose-binding domain anchored to the cellulose fibers and a rotation of the extended molecule around this axis, it was calculated that the catalytic domain has a 40-fold higher accessible surface area of substrate when compared with a mesophilic cellulase possessing a much shorter linker. Here also, increasing the available surface of the insoluble substrate to the catalytic domain should improve the activity of this enzyme at low temperatures.

## 1.9 Active Site Dynamics

The heat-labile activity of psychrophilic enzymes suggests that the dynamics of the functional side chains at the active site is improved in order to contribute to cold-activity and the above-mentioned structural adaptations seem to favor a better accessibility to the substrate and release of the product (Tsigos et al. 1998; Smalas et al. 2000). This active site flexibility of cold-active enzymes in solution is also well demonstrated by the psychrophilic α-amylase (D'Amico et al. 2006b). In this specific case, the above-mentioned structural identity of the catalytic cleft with its mesophilic homologue from pig

precludes the involvement of adaptive mutations within the active site in the analysis of the results. As shown in Table 3, both the psychrophilic and mesophilic α-amylases degrade large macromolecular polysaccharides made of glucose units linked by α-1,4 bonds. These substrates have a complex structure and are generally branched. Taking the natural substrate, starch, as the reference, it can be seen that the psychrophilic enzyme is more active on all these large substrates. Being more flexible, the active site can accommodate easily these macromolecular polysaccharides. Considering the small substrates, the reverse situation is observed. Both enzymes are active on short oligosaccharides of at least four glucose units, but in this case, the psychrophilic α-amylase is less active on all these small substrates. Apparently, the flexible active site accommodates less efficiently these short oligosaccharides.

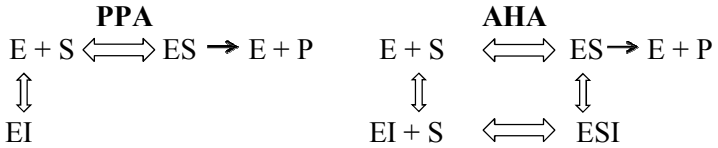


**Fig. 23.** Inhibition models of α-amylases. Reaction pathways for the competitive inhibition of starch hydrolysis by maltose for the mesophilic α-amylase PPA and of the mixed type inhibition for the psychrophilic α-amylase AHA. Under identical experimental conditions, the cold-active enzyme forms the ternary complex ESI (D'Amico et al. 2006b)

**Table 3:** Relative activity of the psychrophilic (AHA) and the mesophilic (PPA) α-amylases on macromolecular polysaccharides and on maltooligasaccharides. Adapted from D'Amico et al., 2006b

| Substrate | Relative activity (%) | |
|---|---|---|
| | AHA | PPA |
| Macromolecular substrates | | |
| Starch | 100 | 100 |
| Amylopectin | 96 | 68 |
| Amylose | 324 | 214 |
| Dextrin | 108 | 95 |
| Glycogen | 74 | 59 |
| Short oligosaccharides | | |
| Maltotetraose G4 | 17 | 22 |
| Maltopentose G5 | 69 | 145 |
| Maltohexaose G6 | 94 | 147 |
| Maltoheptaose G7 | 119 | 155 |
| Maltooligosaccharides (G4–G10 mix) | 64 | 101 |

The inhibition patterns provide additional insights into the specific properties of psychrophilic active sites (Fig. 23). Both the mesophilic and the psychrophilic α-amylases are inhibited by maltose, the end product of starch hydrolysis. In the case of the mesophilic enzyme, the enzyme can bind either the substrate (in a productive mode) or the inhibitor, but not both. By contrast, the cold-active enzyme

can also bind either the substrate or the inhibitor but also both, forming the ternary complex ESI, once again suggesting a more accessible and flexible active site.

## 1.10 Adaptive Drift and Adaptive Optimization of Substrate Affinity

As a consequence of the improved active site dynamics in cold-active enzymes, substrates bind less firmly in the binding site (if no point mutations have occurred) giving rise to higher $K_m$ values. An example is given in Table 4 showing that the psychrophilic α-amylase is more active on its macromolecular substrates whereas the $K_m$ values are up to 30-fold larger, i.e., the affinity for the substrates is up to 30-fold lower. Ideally, a functional adaptation to cold would mean optimizing both $k_{cat}$ and $K_m$. However, a survey of the available data on psychrophilic enzymes (Xu et al. 2003) showed that optimization of the $k_{cat}$ / $K_m$ ratio is far from a general rule but on the contrary that the majority of cold-active enzymes improve the $k_{cat}$ value at the expense of $K_m$, therefore leading to suboptimal values of the $k_{cat}$ / $K_m$ ratio, as also shown in Table 4. There is in fact an evolutionary pressure on $K_m$ to increase in order to maximize the overall reaction rate. Such adaptive drift of $K_m$ has been well illustrated by the lactate dehydrogenases from Antarctic fish (Fields and Somero 1998) and by the psychrophilic α-amylase (D'Amico et al. 2001) because both enzymes display rigorously identical substrate binding site and active site architecture when compared with their mesophilic homologues. In both cases, temperature-adaptive increases in $k_{cat}$ occur concomitantly with increases in $K_m$ in cold-active enzymes. As already mentioned, such identity of the sites also implies that adjustments of the kinetic parameters are obtained by structural changes occurring distantly from the reaction center. This aspect has received strong experimental support (D'Amico et al. 2003a) as discussed latter in this chapter.

**Table 4:** Kinetic parameters for the hydrolysis of polysaccharides at 25°C by the psychrophilic (AHA) and the mesophilic (PPA) α-amylases. Adapted from D'Amico et al., 2006b

| | AHA | | | PPA | | |
|---|---|---|---|---|---|---|
| Substrate | $k_{cat}$ $s^{-1}$ | $K_m$ mg $l^{-1}$ | $k_{cat}/K_m$ $s^{-1}$ mg$^{-1}$ l | $k_{cat}$ $s^{-1}$ | $K_m$ mg $l^{-1}$ | $k_{cat}/K_m$ $s^{-1}$ mg$^{-1}$ l |
| Starch | 663 | 155 | 4.3 | 327 | 41 | 8.0 |
| Amylopectin | 636 | 258 | 2.5 | 222 | 53 | 4.2 |
| Amylose | 2148 | 178 | 12.1 | 700 | 36 | 19.4 |
| Dextrin | 716 | 586 | 1.2 | 311 | 61 | 5.1 |
| Glycogen | 491 | 1344 | 0.3 | 193 | 46 | 4.2 |

Several enzymes, especially in some cold-adapted fish, counteract this adaptive drift of $K_m$ in order to maintain or to improve the substrate binding affinity by amino acid substitutions within the active site (Smalas et al. 2000). The first reason for these enzymes to react against the drift is obvious when considering the regulatory function associated with $K_m$, especially for intracellular enzymes. The second reason is related to the temperature dependence of weak interactions. Substrate binding is an

especially temperature sensitive step because both the binding geometry and interactions between binding site and ligand are governed by weak interactions having sometimes opposite temperature dependencies. Hydrophobic interactions form endothermically and are weakened by a decrease in temperature. By contrast, interactions of electrostatic nature (ion pairs, hydrogen bounds, Van der Waals interactions) form exothermically and are stabilized at low temperatures. Therefore low temperatures do not only reduce the enzyme activity ($k_{cat}$), but can also severely alter the substrate binding mode according to the type of interaction involved.

The chitobiase from Antarctic bacteria nicely illustrates both aspects, as well as the extent of the kinetic optimization that can be reached during cold adaptation of enzymes (Lonhienne et al. 2001). Figure 24 shows that the $k_{cat}$ of the cold-active chitobiase is eight times higher than that of a mesophilic chitobiase at 5°C. However, the $K_m$ for the substrate is 25 times lower at this temperature, and as a result, the $k_{cat}$ / $K_m$ for the cold-active enzyme is nearly 200 times greater at low temperature. Because the cell-bound bacterial chitobiase has to access its substrate in the extracellular medium, the physiological advantage of a high affinity for the substrate is clear. In addition, the cross-shaped plot of $K_m$ shows that the $K_m$ of each enzyme tends to minimal and optimal values in the range of the corresponding environmental temperatures, reflecting the fine tuning of this parameter reached in the course of thermal adaptation. In the case of the mesophilic chitobiase, the 3D-structure indicates that two tryptophan residues are the main substrate binding ligands and perform hydrophobic interactions with the substrate. This can be related to the decrease of $K_m$ with temperature, according to the above-mentioned thermal dependence of hydrophobic interactions. Interestingly, the two tryptophan residues are not found in the cold-active chitobiase but are replaced by polar residues that are able to perform stronger interactions as the temperature is decreased.

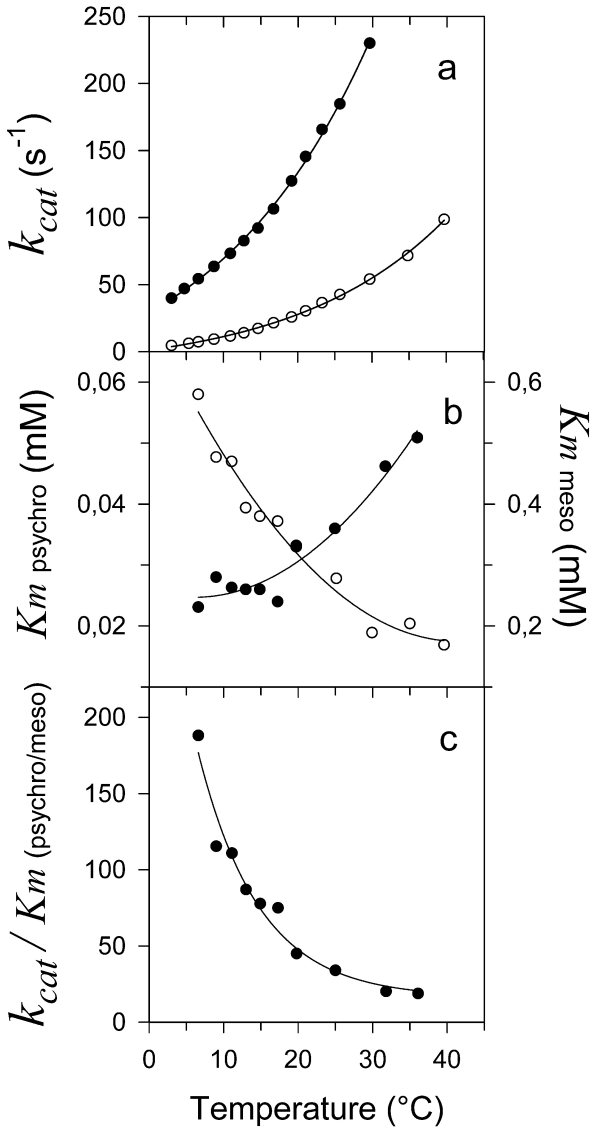


**Fig. 24.** Kinetic optimization in a cold-active chitobiase. Temperature dependence of the kinetic parameters for psychrophilic (closed symbols) and mesophilic (open symbols) chitobiases. Data for **(a)** the catalytic rate constant $k_{cat}$; **(b)** the Michaelis parameter $K_m$, note the different scales used; and **(c)** the relative catalytic efficiency $k_{cat}/ K_m$ (psychrophile/mesophile). The cold-adapted chitobiase is characterized by a higher activity, an optimal $K_m$ value at low temperatures, and a 200 times higher catalytic efficiency at 7°C. Adapted from (Lonhienne et al. 2001)

## 1.11 Energetics of Activity at Low Temperatures

Referring to Eq. 1, the high activity of cold-adapted enzymes corresponds to a decrease of the free energy of activation $\Delta G^{\#}$. Two strategies have been highlighted to reduce the height of this energy barrier. Figure 25 illustrates the first strategy where an evolutionary pressure increases $K_m$ in order to maximize the reaction rate. According to the transition state theory, when the enzyme encounters its substrate, the enzyme-substrate complex ES falls into an energy pit. For the reaction to proceed, an activated state $ES^{\#}$ has to be reached, which eventually breaks down into the enzyme and the product.

The height of the energy barrier between the ground state ES and the transition state $ES^{\#}$ is defined as the free energy of activation $\Delta G^{\#}$: the lower this barrier, the higher the activity as reflected in Eq. 1. In the case of cold-active enzymes displaying a weak affinity for the substrate, the energy pit for the ES complex is less deep (dashed in Fig. 25). It follows that the magnitude of the energy barrier is reduced and therefore the activity is increased. This thermodynamic link between affinity and activity is valid for most enzymes (extremophilic or not) under saturating substrate concentrations and this link appears to be involved in the improvement of activity at low temperatures in numerous cold-active enzymes (Fields and Somero 1998; Xu et al. 2003).

The second and more general strategy involves the temperature dependence of the reaction catalyzed by cold-active enzymes. Table 5 reports the enthalpic and entropic contributions to the free energy of activation in extremophilic α-amylases. The free energy of activation $\Delta G^{\#}$ is calculated from Eq. 1 using the $k_{cat}$ value at a given temperature and the enthalpy of activation $\Delta H^{\#}$ is obtained by recording the temperature dependence of the activity (Lonhienne et al. 2000). Finally, the entropic contribution $T\Delta S^{\#}$ is deduced from the Gibbs–Helmholtz equation:

$$\Delta G^{\#} = \Delta H^{\#} - T\Delta S^{\#} \qquad (2)$$

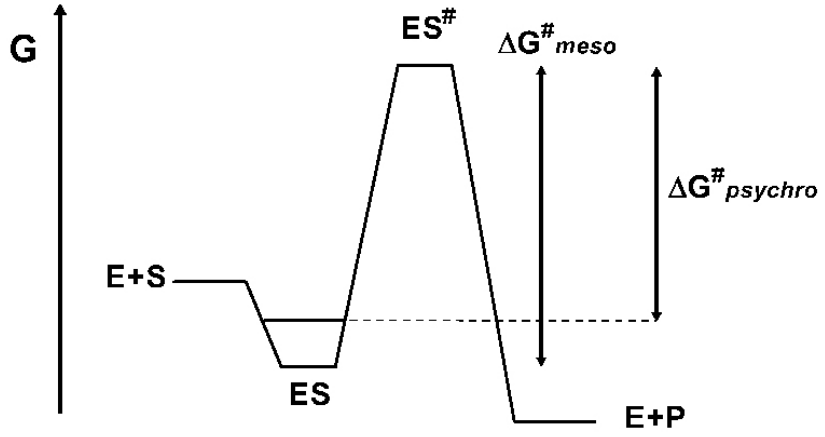


**Fig. 25.** Optimization of activity by decreasing substrate affinity in psychrophilic enzymes. Reaction profile for an enzyme-catalyzed reaction with Gibbs energy changes under saturating substrate concentration. Weak substrate binding (dashed line) decreases the activation energy ($\Delta G^{\#}_{psychro}$) and thereby increases the reaction rate (see text for details)

The enthalpy of activation $\Delta H^{\#}$ depicts the temperature dependence of the activity: the lower this value, the lower the variation of activity with temperature. The low value found for almost all psychrophilic enzymes demonstrates that their reaction rate is less reduced than for other enzymes when the temperature is lowered. Accordingly, the decrease of the activation enthalpy in the enzymatic reaction of psychrophilic enzymes can be considered as the main adaptive character to low

temperatures. This decrease is structurally achieved by a decrease in the number of enthalpy-driven interactions that have to be broken during the activation steps. These interactions also contribute to the stability of the protein folded conformation, and, as a corollary, the structural domain of the enzyme bearing the active site should be more flexible. It is interesting to note that such a macroscopic interpretation of the low activation enthalpy in cold-active enzymes fits with the experimental observation of a markedly heat-labile activity illustrated in Fig. 21. Table 5 shows that the entropic contribution $T\Delta S^{\#}$ for the cold-active enzyme is larger and negative. This has been interpreted as a large reduction of the apparent disorder between the ground state with its relatively loose conformation and the well organized and compact transition state (Lonhienne et al. 2000). The heat-labile activity of cold-active enzymes suggests a macroscopic interpretation for this thermodynamic parameter. As a consequence of active site flexibility, the enzyme-substrate complex ES occupies a broader distribution of conformational states translated into increased entropy of this state, compared to that of the mesophilic or thermophilic homologues. This assumption has received strong experimental support by using microcalorimetry to compare the stabilities of free extremophilic enzymes with the same enzymes trapped in the transition state conformation by a non-hydrolysable substrate analog (D'Amico et al. 2003b). The larger increase in stability for the psychrophilic enzyme in the transition state conformation demonstrated larger conformational changes between the free and bound states when compared to mesophilic and thermophilic homologues. Furthermore, a broader distribution of the ground state ES should be accompanied by a weaker substrate binding strength, as indeed observed for numerous psychrophilic enzymes.

**Table 5:** Activation parameters of the hydrolytic reaction of α-amylases at 10°C. Adapted from (D'Amico *et al.* 2003b)

| | $k_{cat}$ $s^{-1}$ | $\Delta G^{\#}$ kcal $mol^{-1}$ | $\Delta H^{\#}$ kcal $mol^{-1}$ | $T\Delta S^{\#}$ kcal $mol^{-1}$ |
|---|---|---|---|---|
| Psychrophile | 294 | 13.3 | 8.3 | 5.5 |
| Mesophile | 97 | 14.0 | 11.1 | 2.9 |
| Thermophile | 14 | 15.0 | 16.8 | 1.8 |

## 1.12 Conformational Stability of Extremophilic Proteins

Considering the numerous insights for strong relationships between activity and stability in psychrophilic enzymes, the conformational stability of these proteins has been intensively investigated in comparison with mesophilic and thermophilic counterparts. Figure 26 displays the calorimetric records of heat-induced unfolding for psychrophilic, mesophilic, and thermophilic proteins. These enzymes clearly show distinct stability patterns that evolve from a simple profile in the unstable psychrophilic proteins to a more complex profile in very stable thermophilic counterparts. The unfolding of the cold-adapted enzymes occurs at lower temperatures as indicated by the temperature of

half-denaturation $T_m$, given by the top of the transition. This property, known for decades, has been highlighted by various techniques. By contrast, the energetics of structure stability was essentially revealed by microcalorimetry (D'Amico et al. 2001; Collins et al. 2003; Georlette et al. 2003). The calorimetric enthalpy $\Delta H_{cal}$ (area under the curves in Fig. 26), corresponding to the total amount of heat absorbed during unfolding, reflects the enthalpy of disruption of bonds involved in maintaining the compact structure and is markedly lower for the psychrophilic enzymes. In addition, there is a clear trend for increasing $\Delta H_{cal}$ values in the order psychrophile < mesophile < thermophile. The transition for the psychrophilic enzymes is sharp and symmetric whereas other enzymes are characterized by a flattening of the thermograms.

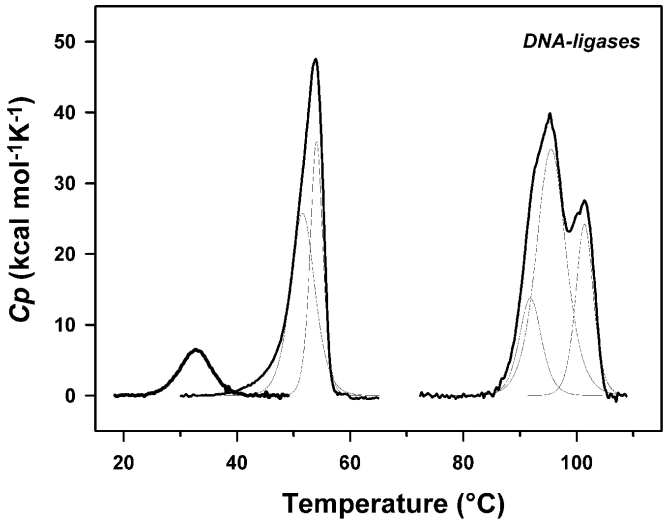


**Fig. 27.** Thermal unfolding of extremophilic enzymes. Thermograms of DNA-ligases recorded by differential scanning microcalorimetry showing, from left to right, psychrophilic (heavy line), mesophilic, and thermophilic proteins. The cold-active enzyme is characterized by a lower $T_m$ (top of the transition) and $\Delta H_{cal}$ (area under the transition), by a sharp and cooperative transition, and by the lack of stability domains (indicated by thin lines in stable proteins). Adapted from (Georlette et al. 2003)

This indicates a pronounced cooperativity during unfolding of the psychrophilic enzymes: the structure is stabilized by fewer weak interactions and disruption of some of these interactions strongly influences the whole molecular edifice and promotes its unfolding. The psychrophilic enzymes unfold according to an all-or-none process, revealing a uniformly low stability of the architecture. By contrast, all other homologous enzymes display two to three transitions (indicated by deconvolution of the heat capacity function in Fig. 26). Therefore, the conformation of these mesophilic and thermophilic enzymes contains structural blocks or units of distinct stability that unfold independently. Finally, the unfolding of the psychrophilic proteins is frequently more reversible than that of other homologous enzymes that are irreversibly unfolded after heating. The weak hydrophobicity of the core clusters in cold-adapted enzymes and the low $T_m$ at which hydrophobic interactions are restrained certainly account for this reversible character because, unlike mesophilic proteins, aggregation does not occur or

occurs to a lower extent.

As a practical and useful consequence of the unfolding reversibility, it has been possible to calculate accurately the conformational stability of a psychrophilic α-amylase over a broad range of temperatures (Feller et al. 1999). The comparison of these data with those of other proteins reveals some unsuspected properties of cold-adapted proteins. The thermodynamic stability of a protein that unfolds reversibly according to a two-state mechanism

$$N \leftrightarrow U \qquad (3)$$

is described by its stability curve, i.e., the free energy of unfolding as a function of temperature (Fig. 27). By definition, this stability is nil at $T_m$ (equilibrium constant $K$ = [U]/[N] = 1 and $\Delta G = RT\,lnK$). At temperatures below $T_m$, the stability increases, as expected, but perhaps surprisingly for the non-specialist, the stability reaches a maximum close to room temperature then it decreases at lower temperatures (Fig. 27). In fact, this function predicts a temperature of cold unfolding, which is generally not observed because it occurs below 0°C. Nevertheless, cold unfolding has been well demonstrated under specific conditions (Privalov 1990). Increasing the stability of a protein is essentially obtained by lifting the curve toward higher free energy values (Kumar and Nussinov 2004). As far as extremophiles are concerned, one of the most puzzling observations of the last decade is that most proteins obey this pattern, i.e., whatever the microbial source, the maximal stability of their proteins is clustered around room temperature (for more details see Kumar and Nussinov 2004). Accordingly, the environmental temperatures for mesophiles and (hyper)thermophiles lie on the right limb of the bell-shaped stability curve and, obviously, the thermal dissipative force is used to promote molecular motions in these molecules. By contrast, the environmental temperatures for psychrophiles lie on the left limb of the stability curve. It follows that molecular motions in proteins at low temperatures are gained from the factors ultimately leading to cold unfolding (Feller et al. 1999), i.e., the hydration of polar and nonpolar groups (Makhatadze and Privalov 1995). The origin of flexibility in psychrophilic enzymes at low temperatures is therefore drastically different from mesophilic and thermophilic proteins, the latter taking advantage of the conformational entropy rise with temperature to gain in mobility.

A surprising consequence of the free energy function for the psychrophilic protein shown in Fig. 27 is its weak stability at low temperatures when compared with mesophilic and thermophilic proteins, whereas it was intuitively expected that cold-active proteins should also be cold stable. This protein is in fact both heat and cold labile. Assuming constant properties of the solvent below 0°C (i.e., no freezing) and the absence of protective effects from cellular components, this α-amylase should unfold at 10°C. Therefore, cold denaturation of some key enzymes in psychrophiles can be an additional, though unsuspected factor fixing the lower limit of life at low temperatures. It has also been shown that the psychrophilic α-amylase has reached a state close to the lowest possible stability of the native

state (D'Amico et al. 2001). If psychrophilic enzymes have indeed gained in flexibility at the expense of stability in the course of evolution, this implies that the actual native state precludes further adaptation toward a more mobile structure. This aspect can account for the imperfect adaptation of the catalytic function in some psychrophilic enzymes, mentioned at the beginning of this chapter and illustrated in Fig. 18.

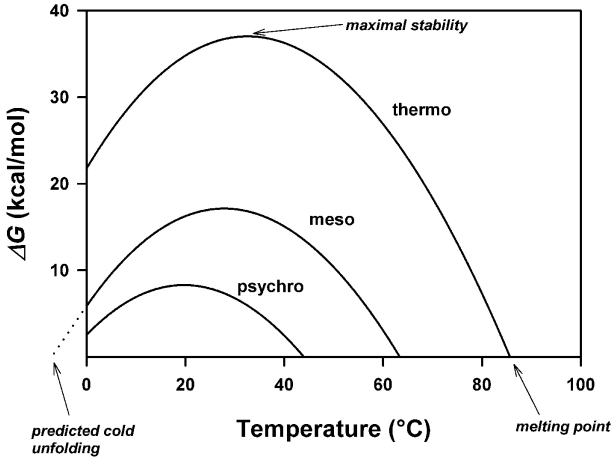


**Fig. 27.** Representative stability curves of homologous extremophilic proteins. The energy required to disrupt the native state (i.e., the conformational stability) is plotted as a function of temperature. At the melting point, this energy = 0 and in addition, the curves also predict cold unfolding and a maximal stability close to room temperature. A high stability in thermophiles is reached by lifting the curve toward higher free energy values, whereas the low stability in psychrophiles corresponds to a collapse of the bell-shaped stability curve. Adapted from (D'Amico et al. 2003b)

## 1.13 Structural Basis of Low Stability

The number of X-ray crystal structures from psychrophilic enzymes has increased dramatically, demonstrating the growing interest for these peculiar proteins. However, the interpretation of these structural data is frequently difficult for two main reasons. First, the structural adaptations are extremely discrete and can easily escape the analysis. Second, these structural adaptations are very diverse, reflecting the complexity of factors involved in the stability of a macromolecule at the atomic level. For instance, it was found that all structural factors currently known to stabilize the protein molecule could be attenuated in strength and number in the structure of cold-active enzymes (Smalas et al. 2000; Russell 2000; Gianese et al. 2002). An exhaustive description of all these factors is beyond the scope of this chapter and only the essential features are summarized below. Two review articles can be consulted for a comprehensive discussion of this topic (Smalas et al. 2000; Siddiqui and Cavicchioli 2006). The observable parameters related to protein stability include structural factors and mainly weak interactions between atoms of the protein structure. In psychrophilic proteins, this involves the clustering of glycine residues (providing local mobility), the disappearance of proline residues in loops (enhancing chain flexibility between secondary structures), a reduction in arginine

residues which are capable of forming multiple salt bridges and H-bonds, as well as a lower number of ion pairs, aromatic interactions or H-bonds, compared to mesophilic enzymes. The size and relative hydrophobicity of nonpolar residue clusters forming the protein core are frequently smaller, lowering the compactness of the protein interior by weakening the hydrophobic effect on folding. The N- and C-caps of α-helices are also altered (weakening the charge-dipole interaction) and loose or relaxed protein extremities appear to be preferential sites for unzipping. The binding of stabilizing ions, such as calcium, can be extremely weak, with binding constants differing from mesophiles by several orders of magnitude. Insertions and deletions are sometimes responsible for specific properties such as the acquisition of extra-surface charges (insertion) or the weakening of subunit interactions (deletion).

Calculation of the solvent accessible area showed that some psychrophilic enzymes expose a higher proportion of nonpolar residues to the surrounding medium (Aghajari et al. 1998b; Russell et al. 1998). This is an entropy-driven destabilizing factor caused by the reorganization of water molecules around exposed hydrophobic side chains. Calculations of the electrostatic potential revealed in some instances an excess of negative charges at the surface of the protein and, indeed, the pI of cold-active enzymes is frequently more acidic than that of their mesophilic or thermophilic homologues. This has been related to improved interactions with the solvent, which could be of prime importance in the acquisition of flexibility near 0 (Feller et al. 1999). Besides the balance of charges, the number of salt bridges covering the protein surface is also reduced. There is a clear correlation between surface ion pairs and temperature adaptation, since these weak interactions significantly increase in number from psychrophiles to mesophiles, to thermophiles and hyperthermophiles, the latter showing arginine-mediated multiple ion pairs and interconnected salt bridge networks (Yip et al. 1995; Vetriani et al. 1998). Such an altered pattern of electrostatic interactions is thought to improve the dynamics or the ‘‘breathing’’ of the external shell of cold-active enzymes.

However, each enzyme adopts its own strategy by using one or a combination of these altered structural factors in order to improve the local or global mobility of the protein edifice. Comparative structural analyses of psychrophilic, mesophilic, and thermophilic enzymes indicate that each protein family displays different structural strategy to adapt to temperature. However, some common trends are observed: the number of ion pairs, the side-chain contribution to the exposed surface, and the apolar fraction of the buried surface show a consistent decrease with decreasing optimal temperatures (Gianese et al. 2002; Bell et al. 2002; Bae and Phillips 2004; Mandrich et al. 2004). As a result of the great diversity of factors involved in protein stability, the bias in the amino acid composition observed in individual psychrophilic protein (low proline or arginine content, etc.) is not found when analyzing the mean amino acid composition of the whole genome. On the contrary, the available genomic data have produced ambiguous results (Gerday and Glansdorff 2007; Margesin et al. 2008) and it is currently difficult to correlate the reported trends in genomic amino acid composition with adaptations to low temperatures or with species-specific differences.

## 1.14 Activity–Stability Relationships: Experimental Insights

In order to check the validity of the proposed relationships between the activity and the stability in cold-active enzymes, a psychrophilic α-amylase has been used as a model because the identical architecture of its active site, when compared with a close mesophilic homologue, indicates that structural adaptations affecting the active site properties occur outside from the catalytic cavity. Accordingly, the crystal structure (Aghajari et al. 1998a, b) has been closely inspected to identify structural factors involved in its weak stability, such as those described in the previous section. On this basis, 17 mutants of this enzyme were constructed, each of them bearing an engineered residue forming a weak interaction found in mesophilic α-amylases but absent in the cold-active α-amylase, or a combination of up to six stabilizing structural factors (D'Amico et al. 2001, 2002b, 2003a). As illustrated in Fig. 28, it was found that single amino acid side-chain substitutions can significantly modify the melting point $T_m$ and the calorimetric enthalpy $\Delta H_{cal}$ but also the cooperativity and reversibility of unfolding as well as the thermal inactivation rate constant. Therefore, these mutants of the psychrophilic α-amylase consistently approximate and reproduce the unfolding patterns of the heat-stable enzymes depicted in Fig. 26.

However, in the context of catalysis at low temperatures, the most significant observation was that these mutations tend to decrease both $k_{cat}$ and $K_m$. As shown in Fig. 29, stabilizing the cold-active α-amylase tends to decrease the $k_{cat}$ values and concomitantly the $K_m$ values of the mutant enzymes, revealing the high correlation between both kinetic parameters (illustrated in Fig. 28). In fact, in addition to an engineered mesophilic-like stability, the multiple-mutant bearing six stabilizing structural factors also displays an engineered mesophilic-like activity in terms of alterations in $k_{cat}$ and $K_m$ values and even in thermodynamic parameters of activation (D'Amico et al. 2003a). Considering the various available data on the psychrophilic α-amylase, it can be concluded that the improved molecular motions of the side chains forming the active site (motions responsible for the high activity, the low affinity and heat-lability) originate from the lack of structure-stabilizing interactions in the vicinity or even far from the active site. This is another strong indication that structural flexibility is an essential feature related to catalysis at low temperatures in psychrophilic enzymes.

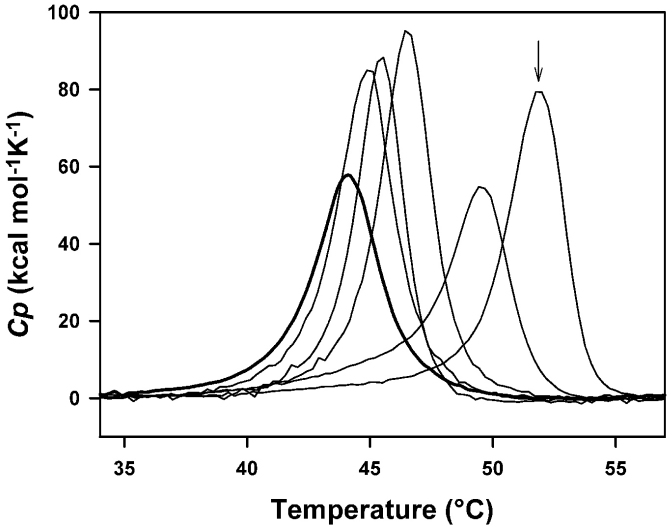


**Fig. 28.** Engineering mesophilic-like stability in mutants of the psychrophilic α-amylase. Structure-stabilizing interactions have been introduced in the heat-labile enzyme (heavy line). As shown by the microcalorimetric thermograms, the resulting mutants (thin lines) display increased melting points (top of the transitions) and calorimetric enthalpies (area below the curves). The most stable mutant (arrow) bears six additional interactions. Adapted from (D'Amico et al. 2001, 2003a)

## 1.15 Psychrophilic Enzymes in Folding Funnels

The various properties of psychrophilic enzymes that have been presented in this chapter can be integrated in a model based on folding funnels (Dinner et al. 2000; Schultz 2000) to describe the activity–stability relationships in extremophilic enzymes. Figure 30 depicts the energy landscapes of psychrophilic and thermophilic enzymes. The top of the funnel is occupied by the unfolded state and having a high free energy (considering the spontaneous folding reaction), whereas the bottom of the funnel is occupied by the stable (low free energy) native state. The height of the funnel, i.e., the free energy of folding, also corresponding to the conformational stability, has been fixed here in a 1–5 ratio according to the stability curves shown in Fig. 27.

The upper edge of the funnels is occupied by the unfolded state in random coil conformations but it should be noted that psychrophilic enzymes tend to have a lower proline content than mesophilic and thermophilic enzymes, a lower number of disulfide bonds and a higher occurrence of glycine clusters (Russell 2000; Smalas et al. 2000; Gianese et al. 2002; Siddiqui and Cavicchioli 2006). Accordingly, the edge of the funnel for the psychrophilic protein is slightly larger (broader distribution of the unfolded state) and is located at a higher energy level. When the polypeptide is allowed to fold, the free energy level decreases, as well as the conformational ensemble. However, thermophilic proteins pass through intermediate states corresponding to local minima of energy. These minima are responsible for the ruggedness of the funnel slopes and for the reduced cooperativity of the folding-unfolding reaction, as demonstrated by heat-induced unfolding (Fig. 26). By contrast, the structural elements of psychrophilic proteins generally unfold cooperatively without intermediates, as a result of

fewer stabilizing interactions and stability domains (Feller et al. 1999; D'Amico et al. 2001; Georlette et al. 2003) and therefore the funnel slopes are steep and smooth. The bottom of the funnel depicts the stability of the native state ensemble.

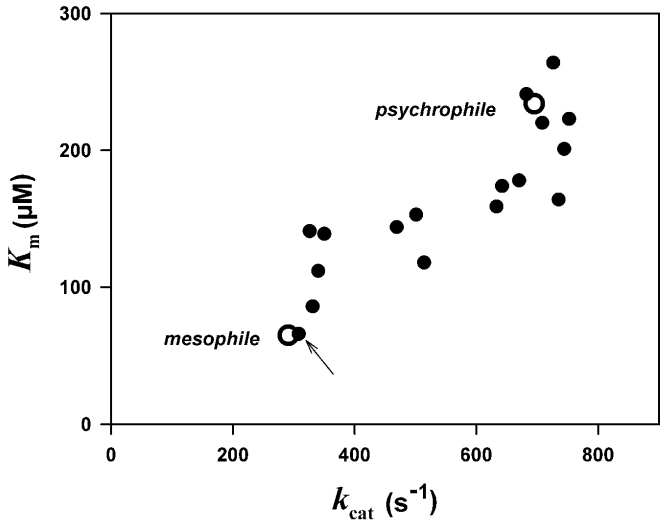


**Fig. 29.** Engineering mesophilic-like activity in mutants of the psychrophilic α-amylase. This plot of the kinetic parameters for the stabilized mutants (filled symbols) shows that the general trend is to decrease the activity and to increase the affinity for the substrate of the wild-type psychrophilic enzyme (open symbol). The most stable mutant bearing six additional interactions (arrow) displays kinetic parameters nearly identical to those of the mesophilic homologue (open symbol). Adapted from (D'Amico et al. 2001, 2003a)

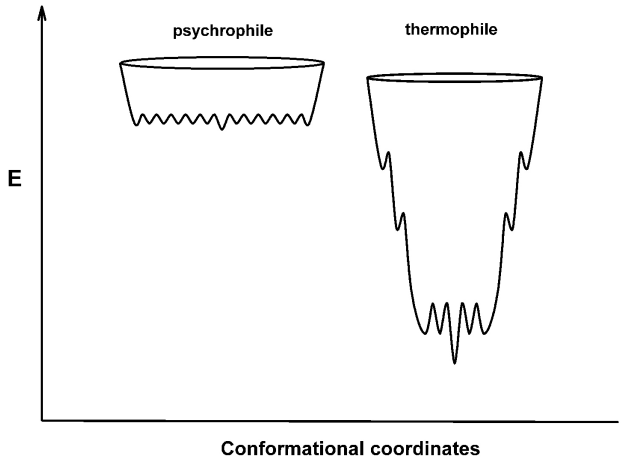


**Fig. 30.** Folding funnel model for extremophilic enzymes. In these schematic energy landscapes, the free energy of folding (E) is depicted as a function of the conformational diversity. The height of the funnels is deduced from the determination of the conformational stabilities. The top of the funnels is occupied by the unfolded states in the numerous random coil conformations, whereas the bottom of the funnels corresponds to native and catalytically active conformations. The ruggedness of the bottom depicts the energy barriers for interconversion, or structural fluctuations of the native state (D'Amico et al. 2003b)

The bottom for a very stable and rigid thermophilic protein can be depicted as a single global minimum or as having only a few minima with high energy barriers between them, whereas the bottom for an unstable and flexible psychrophilic protein is rugged and depicts a large population of conformers with low energy barriers to flip between them. Rigidity of the native state is therefore a direct function of the energy barrier height (Tsai et al. 1999; Kumar et al. 2000) and is drawn here according to the results of fluorescence quenching (Fig. 19) and neutron scattering experiments (Tehei et al. 2004). In this context, the activity–stability relationships in these extremophilic enzymes depend on the bottom properties. Indeed, it has been argued that upon substrate binding to the association-competent sub-population, the equilibrium between all conformers is shifted toward this sub-population, leading to the active conformational ensemble (Tsai et al. 1999; Kumar et al. 2000; Ma et al. 2000; Benkovic et al. 2008). In the case of the rugged bottom of psychrophilic enzymes, this equilibrium shift only requires a modest free energy change (low energy barriers), a low enthalpy change for interconversion of the conformations, but is accompanied by a large entropy change for fluctuations between the wide conformer ensemble. The converse picture holds for ther- mophilic enzymes, in agreement with the activation parameters shown in Table 5 and with the proposed macroscopic interpretation. Such energy landscapes integrate nearly all biochemical and biophysical data currently available for extremophilic enzymes but they will certainly be refined by future investigations of other series of homologous proteins from psychrophiles, mesophiles and thermophiles. This model has nevertheless received support from independent studies (Bjelic et al. 2008; Xie et al. 2009).

# References


Aghajari N, Feller G, Gerday C, Haser R (1998a) Crystal structures of the psychrophilic α-amylase from *Alteromonas haloplanctis* in its native form and complexed with an inhibitor. Protein Sci 7:564–572

Aghajari N, Feller G, Gerday C, Haser R (1998b) Structures of the psychrophilic *Alteromonas haloplanctis* α-amylase give insights into cold adaptation at a molecular level. Structure 6:1503–1516

Aghajari N, Roth M, Haser R (2002) Crystallographic evidence of a transglycosylation reaction: ternary complexes of a psychrophilic alpha-amylase. Biochemistry 41:4273–4280

Aghajari N, Van Petegem F, Villeret V, Chessa JP, Gerday C, Haser R, Van Beeumen J (2003) Crystal structures of a psychrophilic metalloprotease reveal new insights into catalysis by cold-adapted proteases. Proteins 50:636–647

Bae E, Phillips GN Jr (2004) Structures and analysis of highly homologous psychrophilic, mesophilic, and thermophilic adenylate kinases. J Biol Chem 279:28202–28208

Bae E, Phillips GN Jr (2006) Roles of static and dynamic domains in stability and catalysis of adenylate kinase. Proc Natl Acad Sci USA 103:2132–2137

Bell GS, Russell RJ, Connaris H, Hough DW, Danson MJ, Taylor GL (2002) Stepwise adaptations of citrate synthase to survival at life's extremes. From psychrophile to hyperthermophile. Eur J Biochem 269:6250–6260

Benkovic SJ, Hammes GG, Hammes-Schiffer S (2008) Free-energy landscape of enzyme catalysis. Biochemistry 47:3317–3321

Bjelic S, Brandsdal BO, Aqvist J (2008) Cold adaptation of enzyme reaction rates. Biochemistry 47:10049–10057

Brandsdal BO, Smalas AO, Aqvist J (2001) Electrostatic effects play a central role in cold adaptation of trypsin. FEBS Lett 499:171–175

Casanueva A, Tuffin M, Cary C, Cowan DA (2010) Molecular adaptations to psychrophily: the impact of 'omic' technologies. Trends Microbiol 18:374–381

Cherry JR, Lamsa MH, Schneider P, Vind J, Svendsen A, Jones A, Pedersen AH (1999) Directed evolution of a fungal peroxidase. Nat Biotechnol 17:379–384

Chiuri R, Maiorano G, Rizzello A, del Mercato LL, Cingolani R, Rinaldi R, Maffia M, Pompa PP (2009) Exploring local flexibility/rigidity in psychrophilic and mesophilic carbonic anhydrases. Biophys J 96:1586–1596

Claverie P, Vigano C, Ruysschaert JM, Gerday C, Feller G (2003) The precursor of a psychrophilic alpha-amylase: structural characterization and insights into cold adaptation. Biochim Biophys Acta 1649: 119–122

Collins T, Meuwis MA, Gerday C, Feller G (2003) Activity, stability and flexibility in glycosidases adapted to extreme thermal environments. J Mol Biol 328:419–428

D'Amico S, Gerday C, Feller G (2001) Structural determinants of cold adaptation and stability in a large protein. J Biol Chem 276:25791–25796

D'Amico S, Claverie P, Collins T, Georlette D, Gratia E, Hoyoux A, Meuwis MA, Feller G, Gerday C (2002a) Molecular basis of cold adaptation. Philos Trans R Soc Lond B Biol Sci 357:917–925

D'Amico S, Gerday C, Feller G (2002b) Dual effects of an extra disulfide bond on the activity and stability of a cold-adapted alpha-amylase. J Biol Chem 277: 46110–46115

D'Amico S, Gerday C, Feller G (2003a) Temperature adaptation of proteins: engineering mesophilic-like activity and stability in a cold-adapted alpha-amylase. J Mol Biol 332:981–988

D'Amico S, Marx JC, Gerday C, Feller G (2003b) Activity-stability relationships in extremophilic enzymes. J Biol Chem 278:7891–7896

D'Amico S, Collins T, Marx JC, Feller G, Gerday C (2006a) Psychrophilic microorganisms: challenges for life. EMBO Rep 7:385–389

D'Amico S, Sohier JS, Feller G (2006b) Kinetics and energetics of ligand binding determined by microcalorimetry: insights into active site mobility in a psychrophilic alpha-amylase. J Mol Biol 358: 1296–1304

De Vos D, Collins T, Nerinckx W, Savvides SN, Claeyssens M, Gerday C, Feller G, Van Beeumen J (2006) Oligosaccharide binding in family 8 glycosidases: crystal structures of active-site mutants of the beta-1, 4- xylanase pXyl from *Pseudoaltermonas haloplanktis* TAH3a in complex with substrate and product. Biochemistry 45:4797–4807

Dinner AR, Sali A, Smith LJ, Dobson CM, Karplus M (2000) Understanding protein folding via free-energy surfaces from theory and experiment. Trends Biochem Sci 25:331–339

Feller G, Gerday C (2003) Psychrophilic enzymes: hot topics in cold adaptation. Nat Rev Microbiol 1: 200–208

Feller G, D'Amico D, Gerday C (1999) Thermodynamic stability of a cold-active α-amylase from the Antarctic bacterium *Alteromonas haloplanctis*. Biochemistry 38:4613–4619

Fields PA, Somero GN (1998) Hot spots in cold adaptation: localized increases in conformational flexibility in lactate dehydrogenase A(4) orthologs of Antarctic notothenioid fishes. Proc Natl Acad Sci USA 95:11476–11481

Garsoux G, Lamotte J, Gerday C, Feller G (2004) Kinetic and structural optimization to catalysis at low temperatures in a psychrophilic cellulase from the Antarctic bacterium *Pseudoalteromonas haloplanktis* Biochem J 384:247–253

Georlette D, Damien B, Blaise V, Depiereux E, Uversky VN, Gerday C, Feller G (2003) Structural and functional adaptations to extreme temperatures in psychrophilic, mesophilic, and thermophilic DNA ligases. J Biol Chem 278:37015–37023

Gerday C, Glansdorff N (2007) Physiology and biochemistry of extremophiles. ASM Press, Washington

Gianese G, Bossa F, Pascarella S (2002) Comparative structural analysis of psychrophilic and meso- and thermophilic enzymes. Proteins 47:236–249

Giver L, Gershenson A, Freskgard PO, Arnold FH (1998) Directed evolution of a thermostable esterase. Proc Natl Acad Sci USA 95:12809–12813

Gorfe AA, Brandsdal BO, Leiros HK, Helland R, Smalas AO (2000) Electrostatics of mesophilic and psychrophilic trypsin isoenzymes: qualitative evaluation of electrostatic differences at the substrate binding site. Proteins 40:207–217

Kim SY, Hwang KY, Kim SH, Sung HC, Han YS, Cho YJ (1999) Structural basis for cold adaptation. Sequence, biochemical properties, and crystal structure of malate dehydrogenase from a psychrophile *Aquaspirillium arcticum*. J Biol Chem 274: 11761–11767

Kumar S, Nussinov R (2004) Experiment-guided thermodynamic simulations on reversible two-state proteins: implications for protein thermostability. Biophys Chem 111:235–246

Kumar S, Ma B, Tsai CJ, Sinha N, Nussinov R (2000) Folding and binding cascades: dynamic landscapes and population shifts. Protein Sci 9:10–19

Leiros I, Moe E, Lanes O, Smalas AO, Willassen NP (2003) The structure of uracil-DNA glycosylase from Atlantic cod (*Gadus morhua*) reveals cold-adaptation features.

Acta Crystallogr D Biol Crystallogr 59:1357–1365
Lonhienne T, Gerday C, Feller G (2000) Psychrophilic enzymes: revisiting the thermodynamic parameters of activation may explain local flexibility. Biochim Biophys Acta 1543:1–10
Lonhienne T, Zoidakis J, Vorgias CE, Feller G, Gerday C, Bouriotis V (2001) Modular structure, local flexibility and cold-activity of a novel chitobiase from a psychrophilic Antarctic bacterium. J Mol Biol 310:291–297
Ma B, Kumar S, Tsai CJ, Hu Z, Nussinov R (2000) Transition-state ensemble in enzyme catalysis: possibility, reality, or necessity? J Theor Biol 203:383–397
Makhatadze GI, Privalov PL (1995) Energetics of protein structure. Adv Protein Chem 47:307–425
Mandrich L, Pezzullo M, Del Vecchio P, Barone G, Rossi M, Manco G (2004) Analysis of thermal adaptation in the HSL enzyme family. J Mol Biol 335:357–369
Margesin R, Schinner F, Marx JC, Gerday C (2008) Psychrophiles, from biodiversity to biotechnology. Springer, Berlin/Heidelberg
Privalov PL (1990) Cold denaturation of proteins. Crit Rev Biochem Mol Biol 25:281–305
Qian M, Haser R, Buisson G, Duee E, Payan F (1994) The active center of a mammalian alpha-amylase. Structure of the complex of a pancreatic alpha-amylase with a carbohydrate inhibitor refined to 2.2-Å resolution. Biochemistry 33:6284–6294
Russell NJ (2000) Toward a molecular understanding of cold activity of enzymes from psychrophiles. Extremophiles 4:83–90
Russell RJ, Gerike U, Danson MJ, Hough DW, Taylor GL (1998) Structural adaptations of the cold-active citrate synthase from an Antarctic bacterium. Structure 6:351–361
Schultz CP (2000) Illuminating folding intermediates. Nat Struct Biol 7:7–10
Siddiqui KS, Cavicchioli R (2006) Cold-adapted enzymes. Annu Rev Biochem 75:403–433
Siddiqui KS, Feller G, D'Amico S, Gerday C, Giaquinto L, Cavicchioli R (2005) The active site is the least stable structure in the unfolding pathway of a multidomain cold-adapted alpha-amylase. J Bacteriol 187: 6197–6205
Skalova T, Dohnalek J, Spiwok V, Lipovova P, Vondrackova E, Petrokova H, Duskova J, Strnad H, Kralova B, Hasek J (2005) Cold-active beta-galactosidase from *Arthrobacter sp.* C2-2 forms compact 660 kDa hexamers: crystal structure at 1.9 Å resolution. J Mol Biol 353:282–294
Smalas AO, Leiros HK, Os V, Willassen NP (2000) Cold adapted enzymes. Biotechnol Annu Rev 6:1–57
Somero GN (1995) Proteins and temperature. Annu Rev Physiol 57:43–68
Suzuki Y, Takano K, Kanaya S (2005) Stabilities and activities of the N- and C-domains of FKBP22 from a psychrotrophic bacterium overproduced in *Escherichia coli*. FEBS J 272:632–642
Tehei M, Franzetti B, Madern D, Ginzburg M, Ginzburg BZ, Giudici-Orticoni MT, Bruschi M, Zaccai G (2004) Adaptation to extreme environments: macromolecular dynamics in bacteria compared in vivo by neutron scattering. EMBO Rep 5:66–70
Tsai CJ, Ma B, Nussinov R (1999) Folding and binding cascades: shifts in energy landscapes. Proc Natl Acad Sci USA 96:9970–9972
Tsigos I, Velonia K, Smonou I, Bouriotis V (1998) Purification and characterization of an alcohol dehydrogenase from the Antarctic psychrophile *Moraxella sp*. TAE123. Eur J Biochem 254:356–362
Vetriani C, Maeder DL, Tolliday N, Yip KS, Stillman TJ, Britton KL, Rice DW, Klump HH, Robb FT (1998) Protein thermostability above 100 C: a key role for ionic interactions. Proc Natl Acad Sci USA 95:12300–12305
Violot S, Aghajari N, Czjzek M, Feller G, Sonan GK, Gouet P, Gerday C, Haser R, Receveur-Brechot V (2005) Structure of a full length psychrophilic cellulase from *Pseudoalteromonas haloplanktis* revealed by X-ray diffraction and small angle X-ray scattering. J Mol Biol 348:1211–1224
Wintrode PL, Arnold FH (2000) Temperature adaptation of enzymes: lessons from laboratory evolution. Adv Protein Chem 55:161–225
Xie BB, Bian F, Chen XL, He HL, Guo J, Gao X, Zeng YX, Chen B, Zhou BC, Zhang YZ (2009) Cold adaptation of zinc metalloproteases in the thermolysin family from deep sea and arctic sea ice bacteria revealed by catalytic and structural properties and molecular dynamics: new insights into relationship between conformational flexibility and hydrogen bonding. J Biol Chem 284:9257–9269
Xu Y, Feller G, Gerday C, Glansdorff N (2003) Metabolic enzymes from psychrophilic bacteria: challenge of adaptation to low temperatures in ornithine carbamoyltransfase from *Moritella abyssi*. J Bacteriol 185:2161–2168
Yip KS, Stillman TJ, Britton KL, Artymiuk PJ, Baker PJ, Sedelnikova SE, Engel PC, Pasquo A, Chiaraluce R, Consalvi V (1995) The structure of *Pyrococcus furiosus* glutamate dehydrogenase reveals a key role for ion-pair networks in maintaining enzyme stability at extreme temperatures. Structure 3:1147–1158

# Chapitre 2 : Objectifs du travail

L'adaptation aux températures est un sujet clé tant sur un plan fondamental que pour des applications biotechnologiques. Bien que de nombreuses études aient été réalisées dans le domaine, une compréhension fine et générale des mécanismes moléculaires responsables de cette adaptation n'en est qu'à ses débuts. La relation entre les paramètres thermodynamiques de stabilité et les paramètres cinétiques d'activité est aujourd'hui admise mais démontrer le rôle de la flexibilité de la structure protéique en tant que facteur majeur de l'adaptation aux températures n'est pas chose aisée. De même, peu d'études sur l'origine cinétique du repliement/dépliement des protéines extremophiles ont été réalisées.

Durant cette thèse, nous nous sommes donc attachés à déterminer l'origine cinétique de la stabilité de l'α-amylase psychrophile AHA et du gain de stabilité de deux mutants multiples de celle-ci présentant les caractères d'une enzyme mésophile et pouvant donc être considérés comme des intermédiaires dans l'évolution d'une enzyme psychrophile vers une mésophile. De plus nous tenterons de contribuer, par une caractérisation plus poussée, à l'amélioration de la compréhension du mécanisme de "mésophilisation" de ces deux mutants et du rôle joué par les interactions faibles dans l'adaptation thermique des protéines.

Dans un deuxième temps, suite aux récentes avancées en terme de séquençage de génomes et d'identification des protéines sur base de leur structure primaire, nous avons noté l'existence d'α-amylases de type chlorure-dépendantes (initialement découverte uniquement chez les mammifères et *P.haloplanktis*) chez d'autres microorganismes. En plus de présenter les mêmes ligands que les autres α-amylases chlorure-dépendantes, l'une d'entre elles était issue d'un actinomycète thermophile. Nous avions donc pour la première fois la possibilité d'étudier l'adaptation aux températures extrêmes chez une protéine psychrophile AHA, une mésophile PPA et une thermophile, à savoir TFA de *Thermobifida fusca*. Pour affiner davantage notre compréhension de la relation activité-stabilité responsable de l'adaptation aux températures des protéines, nous avons ajouté à ce travail l'α-amylase mésophile DMA de *Drosophila melanogaster*. Ainsi nous couvrions toute la gamme des températures physiologiques des organismes vivants, du psychrophile au thermophile en passant par deux mésophiles, PPA issue d'un organisme homéotherme et DMA issu d'un organisme ectotherme pour comprendre le lien entre la température de l'environnement d'une protéine et ses adaptations moléculaires aux températures.

# Chapitre 3 : Préambule aux résultats

Projet initial et réorientation…

Le titre de mon projet était à l'origine « *Identification des facteurs structuraux responsables de l'activité aux basses températures chez une α-amylase produite par une bactérie psychrophile de l'Antarctique* ». Deux aspects essentiels de l'adaptation de la structure enzymatique aux basses températures y étaient abordés. Premièrement, suivant certains auteurs, l'accroissement de flexibilité, responsable de l'activité élevée, serait localisée (Fields *et al.,* 1998 ; Bae *et al.,* 2006) et concernerait principalement les régions bordant le site actif, la composition de ce dernier étant inchangée afin de maintenir le mécanisme catalytique. Ces régions formeraient un domaine dynamique alors que d'autres régions constitueraient des domaines statiques assurant la stabilité de l'édifice (Bae *et al.,* 2006). Afin de vérifier cette hypothèse, les trois domaines structuraux de l'α-amylase de drosophile, ainsi que des fragments de domaine, devaient être remplacés par les domaines correspondants de l'α-amylase psychrophile.

D'autres observations indiquaient qu'une mobilité accrue de l'ensemble de la structure protéique est nécessaire afin de promouvoir la dynamique du site actif (Aghajari *et al.,* 1998; D'Amico *et al.,* 2001; Závodszky *et al.,* 1998). Dans ce contexte, diverses interactions faibles, ainsi que des facteurs structuraux, stabilisant l'α-amylase de drosophile devaient être éliminés par mutagenèse dirigée sur base de l'absence de ces interactions et facteurs observée chez l'enzyme psychrophile.

On notera que les deux hypothèses mentionnées ci-dessus ne sont pas mutuellement exclusives. L'approche proposée devait permettre d'affiner notre compréhension des adaptations moléculaires à la température, et d'aboutir *in fine* au transfert des propriétés psychrophiles à une enzyme mésophile.

Pour initier ce projet, les méthodes de production et de purification de l'α-amylase de drosophile, DMA, ont été établies et l'enzyme a été caractérisée. De plus, ces productions ont permis la résolution de la structure cristallographique de DMA (N. Aghajari, CNRS, Lyon, communication personnelle).

Nous avons ensuite entamé la construction et la production des divers mutants et chimères. Malheureusement, la construction des chimères par remplacement de domaines mésophiles (DMA) par leurs équivalents psychrophiles (AHA) et la suppression d'interactions faibles et de facteurs stabilisants sur l' α-amylase mésophiles (DMA) ont abouti à des problèmes de production avec la formation de corps d'inclusion. Dès les premiers signes de la formation de ces corps d'inclusion, nous avons initié en parallèle la production, sous forme recombinante chez *E.coli*, de l'α-amylase de porc PPA puisque celle-ci avait été utilisée comme modèle mésophile pour de précédentes études (D'Amico *et al.,* 2003a). Cependant, ici aussi, la production de PPA a conduit à la formation de corps d'inclusion. Face à ces problèmes, nous avons tenté de solubiliser ces corps d'inclusion par des tests de dénaturation/renaturation au chlorure de guanidinium, par l'utilisation de kits (ex : « Protein refolding kit » de Novagen), en variant les conditions de production (températures de 15, 18, 25 et

37°C ; milieux de cultures différents (LB, TB, …) ; inductions à des $A_{600}$ variables ; diverses souches d'*E.coli* (Rosetta, KRX) ainsi que l'utilisation des vecteurs pCold DNA-I et pUC-12). Que ce soit dans le cas des chimères, de mutants ponctuels ou de PPA, il n'a pas été possible de produire d'enzyme repliée et active.

A ce stade, il était donc nécessaire de revoir le projet et de le réorienter avec l'approbation du comité de thèse. Nous avons opté pour une approche qui n'avait pas encore été envisagée dans l'étude de l'adaptation thermique des protéines, à savoir déterminer l'origine cinétique du gain de stabilité d'une enzyme psychrophile vers une enzyme "mésophilisée". Les résultats de ce travail sont décrits dans le chapitre 3 : section I et publiés dans « *Journal of Biological Chemistry*».

Durant ce travail, nous avons noté, grâce à l'article de Da Lage *et al*., 2004, l'existence d'une α-amylase thermophile de *Thermobifida fusca*, TFA. Il nous est donc apparu opportun de tenter de produire cette enzyme thermophile chlorure-dépendante. Ceci nous permettrait pour la première fois, de comparer l'activité et la stabilité d'homologues d'α-amylases psychrophile AHA, mésophile ectotherme DMA, mésophile homéotherme PPA et thermophile TFA. Ces résultats sont décrits dans le chapitre 3 : section II et sont sous presse dans la revue « Biochimie ».

# Chapitre 3 : Résultats

## *Section I: Stepwise adaptations to low temperature as revealed by multiple mutants of a psychrophilic α-amylase from an Antarctic bacterium.*

**(J. Biol. Chem., *2011*. 286(44): 38348-38355)**

# Stepwise adaptations to low temperature as revealed by multiple mutants of a psychrophilic α-amylase from an Antarctic bacterium*

**Alexandre Cipolla**[‡], Salvino D'Amico[‡], Roya Barumandzadeh[§], André Matagne[§] and Georges Feller[‡1]

[‡] From the Laboratory of Biochemistry and [§]the Laboratory of Enzymology and Protein Folding, Centre for Protein Engineering, University of Liège, B-4000 Liège-Sart Tilman, Belgium

## SYNOPSIS

The mutants Mut5 and Mut5CC from a psychrophilic α-amylase bear representative stabilizing interactions found in the heat-stable porcine pancreatic α-amylase but lacking in the cold-active enzyme from an Antarctic bacterium. From an evolutionary perspective, these mutants can be regarded as structural intermediates between the psychrophilic and the mesophilic enzymes. We found that these engineered interactions improve all the investigated parameters related to protein stability: the compactness, the kinetically-driven stability, the thermodynamic stability, the resistance towards chemical denaturation and the kinetics of unfolding/refolding. Concomitantly to this improved stability, both mutants have lost the kinetic optimization to low temperature activity displayed by the parent psychrophilic enzyme. These results provide strong experimental support to the hypothesis assuming that the disappearance of stabilizing interactions in psychrophilic enzymes increases the amplitude of concerted motions required by catalysis and the dynamics of active site residues at low temperature, leading to a higher activity.

## ABBREVIATIONS

AHA, α-amylase from *Pseudoalteromonas haloplanktis*

PPA, α-amylase from pig pancreas

Mops, 3-morpholinopropanesulfonic acid

DSC, differential scanning calorimetry

NDSB, nondetergent sulfobetaine

GdmCl, guanidinium chloride

# INTRODUCTION

One frequently overlooks that over 80% of the Earth's biosphere is permanently cold (1) but also that these cold biotopes have been successfully colonized by diverse organisms. Psychrophiles are such cold-adapted organisms thriving permanently at temperatures close to 0°C and found for instance in Antarctica, the Arctic regions, deep-sea water and sediments or in the permafrost. They include a large range of representatives from all three domains (*Bacteria*, *Archaea*, *Eukarya*) and are the most abundant extremophiles in terms of biomass, diversity and distribution (2,3). The observation of metabolically active bacteria at -20°C in the brine veins between sea-ice crystals illustrates the remarkable adaptations of psychrophiles (4).

Amongst the numerous adverse effects of low temperature on the cell (1, 5, 6), the major constraint is exerted on enzyme activity, which is exponentially reduced by temperature decreases. In psychrophiles, this constraint is alleviated by the synthesis of cold-active enzymes in order to maintain metabolic fluxes compatible with life. The prevailing hypothesis assumes that cold-adapted enzymes have acquired a high catalytic activity at low temperature by improving their conformational flexibility at the expense of stability (7-10). It has been shown that the crystal structure of psychrophilic enzymes is characterized by the disappearance of various non-covalent stabilizing interactions, resulting in both an improved dynamics of the enzyme conformation and in a weak stability (11-17). There is indeed a clear decrease in the number and strength of all known weak interactions and structural factors involved in protein stability, from thermophiles, mesophiles to psychrophiles (17- 19).

The heat-labile α-amylase (AHA)[1] from the Antarctic bacterium *Pseudoalteromonas haloplanktis* (18) is the best characterized psychrophilic enzyme. It displays striking sequence and structure similarities with its mesophilic homologue from pig pancreas (PPA) (11,21-23). For instance, all 24 residues forming the catalytic cleft (Fig.1) and involved in substrate binding are strictly conserved in both the psychrophilic and the mesophilic homologues (11,24). This outstanding example of active site identity demonstrates that cold activity is reached without any amino acid substitution in the reaction center. As a consequence, changes occurring elsewhere in the molecule are responsible for the optimization of the catalytic parameters at low temperature, by adjustments of the active site residue dynamics. In order to probe the activity-flexibility-stability hypothesis, numerous mutants of AHA have been constructed, each bearing additional weak interactions mediated by the replacement of a specific residue, as well as a disulfide bond as found in PPA. It has been shown that single amino acid side chain substitutions significantly modify the stability parameters, the cooperativity and reversibility of unfolding, the thermal inactivation rate constant and the kinetic parameters $k_{cat}$ and $K_m$ (25-27). Here we report the activity and mainly the stability properties of two stabilized multiple mutants (Fig. 1 and Fig.2) of the heat-labile α-amylase AHA: Mut5, bearing five mutations and Mut5CC, also bearing an extra disulfide bond specific to α-amylases from warm-blooded animals (28). The five mutations

shared by both multiple mutants have been selected on the basis of the DSC thermograms of single mutants (25) that showed a global stabilization of the protein (higher melting point $T_m$ and calorimetric enthalpy $\Delta H_{cal}$), without evidence for local destabilization (identical or higher temperature of transition start). The lack of interferences between individual mutations, modeled in the crystal structure of AHA, was also checked. These multiple mutants provide clear insights into the structure-function relationships allowing psychrophilic enzymes to fulfill their biochemical functions at low temperatures.

```
AHA          --------TPTTFVHLFEWNWQDVAQECEQYLGPKGYAAVQVSPPNEHITGS----QWWT  48
Mut5         --------TPTTFVHLFEWNWQDVAQECEQYLGPKGYAAVQVSPPNEHITGS----QWWT  48
Mut5CC       --------TPTTFVHLFEWNWQDVAQECEQYLGPKGYAAVQVSPPNEHITGS----QWWT  48
PPA          QYAPQTQSGRTSIVHLFEWRWVDIALECERYLGPKGFGGVQVSPPNENIVVTNPSRPWWE  60

AHA          RYQPVSYELQSRGGNRAQFIDMVNRCSAAGVDIYVDTLINHMA---AGSGTGT-AGNSFG 104
Mut5         RYQPVSYELQSRGGNRAQFIDMVNRCSAAGVDIYVDTLINHMA---AGSGTGT-AGNSFG 104
Mut5CC       RYQPVSYELCSRGGNRAQFIDMVNRCSAAGVDIYVDTLINHMA---AGSGTGT-CGNSFG 104
PPA          RYQPVSYKLCTRSGNENEFRDMVTRCNNVGVRIYVDAVINHMCGSGAAAGTGTTCG-SYC 119

AHA          N---KSFP--IYSPQDFHES-CTINNS--DYGNDRYRVQNCELVGLADLDTASNYVQNTI 156
Mut5         N---KSFP--IYSPQDFHES-CTINNS--DYGNDRYRVQNCELVGLADLDTASDYVQNTI 156
Mut5CC       N---KSFP--IYSPQDFHES-CTINNS--DYGNDRYRVQNCELVGLADLDTASDYVQNTI 156
PPA          NPGNREFPAVPYSAWDFNDGKCKTASGGIESYNDPYQVRDCQLVGLLDLALEKDYVRSMI 179

AHA          AAYINDLQAIGVKGFRFDASKHVAASDIQSLMAKVN---------GS-PVVFQEVIDQGG 206
Mut5         AAYINDLIAIGVKGFRFDASKHVAASDIQSLMAKVN---------GS-PFVFQEVIDQGG 206
Mut5CC       AAYINDLIAIGVKGFRFDASKHVAASDIQSLMAKVN---------GS-PFVFQEVIDQGG 206
PPA          ADYLNKLIDIGVAGFRIDASKHMWPGDIKAVLDKLHNLNTNWFPAGSRPFIFQEVIDLGG 239

AHA          EAVGASEYLSTGLVTEFKYSTELGNTFRNGS---LAWLSNFGEGWGFMPSSSAVVFVDNH 263
Mut5         EAVGASEYLSTGLVTEFKYSTELGNVFRNGS---LAWLSNFGEGWGFMPSSSAVVFVDNH 263
Mut5CC       EAVGASEYLSTGLVTEFKYSTELGNVFRNGS---LAWLSNFGEGWGFMPSSSAVVFVDNH 263
PPA          EAIQSSEYFGNGRVTEFKYGAKLGTVVRKWSGEKMSYLKNWGEGWGFMPSDRALVFVDNH 299

AHA          DNQRGHGGAGN-VI-TFEDGRLYDLANVFMLAYPYGYPKVMSSYDF----HGDTDA---- 313
Mut5         DNQRGHGGAGN-VI-TFEDGRLYDLANVFMLAYPYGYPRVMSSYDF----HGDTDA---- 313
Mut5CC       DNQRGHGGAGN-VI-TFEDGRLYDLANVFMLAYPYGYPRVMSSYDF----HGDTDA---- 313
PPA          DNQRGHG-AGGASILTFWDARLYKVAVGFMLAHPYGFTRVMSSYRWARNFVNGQDVNDWI 358

AHA          GGPNVPVHN-----NGNLECFASNWKCEHRWSYIAGGVDFRNNTADNWAVTNWWDNTNNQ 368
Mut5         GGPNVPVHN-----NGNLECFASNWKCEHRWSYIAGGVDFRNNTADNWAVTNWWDNTNNQ 368
Mut5CC       GGPNVPVHN-----NGNLECFASNWKCEHRWSYIAGGVDFRNNTADNWAVTNWWDNTNNQ 368
PPA          GPPNNNGVIKEVTINADTTC-GNDWVCEHRWRQIRNMVWFRN-VVDGQPFANWWANGSNQ 416

AHA          ISFGRGSSGHMAINKEDSTLTATVQTDMASGQYCNVLKGELSADAKSCSGEVITVNSDGT 428
Mut5         ISFGRGSSGHMAINKEDSTLTATVQTDMASGQYCNVLKGELSADAKSCSGEVITVNSDGT 428
Mut5CC       ISFGRGSSGHMAINKEDSTLTATVQTDMASGQYCNVLKGELSADAKSCSGEVITVNSDGT 428
PPA          VAFGRGNRGFIVFNNDDWQLSSTLQTGLPGGTYCDVISGDKVG--NSCTGIKVYVSSDGT 474

AHA          INLNIG--AWD-AMAIHKNAKLNTSSAS 453
Mut5         INLNIG--AWD-AMAIHKNAKLNTSSAS 453
Mut5CC       INLNIG--AWD-AMAIHKNAKLNTSSAS 453
PPA          AQFSISNSAEDPFIAIHAESKL------ 496
```

**Fig. 1**. Sequence alignment of the psychrophilic AHA, its multiple mutants Mut5 and Mut5CC, and of the mesophilic PPA. The mutations engineered in Mut5 and in Mut5CC are shown in red. The 24 conserved residues forming the active site cleft are shown in blue.

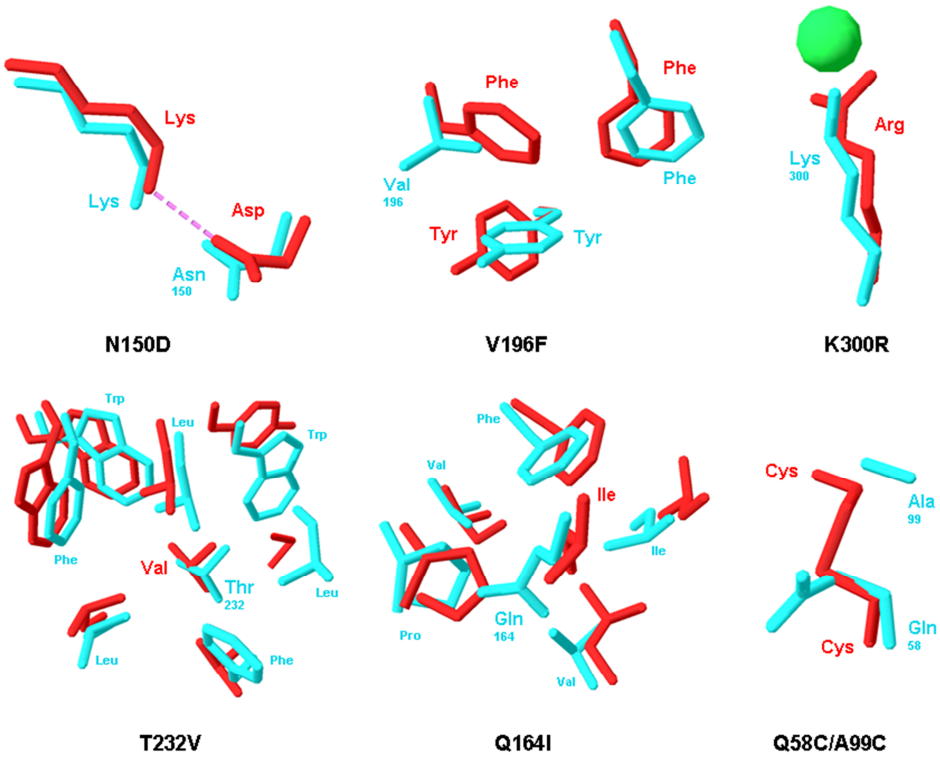


**Fig. 2.** Mutations engineered in the psychrophilic alpha-amylase AHA (blue) based on the structure of the mesophilic homologue PPA (red). The mutation N150D introduces a salt bridge with the corresponding Lys side chain. V196F restores a triple face-to edge aromatic interaction. K300R provides a bidentate coordination of the chloride ion. T232V and Q164I increase the apolarity of hydrophobic core clusters (only AHA side chains are labeled for clarity) and the double mutation Q58C/A99C creates a disulfide bond. PDB coordinates for AHA (1AQH) and for PPA (1PPI).

# EXPERIMENTAL PROCEDURES

***Mutagenesis and protein purification***

The multiple mutants Mut5 and Mut5CC were constructed by combining restriction fragments of the single mutants and by reverse PCR as described (25). The recombinant AHA, Mut5 and Mut5CC were expressed in *E. coli* at 18°C and purified by DEAE-agarose, Sephadex G-100 and Ultrogel AcA54 column chromatography, as described previously (25). The following parameters were used for calculation: AHA (49 343.1 Da), Mut5 (49 403.2 Da) and Mut5CC (49 410.3 Da) on 453 aa.

***Enzyme assays***

α-Amylase activity was recorded using 3.5 mM 4-nitrophenyl-α-D-maltoheptaoside-4,6-O-ethylidene as substrate and by the dinitrosalicylic acid method using 1% soluble starch as substrate (25). Microcalorimetric determination of activity towards various polysaccharides and maltooligosaccharides was performed using an isothermal titration calorimeter as described (29).

***Differential scanning calorimetry***

Measurements were performed using a MicroCal VP-DSC instrument at a scan rate of 60 K $h^{-1}$ and under ~25 psi positive cell pressure. Samples (~2mg/ml) were dialyzed overnight against 30mM MOPS, 50mM NaCl, 1mM $CaCl_2$, pH 7.2 and, when required, were brought to 1 M 3-(1-pyridinio)-1-propanesulfonate (*i.e.* a nondetergent sulfobetaine) as detailed (30). Thermograms of enzyme-acarbose complexes were recorded in the presence of 1 mM acarbose (Bayer). Thermograms were analyzed according to a non-two-state model in which the melting point $T_m$, the calorimetric enthalpy $\Delta H_{cal}$ and the van't Hoff enthalpy $\Delta H_{eff}$ of individual transitions are fitted independently using the MicroCal Origin software (version 7). The magnitude and source of the errors in the $T_m$ and enthalpy values have been discussed elsewhere (31).

Kinetically driven unfolding was recorded without nondetergent sulfobetaine addition and the rate constant $k_{u,i}$ was calculated from the relation (32):

$$k_{u,i} = v\, C_p / \Delta_{cal} - \Delta(T) \qquad \text{(Eq. 1)}$$

where $v$ is the scan rate (K $s^{-1}$), $C_p$ is the excess heat capacity at a temperature $T$, $\Delta_{cal}$ is the total heat of the process and $\Delta(T)$ is the heat evolved at a given temperature $T$.

***Unfolding recorded by intrinsic fluorescence***

Heat-induced unfolding was recorded using an SML-AMINCO Model 8100 spectrofluorometer (Spectronic Instruments) at an excitation wavelength of 280 nm and at an emission wavelength of 350 nm (22). GdmCl-induced unfolding was monitored at 20°C after overnight incubation of the samples at this temperature in 30 mM MOPS, 50 mM NaCl, 1 mM $CaCl_2$, pH 7.2 on a Perkin-Elmer LS50B

spectrofluorometer (22). The equilibrium condition was ascertained by recording unfolding as a function of time. Last-squares analysis of $\Delta G°$ values as a function of GdmCl concentrations allowed estimating the conformational stability in the absence of denaturant, $\Delta G°H_2O$, according to:

$$\Delta G° = \Delta G°H_2O - m\,[\text{GdmCl}] \qquad \text{(Eq. 2)}$$

*Dynamic quenching of fluorescence* - The acrylamide-dependent quenching of intrinsic protein fluorescence was monitored as described (22). The Stern-Volmer quenching constants $K_{SV}$ were calculated according to the relation:

$$F/F_0 = 1 + K_{SV}\,[\text{Q}] \qquad \text{(Eq. 3)}$$

where $F$ and $F_0$ are the fluorescence intensity in the presence and absence of molar concentration of the quencher Q, respectively (33).

***Kinetics of unfolding and refolding***

All kinetic experiments were performed using a Bio-Logic (Claix, France) SFM-3 stopped-flow, coupled with a MOS-200 spectrophotometer and a MPS-51 power supply. Temperature was maintained at 15°C by a Julabo F30-C thermostated bath. Fluorescence measurements were performed using a 1.5 mm pathlength cell (FC-15) and the dead time of the apparatus was found to be ~ 10ms under all experimental settings. This value was estimated by monitoring the fluorescence of the reduction of dichlorophenolindophenol by ascorbic acid, as described by the manufacturer. All experiments were performed in 30 mM MOPS, 50 mM NaCl, 1 mM $CaCl_2$, pH 7.2, using a protein final concentration of 0.1 mg $mL^{-1}$ (~2 µM). To initiate refolding reactions, unfolded α-amylase (1 mg $mL^{-1}$) in 3 M GdmCl was diluted 10-fold with aqueous buffer or with GdmCl solutions of varying concentrations to give the desired final concentrations of GdmCl. Conversely, unfolding reactions were initiated by an 10-fold dilution of native α-amylase with the same buffer containing various amounts of GdmCl, to yield final concentrations ranging from 0.3 to 0.9 M, 0.3 to 1.1 M and 0.3 to 1.25 M, for AHA, Mut5 and Mut5CC, respectively. Unfolding and refolding kinetics were followed by intrinsic fluorescence with an excitation wavelength of 280 nm and total emission above 320 nm was monitored using a high-pass filter. For each experiment, 7000 data points were sampled over the entire time-course.

Kinetic traces resulting from the accumulation of five identical experiments were analyzed according to the sum of two exponential terms (Eq. 4) in the case of refolding and to a simple exponential term (Eq. 5) in the case of unfolding.

$$y_t = y_\infty + A_1 \cdot \exp(-k_1 \cdot t) + A_2 \cdot \exp(-k_2 \cdot t) \qquad \text{(Eq. 4)}$$

$$y_t = y_\infty + A \cdot \exp(-k \cdot t) \qquad \text{(Eq. 5)}$$

Where $y_t$ is the intensity of fluorescence at time $t$, $y_\infty$ is the signal value for an infinite time, $A$ is the amplitude of the signal associated with rate constant $k$. The data sets were averaged to obtain the rate constant and errors were calculated as standard deviations.

The dependence of unfolding and refolding rate constants on denaturant concentration was analyzed according to the following linear relationship (34, 35):

$$\ln(k_{obs}) = \ln(k_f^{H_2O} . \exp(-(m_{kf}/RT) . [\text{GdmCl}]) + k_u^{H_2O} . \exp((m_{ku}/RT) . [\text{GdmCl}])) \quad \text{(Eq. 6)}$$

where $k_{obs}$ is the rate of unfolding or refolding measured at various GdmCl concentrations, $k_f^{H_2O}$ and $k_u^{H_2O}$ are the values for folding and unfolding rates, respectively, in the absence of denaturant, and $m_{kf}/RT$ and $m_{ku}/RT$ are proportionality constants, which describes the denaturant dependence. The programs Bio-Kine 32 V4.51 was used for non-linear least-squares analysis of the data.

# RESULTS AND DISCUSSION

### *Activity of the mutants Mut5 and Mut5CC*

The effects of the single, double and combined mutations on activity towards a chromogenic substrate were described previously (25-27) and are summarized in Fig. 3. The general trend of the mutations combined to create both multiple mutants is to decrease $k_{cat}$ and $K_m$ concomitantly. Furthermore, a mesophilic-like activity was engineered in the multiple mutants Mut5 and Mut5CC as both kinetic parameters are similar to those recorded for the mesophilic homologue PPA.

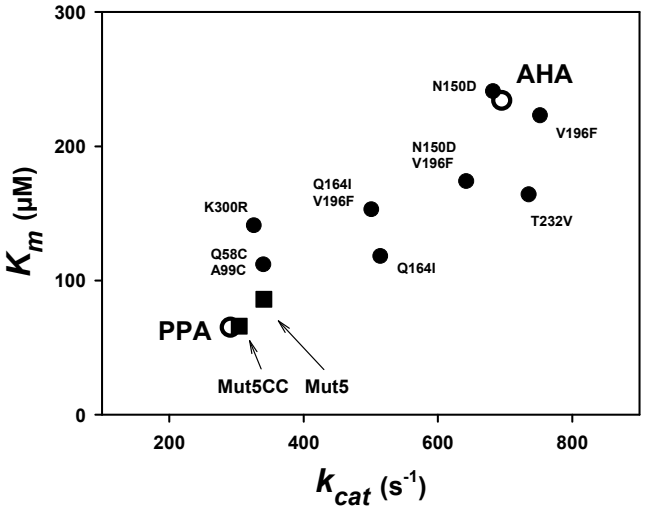


**Fig. 3.** Correlation of the kinetic parameters $k_{cat}$ and $K_m$ in the psychrophilic AHA, the mesophilic PPA (open symbols) and in single and multiple mutants of AHA. Activity towards the chromogenic substrate Et-G7-NP at 25°C. Data from (25-27).

The specificity of both mutants for various polysaccharides was further investigated by microcalorimetry. Table 1 reports the relative activities of the α-amylases, taking soluble starch, the natural substrate, as a reference. Interestingly, the specificity profile of Mut5 and Mut5CC closely follows that of the parent AHA, indicating that the mode of interaction with these polysaccharides has not been modified. By contrast, comparison of the absolute catalytic constants $k_{cat}$ shows that the activity of the mutants is similar to that of the mesophilic homologue, revealing a less efficient active site.

**Table 1**. Relative activity and catalytic constant of Mut5 and Mut5CC on various polysaccharides recorded by microcalorimetry at 25°C.

| Substrate | Relative activity (%) | | | | $k_{cat}$ ($s^{-1}$) | | | |
|---|---|---|---|---|---|---|---|---|
| | AHA | Mut5 | Mut5CC | PPA[a] | AHA | Mut5 | Mut5CC | PPA[a] |
| Starch | 100 | 100 | 100 | 100 | 663 | 352 | 314 | 327 |
| Amylopectin | 96 | 94 | 90 | 68 | 636 | 331 | 283 | 222 |
| Dextrin | 108 | 111 | 112 | 95 | 716 | 391 | 352 | 311 |
| Glycogen | 74 | 73 | 71 | 59 | 491 | 257 | 223 | 193 |
| Maltopentaose | 69 | 50 | 48 | 145 | 457 | 176 | 151 | 474 |
| Et-G7-NP | 105 | 97 | 97 | 101 | 642 | 341 | 304 | 330 |

[a] data from (29)

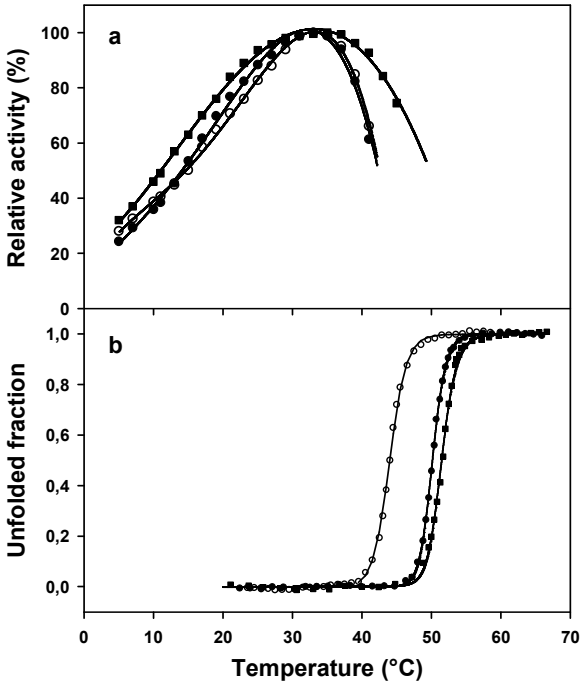


**Fig. 4.** Temperature dependence of activity (a) and heat-induced unfolding recorded by fluorescence (b). Data for the psychrophilic AHA (○), the multiple mutants Mut5 (●) and Mut5CC (■) and the mesophilic PPA (▲, data from (22) and (44)). Activity towards starch as substrate. All experiments were performed at similar protein concentrations (5-40 µg/ml).

Fig. 4b illustrates the increased stability of both multiple mutants as probed by their heat-induced unfolding recorded by intrinsic fluorescence. Despites their higher thermal stability, there was no significant differences in the apparent optimal temperature for activity, which is recorded near 35°C (Fig. 4a). However, Mut5CC displayed a marked protection against heat inactivation at the upper temperatures. This indicates that the disulfide bond bridging the domains forming the active site cleft contributes to thermal stability of activity in the mesophilic homologue PPA. It should be noted that thermal inactivation above 35°C (Fig. 4a) is recorded before any detectable structural change (Fig. 4b). As a result, the active site remains the most heat-labile structural element in both mutants.

### *Dynamic fluorescence quenching*

Determination of molecular flexibility requires the definition of the types and amplitudes of atomic motions as well as a timescale for these motions. In this respect, dynamic fluorescence quenching usefully averages most of these parameters into a single signal (33). The structural permeability of the enzymes was investigated by dynamic fluorescence quenching of aromatic residues (dominated by 12 tryptophan residues in AHA and its mutants) by acrylamide. The individual Stern-Volmer plots for AHA and its multiple mutants at 4 and 30°C are provided in the Fig.6 and the difference between the slopes of the Stern-Volmer plots at 30 and 4°C were used to illustrate the difference in structural permeability of the enzymes with an increase in temperature (Fig. 5). The lower slope for Mut5 and Mut5CC indicates a reduced accessibility of aromatic residues relative to AHA, arising from a lower permeability of the mutant structures to the small quencher molecule. This reveals a more compact conformation undergoing reduced micro-unfolding events of the native state and shorter native state fluctuations for both mutants. The flexibility of these proteins and of the mesophilic homologue also correlates with their difference in stability (*i.e.* AHA<Mut5<Mut5CC<PPA).

**Fig. 5**

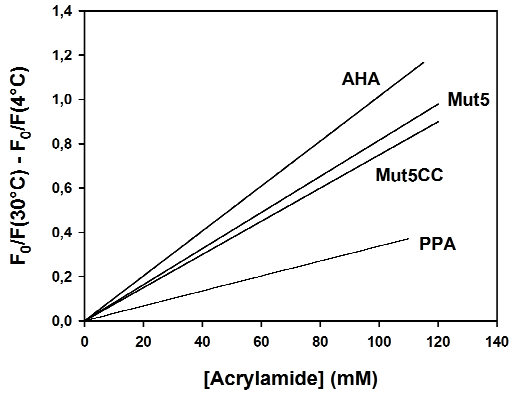


**Fig. 5.** Variation of fluorescence quenching by acrylamide between 4°C and 30°C. Graph constructed by subtracting the regression lines of Stern-Volmer plots at individual temperatures, as shown in Fig. 6. Data for the mesophilic PPA (22) in a similar temperature interval.

**Fig. 6**

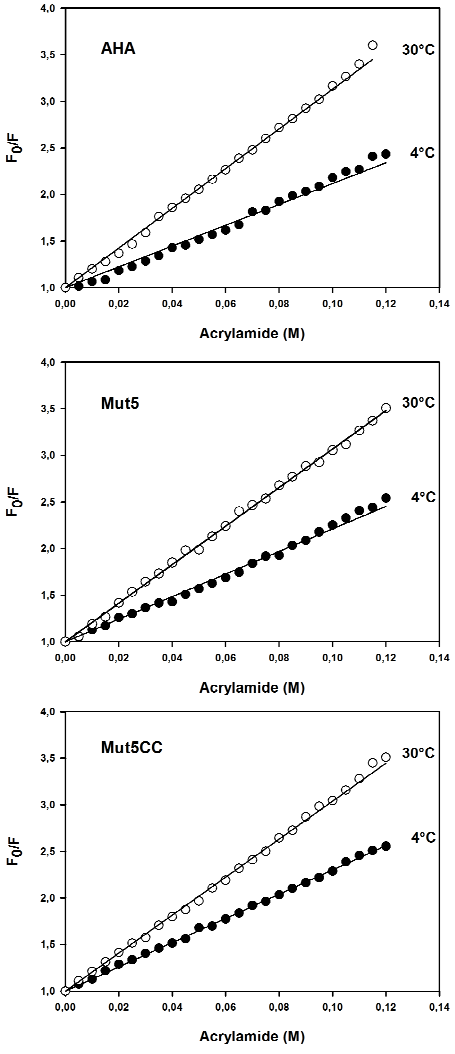


**Fig. 6.** Stern-Volmer plots of fluorescence quenching by acrylamide. The quenching constant $K_{SV}$ values corresponding to the plot slope are 11.7, 12.1 and 13.0 $M^{-1}$ at 4°C and 21.3, 20.7 and 20.4 $M^{-1}$ at 30°C for AHA, Mut5 and Mut5CC, respectively.

***Irreversible unfolding of the stabilized mutants***

Fig. 7 illustrates the correlation between stability of the activity and unfolding reversibility in single and multiple mutants. With the noticeable exception of the disulfide-containing mutant (26), the general trend of the mutations was to protect against heat inactivation but to decrease concomitantly the unfolding reversibility (25). In this respect, both multiple mutants Mut5 and Mut5CC also display mesophilic-like properties.

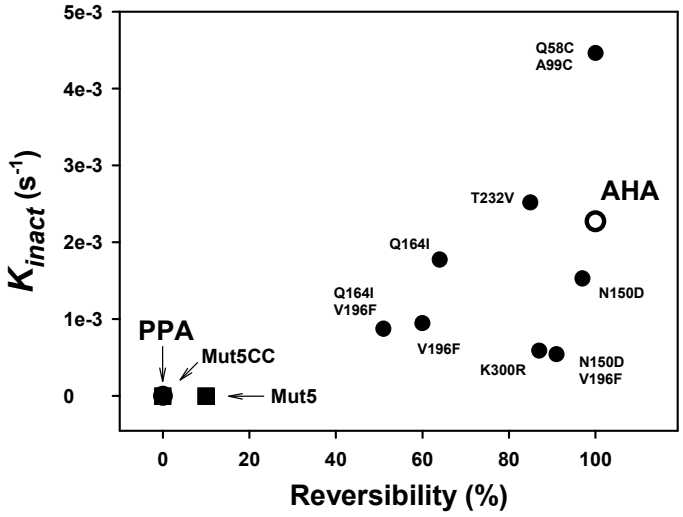


**Fig. 7.** Correlation of stability parameters in the psychrophilic AHA, the mesophilic PPA (open symbols) and in single and multiple mutants of AHA. $k_{inact}$ is the first order rate constant for activity decay at 45°C and unfolding reversibility was calculated from two consecutive DSC scans.

According to the pronounced unfolding irreversibility of both Mut5 and Mut5CC mutants shown in Fig. 7, the kinetically-driven stability was analyzed by DSC in order to determine the rate constant for heat-induced irreversible unfolding, $k_{u,i}$ (32). Such kinetic analysis is not possible for AHA (fully reversible unfolding) and data were obtained from its mutant N12R. The latter displays the same microcalorimetric properties than AHA but only 30% denaturation reversibility (25), ensuring that unfolding is kinetically driven. The temperature dependence of $k_{u,i}$ is shown as an Arrhenius plot in Fig. 8 and the corresponding activation parameters are provided in Table 2.

At an identical temperature of 316 K (43°C), the rate constants for irreversible unfolding differ by several orders of magnitude, which correspond to higher activation energy barriers $\Delta G^*$ in the stabilized mutants (Table 2). Both mutants also display reduced activation enthalpy $\Delta H^*$ as calculated from the slope of the plot in Fig. 8. This mainly reflects a lower temperature dependence of irreversible unfolding and therefore a larger resistance towards unfolding in a given temperature interval, as compared with the parent protein AHA. The lower activation enthalpy value of Mut5 (Table 2) arises from its broader DSC endotherm (see Fig. 10). The weaker entropic contribution in both mutants can be tentatively explained by a less disordered transition state. In other words, the

stabilized mutants would resist against unfolding (before irreversible denaturation) to a larger extent as compared with AHA. As also shown in Fig. 8, PPA unfolds at higher temperatures, which preclude direct comparison. Nevertheless, it is worth noting that Mut5CC tends towards the behavior of PPA in terms of temperature interval for irreversible unfolding and $\Delta H^*$ (slope of the plot).

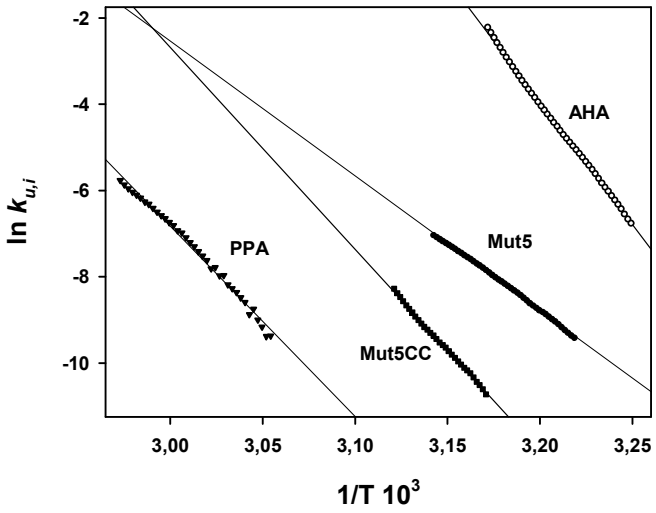


**Fig. 8.** Arrhenius plot of the rate constant for heat-induced irreversible unfolding, $k_{u,i}$. Data were derived from irreversible DSC endotherms according to (32) and Eq. 1.

**Table 2.** Thermodynamic parameters for heat-induced irreversible unfolding of AHA and its stabilized mutants at 316 K (43°C).

| Protein | $k_{u,i}$ $s^{-1}$ | $\Delta G^*$ kcal $mol^{-1}$ | $\Delta H^*$ kcal $mol^{-1}$ | $T\Delta S^*$ kcal $mol^{-1}$ |
|---|---|---|---|---|
| $AHA_{N12R}$ | $1.8\ 10^{-1}$ | 19.6 | 112 | 92 |
| Mut5 | $4.6\ 10^{-4}$ | 23.3 | 61 | 38 |
| Mut5CC | $3.1\ 10^{-5}$ | 25.0 | 92 | 67 |

### *Thermodynamic stability recorded by DSC*

Although heat-induced unfolding of both mutants was irreversible under standard microcalorimetric conditions, we found that addition of the nondetergent sulfobetaine (NDSB) 3-(1-pyridinio)-1-propanesulfonate promotes full unfolding reversibility as illustrated in the Fig. 9. This compound has been reported to protect unfolded proteins from nonspecific interactions by both charge-screening and hydrophobic-screening effects (30, 36, 37). Such reversibility of the heat-induced unfolding reaction allowed to re-investigate the thermodynamic stability (reversible reaction characterized by an equilibrium constant) of Mut5 and Mut5CC, assuming that NDSB does not alter the unfolding parameters, as already demonstrated for the parent enzyme AHA (36). Fig. 10 illustrates the normalized DSC thermograms. The thermodynamic parameters of unfolding derived from reversible

DSC endotherms are close to those previously obtained under non-reversible conditions (27). As shown in Table 3, the improved stability of both mutants is characterized by greater melting points $T_m$ and calorimetric enthalpies $\Delta H_{cal}$. This indicates a significant contribution of the engineered interactions in the enthalpic stability of the protein. Furthermore, the stability curves (Fig. 11) obtained by plotting the Gibbs free energy of unfolding, *i. e.* the work required to disrupt the native state at any temperature (38), clearly illustrate the stability increases brought by the mutations, with, in the case of Mut5CC, values approaching those of the mesophilic homologue PPA.

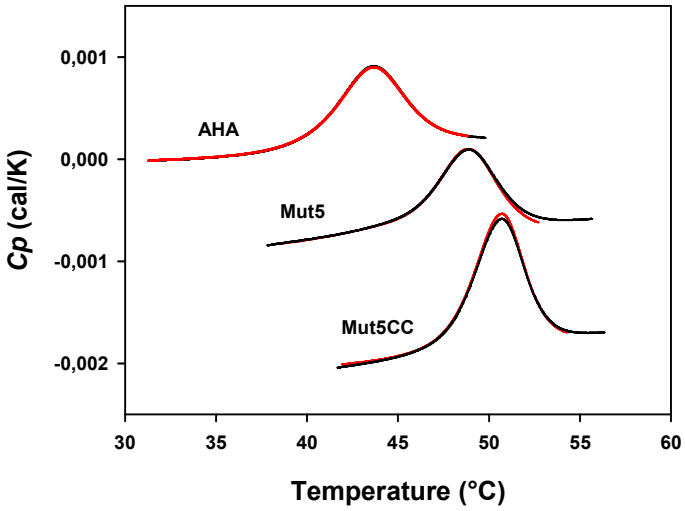


**Fig. 9.** Unfolding reversibility of the mutants in the presence of a nondetergent sulfobetaine. Thermograms were recorded in 30 mM Mops, 50 mM NaCl, 1 mM Ca $Cl_2$, 1 M 3-(1-pyridinio)-1-propanesulfonate, pH 7.2 at a scan-rate of 60 K $h^{-1}$. Red traces: first up-scans interrupted after completion of the unfolding transition. Black traces: second up-scans performed after sample cooling. Raw data have been displaced along the Y axis for clarity.

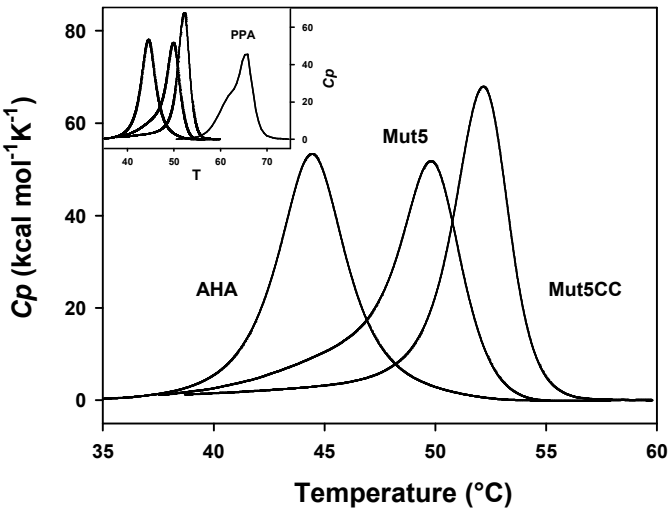


**Fig. 10.** Normalized reversible endotherms of AHA and of its mutants recorded by DSC in the presence of a nondetergent sulfobetaine. Thermograms were recorded in 30 mM Mops, 50 mM NaCl, 1 mM Ca $Cl_2$, pH 7.2 and 1 M 3-(1-pyridinio)-1-propanesulfonate in the case of Mut5 and Mut5CC. Raw data were baseline-subtracted and normalized for protein concentration. Inset: same graph including the irreversible thermogram of PPA (44).

**Table 3.** Thermodynamic parameters of unfolding derived from reversible DSC endotherms

| | $T_m$ °C | $\Delta H_{cal}$ kcal mol$^{-1}$ | $\Delta H_{eff}$ kcal mol$^{-1}$ | $\Delta H_{cal}$ / $\Delta H_{eff}$ | Reversibility % |
|---|---|---|---|---|---|
| AHA | 44.0 | 214 | 203 | 1.05 | >99 |
| Mut5 | 49.7 | 233 | 204 | 1.14[1] | >98 |
| Mut5CC | 52.2 | 280 | 270 | 1.04 | >98 |
| PPA[2] | 65.6 | 319 | --[3] | --[3] | none |

[1] despite a ratio close to 1, unfolding deviates from a two-state model as a result of an asymmetric transition
[2] data from (38)
[3] not applicable, biphasic transition

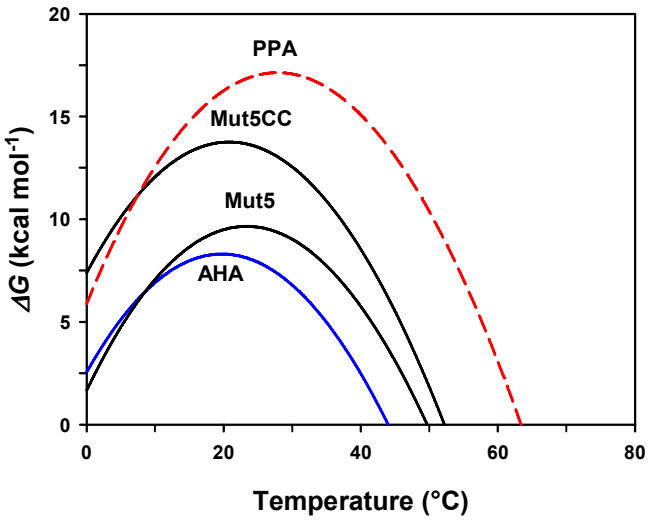


**Fig. 11.** Stability curves calculated from DSC data. The Gibbs free energy of unfolding was calculated as described (20) by the relation:

$$\Delta G(T) = \Delta H_{cal}(1-T/T_m) + \Delta Cp(T-T_m) - T\Delta Cp \ ln \ (T/T_m)$$

using $\Delta Cp$ = 8.47 kcal mol$^{-1}$ K$^{-1}$ as determined experimentally for AHA (38). Dashed, estimation of PPA stability from its irreversible unfolding parameters.

### *Stability of α-amylase-acarbose complexes*

Acarbose is a pseudosaccharide inhibitor containing a *N*-glycosidic bond and acting as a transition state analog (39). It has been shown that stabilization induced by acarbose binding closely follows the activation parameters of the amylolytic reaction (22) between the ground state (free enzyme) and the transition state intermediate (enzyme-acarbose complex). The thermograms of AHA and of its mutants were therefore recorded by DSC in the presence of acarbose (Fig. 12). Table 4 provides the relevant parameters and the full data set is presented in the table 5.

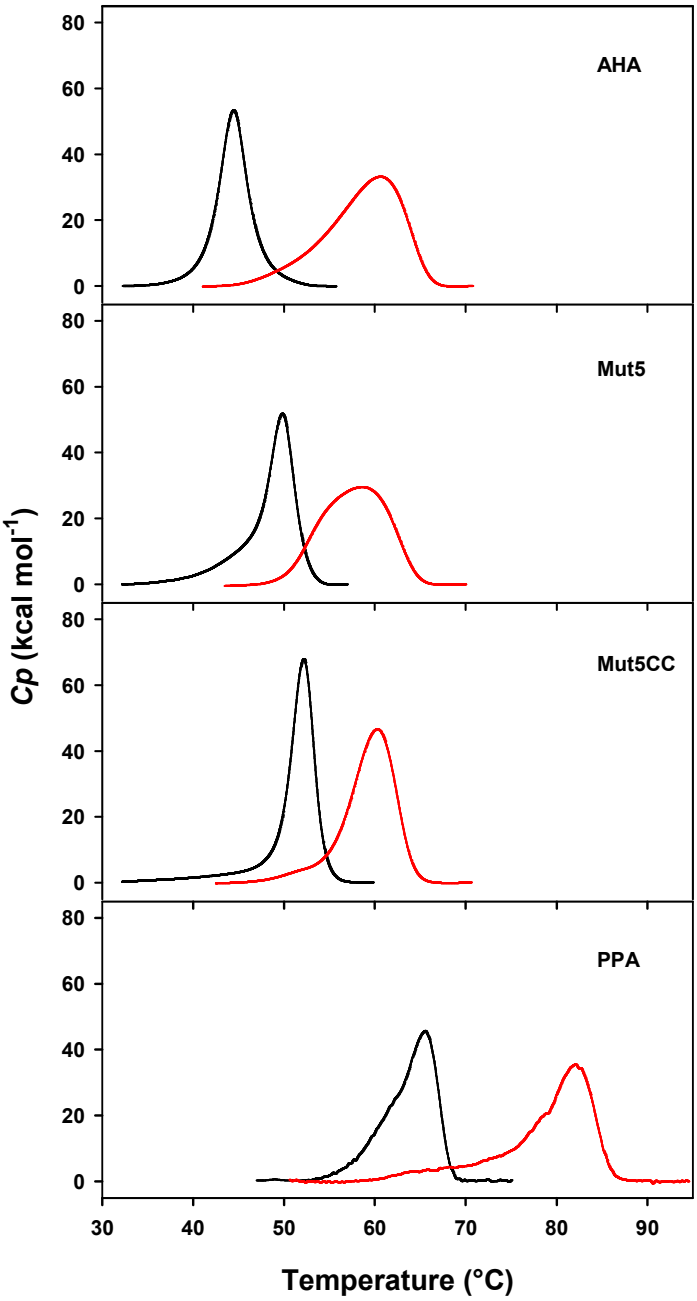


**Fig. 12.** Stability of α-amylase-acarbose complexes. DSC endotherms of α-amylases in the free state (black lines) and in complex with the transition state analog acarbose (red lines). $T_{max}$ corresponds to the top of the transition and $\Delta H_{cal}$ to the surface below the transition (Table 5). Baseline subtracted data have been normalized for protein concentration.

**Table 4:** Microcalorimetric parameters of thermal unfolding for α-amylases in complex with the pseudosaccharide inhibitor acarbose. The values refer to the differences in $T_{max}$ (top of the transition) and in $\Delta H_{cal}$ (area of the transition) with respect to the free enzyme. Activation parameters of the amylolytic reaction at 15°C are also indicated (27).

| | $\Delta T_{max}$ °C | $\Delta\Delta H_{cal}$ kcal mol$^{-1}$ | $\Delta G^{\#}$ kcal mol$^{-1}$ | $\Delta H^{\#}$ kcal mol$^{-1}$ | $T\Delta S^{\#}$ kcal mol$^{-1}$ |
|---|---|---|---|---|---|
| AHA | 16.6[a] | 115[a] | 13.4 | 8.3 | -5.1 |
| Mut5 | 9.0 | 53 | 14.0 | 11.3 | -2.7 |
| Mut5CC | 8.3 | 16 | 14.0 | 11.1 | -2.9 |
| PPA | 16.3[b] | 11 [b] | 14.0 | 11.5 | -2.5 |

[a] data similar to (22)
[b] data from (22)

**Table 5:** Microcalorimetric parameters of thermal unfolding for α-amylases in the free state and in complex with the pseudosaccharide inhibitor acarbose.

| | Free enzyme | | Enzyme-acarbose complex | | $\Delta T_{max}$ | $\Delta\Delta H_{cal}$ |
|---|---|---|---|---|---|---|
| | $T_{max}$ °C | $\Delta H_{cal}$ *kcal mol$^{-1}$* | $T_{max}$ °C | $\Delta H_{cal}$ *kcal mol$^{-1}$* | °C | *kcal mol$^{-1}$* |
| AHA | 44.0 | 214 | 60.6 | 329 | 16.6 | 115 |
| Mut5 | 49.4 | 229 | 58.4 | 282 | 9.0 | 53 |
| Mut5CC | 51.8 | 277 | 60.1 | 293 | 8.3 | 16 |
| PPA[a] | 65.6 | 295 | 81.9 | 306 | 16.3 | 11 |

[a] data from (20)

Upon acarbose binding, AHA is strongly stabilized, as indicated by the large increase of $T_{max}$ and of the calorimetric enthalpy $\Delta H_{cal}$. It has been argued (22) that this reflects the weak number of interactions to be broken to reach the activated state in the cold-active enzyme (low $\Delta H^{\#}$ in Table 4), which in turn implies large structural motions of the loose free enzyme upon substrate binding (high $\Delta S^{\#}$ in Table 4). It is worth mentioning that Mut5 and Mut5CC are less stabilized by acarbose and display intermediate values with PPA (Table 4). Concomitantly, their activation parameters become close to those of PPA. This is a strong indication that the stabilizing interactions engineered in the mutants directly impair the cold activity optimization of the parent psychrophilic α-amylase.

### *Equilibrium unfolding in GdmCl*

The resistance towards chemical denaturation using GdmCl (guanidinium hydrochloride) was probed by equilibrium unfolding recorded by fluorescence (Fig. 13, Table 6). Both mutants unfold reversibly at higher GdmCl concentrations ($C_{1/2}$ values) with respect to AHA and in accordance with their increased thermal stability. The cooperativity of unfolding remains similar to that of AHA, as indicated by the *m* value. Estimation of the conformational stability in the absence of denaturant

($\Delta G°H_2O$) at 20°C using Eq. 2 provides a ratio of 1/1.5/1.8/2 for AHA, Mut5, Mut5CC and PPA, respectively, in reasonable agreement with the values derived from the DSC stability curves (Fig. 11).

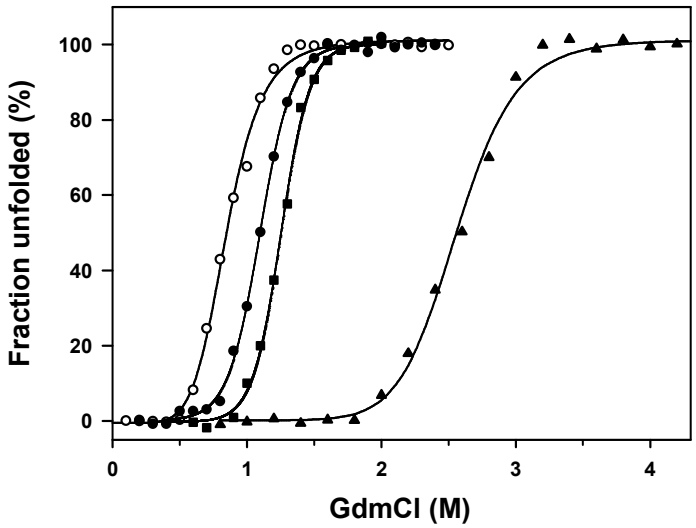


**Fig. 13.** Equilibrium unfolding in GdmCl of AHA and of its mutants as recorded by fluorescence emission. From left to right: AHA (open circles), Mut5 (closed circles), Mut5CC (closed squares) and PPA (closed triangles, data from (22))

**Table 6:** Equilibrium unfolding parameters in GdmCl of AHA and of its mutants

| | $C_{1/2}$ M | $m$ kcal mol$^{-1}$ M$^{-1}$ | $\Delta G°_{H2O}$ kcal mol$^{-1}$ |
|---|---|---|---|
| AHA[a] | 0.86 | 4.3 | 3.7 |
| Mut5 | 1.08 | 5.1 | 5.5 |
| Mut5CC | 1.25 | 5.3 | 6.6 |
| PPA[b] | 2.60 | 2.7 | 6.9 |

[a] data similar to (22)
[b] data from (22)

### *Kinetics of unfolding and refolding*

In order to address the kinetic origin of the gain in stability of the mutants, the folding kinetics in GdmCl were recorded. Indeed, the equilibrium constant $K_{N-U}$ between the native state N and the unfolded state U ($K_{N-U}$ = [U] / [N] ) is also expressed by the ratio $k_{unfold}$ / $k_{fold}$ of the kinetic constants for unfolding and folding, respectively. As shown in Fig. 14, kinetics of unfolding and refolding were determined between 0.3 M and 2 M GdmCl. Under all conditions, unfolding was found to be a monophasic process while refolding was a biphasic process comprising a fast phase (~80% amplitude) and a slow phase (~20% amplitude). In the context of our analysis, the corresponding parameters (Table 7) are restricted to the rate constants in the absence of denaturant ($k_f^{H_2O}$ and $k_u^{H_2O}$) obtained by linear regression (dashed lines in Fig. 14), the corresponding time constants ($\tau = 1/k$), their

dependencies on the denaturant concentration ( $m_{kf}$ and $m_{ku}$) and, when relevant, the transition midpoint $C_{1/2}$. Interestingly, the folding rate constants $k_f^{H_2O}$ for both phases converge towards very similar values in the three enzymes. By contrast, the unfolding rate constants $k_u^{H_2O}$ of both stabilized mutants are reduced: Mut5 unfolds 3.5 times slower and Mut5CC unfolds 13.4 times slower with respect to AHA. It can be concluded that the decreased unfolding rate is the main kinetic determinant of the improved stability in both mutants.

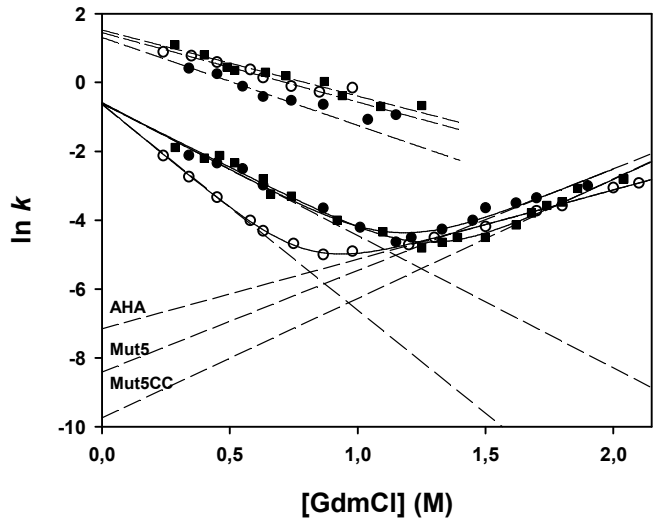


**Fig. 14.** Chevron plots of the GdmCl concentration dependence of the rate constants for unfolding and refolding. Data for AHA (open circles), Mut5 (closed circles) and Mut5CC (closed squares). Unfolding rate constants (right arms of the plot) and refolding rate constants (left arms, slow phase) were fitted on Eq. 6 (solid lines). Dashed lines are extrapolations to 0 M GdmCl allowing the determination of $k_f^{H_2O}$ and $k_u^{H_2O}$, the folding and unfolding rate constants in the absence of denaturant. Upper data set: fast refolding phases.

**Table 7:** Kinetic parameters of unfolding and refolding in GdmCl

| | $\ln k_u^{H_2O}$ | $\ln k_f^{H_2O}$ | $k_u^{H_2O}$ $s^{-1}$ | $k_f^{H_2O}$ $s^{-1}$ | $\tau_u$ s | $\tau_f$ s | $m_{ku}$ kcal $M^{-1}mol^{-1}$ | $m_{kf}$ kcal $M^{-1}mol^{-1}$ | $C_{1/2}$ M |
|---|---|---|---|---|---|---|---|---|---|
| *Slow phases* | | | | | | | | | |
| AHA | -7.15 | -0.62 | 7.8e-4 | 0.53 | 1 282 | 1.88 | 1.15 | -3.51 | 0.81 |
| Mut5 | -8.41 | -0.58 | 2.2e-4 | 0.55 | 4 545 | 1.81 | 1.67 | -2.22 | 1.14 |
| Mut5CC | -9.74 | -0.61 | 5.8e-5 | 0.54 | 17 241 | 1.85 | 1.97 | -2.11 | 1.26 |
| *Fast refolding phase* | | | | | | | | | |
| AHA | | 1.44 | | 4.22 | | 0.24 | | -2.01 | |
| Mut5 | | 1.31 | | 3.69 | | 0.27 | | -2.55 | |
| Mut5CC | | 1.26 | | 4.58 | | 0.22 | | -1.92 | |

# CONCLUSIONS

The mutants Mut5 and Mut5CC bear representative stabilizing interactions found in the heat-stable PPA but lacking in the psychrophilic AHA, *i.e.* a salt bridge (N150D), weakly polar interactions (V196F), short H-bonds (K300R), better hydrophobic effect in core clusters (T232V and Q194I) and a covalent disulfide bond (Q58C/A99C) specific to warm-blooded animals (Fig. 2). From an evolutionary perspective, these mutants can be regarded as structural intermediates between the psychrophilic and the mesophilic enzymes. We have shown here that these engineered interactions improve all the investigated parameters related to protein stability: the compactness (as probed by fluorescence quenching), the kinetically-driven stability (irreversible heat-induced unfolding), the thermodynamic stability (from DSC endotherms), the resistance towards chemical denaturation (equilibrium unfolding in GdmCl) and the kinetics of unfolding/refolding. Concomitantly to this improved stability, both mutants have lost the kinetic optimization to low temperature activity displayed by the parent enzyme AHA, as demonstrated by their kinetic parameters towards a model substrate (Fig. 3), by their activity towards various polysaccharides and oligosaccharides (Table 1) and by their stability in complex with the transition state analog acarbose (Table 4). These results provide strong experimental support to the prevailing hypothesis (7,27): the disappearance of stabilizing interactions in psychrophilic enzymes increases the amplitude of concerted motions required by catalysis and the dynamics of active site residues at low temperature, leading to a higher activity but also to a lower substrate binding strength (Fig. 3). We have argued elsewhere that loosing stability is apparently the easiest strategy to improve molecular dynamics in cold environments where the selective pressure for stable proteins is lacking (8,40).

Two aspects of the present stability studies are also worth commenting. *i*) The role of disulfide bonds has been frequently debated in the general context of protein stability (26). In the case of Mut5CC, there is an unquestionable contribution of the disulfide to all recorded stability parameters. Furthermore, a fascinating aspect, which deserve further investigations, is the observation that the disulfide has a higher contribution to stability when added to Mut5 than to its effect on AHA alone (26), as far as $T_m$ and $\Delta H_{cal}$ variations are concerned. This reflects a very strong cooperativity of stabilizing interactions, rather than a simple additivity, in the maintenance of the native, folded state of proteins. *ii*) The kinetics of unfolding/refolding of Mut5 and Mut5CC demonstrates that the gain in stability is governed by a slow unfolding rate, whereas the folding rate remains unchanged (Fig. 14, Table 7). This perfectly fits with similar experiments performed on hyperthermophilic proteins and aimed at explaining their unusual stability (41, 42). Altogether, these results suggest the occurrence of a transition state on the unfolding pathway, the free energy level of which modulates the stability of proteins adapted to extreme biological temperatures. This aspect should stimulate further investigations, using appropriate extremophilic protein models.

# ACKNOWLEDGEMENTS

We thank H. Bichoff (Bayer AG, Germany) for the kind gift of acarbose. The support of the Institut Polaire Français was also appreciated. AC and RB were FRIA fellows during this work.

# FUNDING

This work was supported by the F.R.S-FNRS, Belgium (Fonds de la Recherche Fondamentale et Collective, contract numbers 2.4535.08 to GF and 2.4530.09 to AM) and the Belgian program of Interuniversity Attraction Poles initiated by the Federal Office for Scientific, Technical and Cultural Affaires (PAI n° P6/19).


# REFERENCES


1. Rodrigues, D. F., and Tiedje, J. M. (2008) *Appl. Environ. Microbiol.* **74**, 1677-1686
2. Gerday, C., and Glansdorff, N. (2007) *Physiology and Biochemistry of Extremophiles*, ASM Press, Washington, D.C.
3. Margesin, R., Schinner, F., Marx, J. C., and Gerday, C. (2008) *Psychrophiles, from Biodiversity to Biotechnology*, Springer-Verlag, Berlin, Heidelberg
4. Deming, J. W. (2002) *Curr. Opin. Microbiol.* **5**, 301-309
5. D'Amico, S., Collins, T., Marx, J. C., Feller, G., and Gerday, C. (2006) *EMBO Rep.* **7**, 385-389
6. Casanueva, A., Tuffin, M., Cary, C., and Cowan, D. A. (2010) *Trends Microbiol.* **18**, 374-381
7. Fields, P. A., and Somero, G. N. (1998) *Proc. Natl. Acad. Sci. U. S. A.* **95**, 11476-11481
8. Feller, G., and Gerday, C. (2003) *Nat. Rev. Microbiol.* **1**, 200-208
9. Feller, G. (2010) *J. Phys.: Condens Mat* **22**, 323101 doi 10.1088/0953-8984/1022/1032/323101
10. Siddiqui, K. S., and Cavicchioli, R. (2006) *Annu. Rev. Biochem.* **75**, 403-433
11. Aghajari, N., Feller, G., Gerday, C., and Haser, R. (1998) *Structure* **6**, 1503-1516
12. Russell, R. J., Gerike, U., Danson, M. J., Hough, D. W., and Taylor, G. L. (1998) *Structure* **6**, 351-361
13. Smalas, A. O., Leiros, H. K., Os, V., and Willassen, N. P. (2000) *Biotechnol. Annu. Rev.* **6**, 1-57
14. Bell, G. S., Russell, R. J., Connaris, H., Hough, D. W., Danson, M. J., and Taylor, G. L. (2002) *Eur. J. Biochem.* **269**, 6250-6260
15. Tehei, M., Franzetti, B., Madern, D., Ginzburg, M., Ginzburg, B. Z., Giudici-Orticoni, M. T., Bruschi, M., and Zaccai, G. (2004) *EMBO Rep.* **5**, 66-70
16. Bae, E., and Phillips, G. N., Jr. (2004) *J. Biol. Chem.* **279**, 28202-28208
17. Coquelle, N., Fioravanti, E., Weik, M., Vellieux, F., and Madern, D. (2007) *J. Mol. Biol.* **374**, 547-562
18. Gianese, G., Bossa, F., and Pascarella, S. (2002) *Proteins* **47**, 236-249
19. Tronelli, D., Maugini, E., Bossa, F., and Pascarella, S. (2007) *Febs J.* **274**, 4595-4608
20. Medigue, C., Krin, E., Pascal, G., Barbe, V., Bernsel, A., Bertin, P. N., Cheung, F., Cruveiller, S., D'Amico, S., Duilio, A., Fang, G., Feller, G., Ho, C., Mangenot, S., Marino, G., Nilsson, J., Parrilli, E., Rocha, E. P., Rouy, Z., Sekowska, A., Tutino, M. L., Vallenet, D., von Heijne, G., and Danchin, A. (2005) *Genome Res.* **15**, 1325-1335
21. Feller, G., Payan, F., Theys, F., Qian, M., Haser, R., and Gerday, C. (1994) *Eur. J. Biochem.* **222**, 441-447
22. D'Amico, S., Marx, J. C., Gerday, C., and Feller, G. (2003) *J. Biol. Chem.* **278**, 7891-7896
23. Da Lage, J. L., Feller, G., and Janecek, S. (2004) *Cell Mol. Life Sci.* **61**, 97-109
24. Aghajari, N., Feller, G., Gerday, C., and Haser, R. (1998) *Protein Sci.* **7**, 564-572
25. D'Amico, S., Gerday, C., and Feller, G. (2001) *J. Biol. Chem.* **276**, 25791-25796.
26. D'Amico, S., Gerday, C., and Feller, G. (2002) *J. Biol. Chem.* **277**, 46110-46115

27. D'Amico, S., Gerday, C., and Feller, G. (2003) *J. Mol. Biol.* **332**, 981-988
28. D'Amico, S., Gerday, C., and Feller, G. (2000) *Gene* **253**, 95-105
29. D'Amico, S., Sohier, J. S., and Feller, G. (2006) *J. Mol. Biol.* **358**, 1296-1304
30. D'Amico, S., and Feller, G. (2009) *Anal. Biochem.* **385**, 389-391
31. Matouschek, A., Matthews, J. M., Johnson, C. M., and Fersht, A. R. (1994) *Protein Eng.* **7**, 1089-1095
32. Sanchez-Ruiz, J. M., Lopez-Lacomba, J. L., Cortijo, M., and Mateo, P. L. (1988) *Biochemistry* **27**, 1648-1652
33. Lakowicz, J. (1983) *Principles of Fluorescence Spectroscopy*, Plenum Press, New York
34. Khorasanizadeh, S., Peters, I. D., and Roder, H. (1996) *Nat. Struct. Biol.* **3**, 193-205
35. Fersht, A. R. (1999) *Structure and Mechanism in Protein Science-A Guide to Enzyme Catalysis and Protein Folding*, W.H. Freeman and Co, New York
36. Collins, T., D'Amico, S., Georlette, D., Marx, J. C., Huston, A. L., and Feller, G. (2006) *Anal. Biochem.* **352**, 299-301
37. Vuillard, L., Braun-Breton, C., and Rabilloud, T. (1995) *Biochem. J.* **305**, 337-343
38. Privalov, P. (1992) Physical basis of the stability of the folded conformations of proteins. in *Protein folding* (Creighton, T. ed.), W.H. Freeman and Company, New York. pp 83-126
39. Qian, M., Haser, R., Buisson, G., Duee, E., and Payan, F. (1994) *Biochemistry* **33**, 6284-6294
40. Roulling, F., Piette, F., Cipolla, A., Struvay, C., and Feller, G. (2011) Psychrophilic enzymes: cool responses to chilly problems. in *Extremophiles Handbook* (Horikoshi, K. ed.), Springer Verlag, Tokyo, Berlin, Heidelberg. pp 891-916
41. Luke, K. A., Higgins, C. L., and Wittung-Stafshedel, P. (2007) *Febs J.* **274**, 4023-4033
42. Perl, D., Welker, C., Schindler, T., Schroder, K., Marahiel, M. A., Jaenicke, R., and Schmid, F. X. (1998) *Nat. Struct. Biol.* **5**, 229-235
43. Aghajari, N., Feller, G., Gerday, C., and Haser, R. (2002) *Protein Sci.* **11**, 1435-1441
44. Feller, G., d'Amico, D., and Gerday, C. (1999) *Biochemistry* **38**, 4613-4619

# Chapitre 3 : Résultats

## *Section II: Temperature adaptations in psychrophilic, mesophilic and thermophilic chloride-dependent alpha-amylases*

**(Soumis dans "*Biochimie*" 2012 May 23. [Epub ahead of print])**

# Temperature adaptations in psychrophilic, mesophilic and thermophilic chloride-dependent alpha-amylases

**Alexandre Cipolla** [a], François Delbrassine [a], Jean-Luc Da Lage [b] and Georges Feller [a]*

[a] *Laboratory of Biochemistry, Center for Protein Engineering, University of Liège, B-4000 Liège-Sart Tilman, Belgium*

[b] *UPR9034 Evolution, Génomes et Spéciation, CNRS, F-91198 Gif-sur-Yvette, France and Université Paris-Sud, 91405 Orsay cedex, France*

*Abbreviations*: AHA, α-amylase from *Pseudoalteromonas haloplanktis* (psychrophile); DMA, α-amylase from *Drosophila melanogaster* (ectothermic mesophile); PPA, α-amylase from pig pancreas (homeothermic mesophile); TFA, α-amylase from *Thermobifida fusca* (thermophile); Et-G7-pNP, 4-nitrophenyl-α-D-maltoheptaoside-4,6-O-ethylidene; GdmCl, guanidine hydrochloride; DSC, differential scanning calorimetry; IF, intrinsic fluorescence; CD, circular dichroism.

## ABSTRACT

The functional and structural adaptations to temperature have been addressed in homologous chloride-dependent α-amylases from a psychrophilic Antarctic bacterium, the ectothermic fruit fly, the homeothermic pig and from a thermophilic actinomycete. This series covers nearly all temperatures encountered by living organisms. We report a striking continuum in the functional properties of these enzymes coupled to their structural stability and related to the thermal regime of the source organism. In particular, thermal stability recorded by intrinsic fluorescence, circular dichroism and differential scanning calorimetry appears to be a compromise between the requirement for a stable native state and the proper structural dynamics to sustain the function at the environmental/physiological temperatures. The thermodependence of activity, the kinetic parameters, the activations parameters and fluorescence quenching support these activity-stability relationships in the investigated α-amylases.

Keywords: alpha-amylase, extremophiles, Antarctic, differential scanning calorimetry, protein stability

# INTRODUCTION

Life has successfully colonized nearly all environments on Earth, from the permanently frozen Polar Regions or the arctic permafrost, to the extremely hot deep-sea hydrothermal vents, hot springs or geysers. The range of temperatures compatible with life is quite large and is currently estimated from -20°C in sea ice [1] to 122°C in hydrothermal vents [2]. Microorganisms living in these environments are able to cope with the local chemical and physical extreme parameters by various adaptive strategies in order to maintain activity and metabolic functions despite these challenging conditions [3,4]. From an evolutionary perspective, current views suggest that the last universal common ancestor (LUCA) was mesophilic or moderately thermophilic and that extant extremophiles have subsequently colonized harsh environments [5]. However, there are also arguments for a hot origin of life [6,7] and even for a cold origin [8,9]. It is therefore of interest to understand the molecular mechanisms of adaptation to temperature in contemporary enzymes. In a first step towards this goal, we have compared homologous psychrophilic, mesophilic and thermophilic α-amylases. Temperature adaptation has been well studied in thermophiles [10] while this remains fragmental in psychrophiles [11]. Furthermore, comparisons of homologous series of extremophilic and mesophilic proteins are scare [12-16].

α-Amylases (α-1,4-glucan-4-glucanohydrolase, EC 3.2.1.1) are ubiquitous and widely distributed in microorganisms, plants and animals. These enzymes belong to family 13 in the glycoside hydrolase classification (http://www.cazy.org/ and [17]) and catalyze the hydrolysis of internal α (1,4)-glycosidic bonds with net retention of the anomeric configuration in starch, amylose, amylopectin, glycogen and other related polysaccharides through multiple attacks toward the non-reducing ends. As a result of the huge diversity of organisms that synthesize α-amylases, these enzymes exhibit in general a very low degree of sequence similarity, although they adopt the same overall fold [18]. Amongst these enzymes, animal-type α-amylases are homologous enzymes present in all bilaterian animals and in some rare microorganisms, a lateral gene transfer having likely occurred between the two groups [19-22]. All animal-type α-amylases isolated so far display the unusual property to bind a chloride ion at a specific site that induces allosteric activation of the full amylolytic activity. It has been shown that the chloride ion is responsible for the p*Ka* shift of catalytic residues via interactions with active site carboxyl groups [23-25].

Chloride-dependent α-amylases from the Antarctic bacterium *Pseudoalteromonas haloplanktis* and its close homologue from pig (*Sus scrofa*) pancreas have been extensively studied in the context of protein adaptation to low temperatures [26-30]. It was shown that the high specific activity at low temperatures of cold-adapted enzymes is a key adaptation to compensate for the exponential decrease of chemical reaction rates as temperature is reduced. Such high biocatalytic activity arises from the disappearance of various non-covalent stabilizing interactions, resulting in an improved flexibility of

the enzyme conformation and in a weak stability [11, 31]. Here, we have extended these earlier observations to the chloride-dependent α-amylases from the ectothermic fruit fly *Drosophila melanogaster* and from the thermophilic actinomycete *Thermobifida fusca*. This series covers nearly all temperatures encountered by living organisms (chloride-dependent α -amylases have not been detected in hyperthermophiles). We report a striking continuum in the functional properties of these enzymes coupled to their structural stability and related to the thermal regime of the source organism.

# MATERIALS AND METHODS

### *Gene cloning*

The naturally intronless *amy-p* gene (coding for DMA α-amylase) has been originally amplified by PCR from genomic DNA of *Drosophila melanogaster* using the forward primer 5'-AACTTCCATCTGGAATCATC-3' and the reverse primer 5'-TGCTCCCCAGCTGTTTAC-3' and the resulting PCR fragment was cloned in the pGEM-T Easy vector (pGEM-AmyD). To construct an expression vector, restriction sites *ClaI* and *XbaI* were introduced by PCR in 5'and 3' of the *amy-p* gene, respectively. The pαH12WT* plasmid, modified with an engineered *Nde*I restriction site at the ATG codon and pGEM-AmyD were digested by *Cla*I and *Xba*I and ligated to produce pα-AmyD in which the residual part of the AHA gene was excised by inverse PCR, producing the pAmyD plasmid. Both pAmyD and pET-22b(+) were digested by *Nde*I/*Hind*III restriction enzymes and ligated to give the pET-AmyD plasmid in which the *amy-p* gene is preceded by the signal peptide of AHA. The nucleotide sequence of this construct is given in the Fig. 1.

Based on the sequence of *Thermobifida fusca* α-amylase Tfu_0985 (GenBank ID: AAZ55023.1), the TFA gene was re-designed in order to replace the native signal sequence by the signal peptide of AHA and to introduce *Nde*I/*Hind*III restriction sites. The codons were optimized for *E.coli* codon usage and this TFA gene was synthesized by GeneArt (Life Technologies) in a pMA vector. PSTFA_pMA plasmid and pET-22b(+) were digested by *Nde*I/*Hind*III restriction enzymes and fragments were ligated to produce the pET-TFA plasmid. The nucleotide sequence of this construct is given in the Fig. 2.

*Nde* I
CATATGAAACTCAATAAAATAATCACCACCGCAGGTTTAAGCCTAGGGTTGCTCTTACCTAGCATTGCGACTGCT
CAATTCGACACCAACTACGCATCCGGTCGTAGTGGAATGGTCCACCTCTTCGAGTGGAAGTGGGACGACATCGCT
GCCGAGTGCGAGAACTTCCTGGGACCCAATGGCTACGCCGGTGTTCAGGTCTCCCCTGTGAACGAGAACGCCGTC
AAGGACAGCCGCCCCTGGTGGGAACGTTACCAGCCCATCTCCTACAAGCTGGAGACCCGCTCCGGAAACGAAGAG
CAGTTCGCCAGCATGGTCAAGCGCTGCAACGCCGTCGGAGTGCGCACCTACGTGGACGTGGTCTTCAACCACATG
GCCGCCGACGGAGGCACCTACGGCACTGGCGGCAGCACCGCCAGCCCCAGCAGCAAGACCTATCCCGGAGTGCCC
TACTCCTCGCTGGACTTCAACCCGACCTGCGCCATCAGCAACTACAACGACGCCAACGAGGTGCGCAACTGCGAG
CTGGTCGGTCTGCGCGACCTTAACCAGGGCAACTCCTACGTGCAGGACAAGGTGGTCGAGTTCCTGGACCATCTG
ATTGATCTCGGCGTGGCCGGATTCCGCGTGGACGCCGCCAAGCACATGTGGCCCGCCGACCTGGCCGTCATCTAT
GGCCGCCTCAAGAACCTGAACACCGACCACGGCTTCGCCTCGGGATCCAAGGCGTACATCGTCCAGGAGGTCATC
GACATGGGCGGCGAGGCCATCAGCAAGTCCGAGTACACCGGACTGGGCGCCATCACCGAGTTCCGCCACTCCGAC
TCCATCGGCAAGGTCTTCCGCGGCAAGGACCAGCTGCAGTATCTGACCAACTGGGGCACCGCCTGGGGCTTCGCT
GCCTCCGACCGCTCCCTGGTATTCGTCGACAACCACGACAACCAGCGCGGACATGGAGCAGGAGGCGCCGACGTG
CTGACCTACAAGGTGCCCAAGCAGTACAAGATGGCCTCCGCCTTTATGCTGGCGCACCCATTCGGCACTCCCCGC
GTGATGTCCTCCTTCTCCTTCACGGACACCGATCAGGGCCCGCCCACCACCGACGGCCACAACATCGCCTCGCCC
ATCTTCAATAGCGACAACTCCTGCAGCGGCGGCTGGGTGTGCGAGCACCGCTGGCGCCAGATCTACAACATGGTG
GCCTTCCGAAACGCCGTGGGCTCGGACGAGATCCAGAACTGGTGGGACAACGGCAGCAACCAGATCTCCTTCAGC
CGAGGCAGCCGCGGCTTCGTGGCCTTCAACAACGACAACTACGACCTGAACAGCTCCCTGCAGACGGGCCTGCCC
GCCGGCACCTACTGCGACGTCATCTCCGGCTCCAAGAGCGGTTCCTCCTGCACGGGCAAGACCGTCACCGTCGGA
TCCGACGGACGGGCTTCCATCAACATTGGCAGCTCCGAGGACGACGGAGTGCTGGCCATTCACGTCAACGCCAAG
TTGTAATCTAGAGTCGACCTGCAGCCCAAGCTT
*Stop* *Hind* III

**Fig. 1.** Nucleotide sequence of DMA engineered for *E. coli* expression

*Nde* I
CATATGAAACTCAATAAAATAATCACCACCGCAGGTTTAAGCCTAGGGTTGCTCTTACCTAGCATTGCGA
CTGCTGCTCCGTCTGGAAATCGTGACGTCATCGTCCACCTGTTCCAATGGCGCTGGAAAAGCATTGCTGA
CGAATGTCGTACCACTCTGGGTCCACATGGGTTTGGCGCTGTCCAAGTGTCTCCTCCTCAAGAGCACGTT
GTACTGCCTGCTGAAGATTATCCTTGGTGGCAGGACTATCAGCCGGTTTCCTATAAACTGGATCAGACTC
GTCGTGGTTCTCGTGCCGACTTTATCGATATGGTCAACACGTGTCGTGAAGCTGGTGTGAAAATCTATGT
CGACGCCGTGATTAATCACATGACCGGGACCGGTAGTGCTGGAGCTGGCCCTGGTTCCGCTGGCTCATCC
TATTCAAAATATGACTATCCGGGCATCTATCAGTCACAGGACTTCAACGATTGCCGTCGTGATATTACCA
ACTGGAATGACAAATGGGAGGTCCAACATTGTGAGCTGGTTGGCCTGGCAGATCTGAAAACCTCTAGCCC
GTATGTCCAGGATCGTATTGCCGCTTATCTGAACGAACTGATCGACCTGGGTGTTGCTGGATTTCGTATC
GACGCTGCTAAACACATTCCGGAAGGCGACCTGCAAGCAATTCTGTCTCGCCTGAAAAACGTTCATCCGG
CATGGGGTGGCGGTAAACCTTATATCTTTCAAGAAGTGATCGCCGATAGCACCATCTCTACAGGGTCCTA
TACACATCTGGGTAGCGTGACCGAGTTCCAGTATCACCGTGACATCAGTCATGCCTTTGCCAATGGGAAT
ATTGCCCATCTGACTGGACTGGGTAGTGGTCTGACACCTTCGGACAAAGCAGTGGTTTTTGTGGTTAACC
ATGACACTCAGCGCTATGAACCGATTCTGACTCATACCGACGGTGCTCGTTATGATCTGGCCCAGAAATT
CATGCTGGCTCACCCGTATGGTACACCGAAAGTCATGTCCTCGTATACCTGGTCAGGGGATGACAAAGCT
GGTCCGCCTATGCATTCTGACGGTACTACTCGTCCTACAGACTGTTCTGCCGATCGCTGGCTGTGTGAAC
ATCGTGCCGTTGCTGGTATGGTTGGCTTCCATAATGCCGTGGCCGGACAGGGAATTGGTAGCGCCGTTAC
CGATGGAAACGGTCGTCTGGCTTTTGCTCGTGGATCCGCCGGTTATGCTGCCTTTAATGCCACGAATACC
GCTTGGACTCGTACCTTTACCACCTCTCTGCCTGATGGCGTTTATTGTGATGTGGCGAATGGCACCTTTG
TTGATGGCGTCTGTGATGGTCCGTCTTATCAGGTTAGTGGGGGCAAATTCACAGCAACTGTTCCGGCAAA
TGGTGCCGTAGCACTGCATGTCGAAGCACCTGGTTCTTGTGGCCCTGATGGTTGTGGCACACCTCCTGGT
GGAGGGGACGACTGTACTACTGTTACAGCCCGCTTTCACGCCACAGTAACAACATGGTATGGCCAAGAAG
TTGCCGTTGTAGGCTCTATCCCTGAACTGGGATCATGGCAACCTGCCCAAGGCGTTCGTCTGCGTACAGA
TTCTGGCACTTATCCGGTGTGGTCTGGTGCCGTTGACCTGCCTGCTGGTGTTGGCTTTGAGTATAAATAT
GTAAAACTGAATCCGGACGGTACTGTTGAGTGGGAGCAGGGTGGGAACCGTATCGCTACTGTCGATGATA
GCGGAGGCGGTTGTTCTCAGAACTTTTATGACTCCTGGCGCTAATAAAAGCTT
*Stop* *Hind* III

**Fig. 2.** Nucleotide sequence of TFA engineered for *E. coli* expression

### *Enzyme production and purification*

The recombinant AHA (pαH12WT* plasmid) was expressed in *Escherichia coli RR1* at 18°C and purified by DEAE-agarose, Sephadex G-100, and Ultrogel AcA54 column chromatography as previously described [32].

The recombinant DMA α-amylase (pET-AmyD plasmid) was expressed in *E.coli* BL21(DE3) at 18°C in TB (Terrific Broth) containing 100mg/l ampicillin and α-amylase production was induced by 0.5 mM IPTG (isopropyl β-D-thiogalactoside) at $A_{600}$ of ~4. After 20 h of induction, cells were recovered by centrifugation at 13,000 g for 50 minutes at 4°C. Bacteria were disrupted on an EmulsiFlex-C3 homogenizer (Avestin) in the presence of benzonase and protease inhibitors and cell debris were removed by centrifugation. Purification of DMA was achieved in five steps: (a) An ammonium sulfate precipitation at 85 % saturation during 1 h at 4°C. The precipitate was centrifuged at 23,000 g for 50 minutes and the pellet was dissolved in a minimum volume of Buffer A (50 mM Tris, 1 mM $CaCl_2$, pH 7,5) and then dialyzed against 2x2 L of Buffer B (20mM Hepes, 20 mM NaCl, pH 7,5). (b) A glycogen precipitation in 40 % cold ethanol [33]. After dropwise ethanol addition, the insoluble material was removed by centrifugation and glycogen was added to the supernatant. The pellet was solubilized and dialyzed against Buffer A. (c) The solution was loaded on a Q Sepharose Fast Flow anion exchanger (2.5 x 40 cm) and eluted with a linear NaCl gradient (0-1 M) in Buffer A. (d)

Fractions displaying amylolytic activity were concentrated to 10 mL by ultrafiltration using a Millipore polyethersulfone membrane (cutoff 10,000 Da) in an Amicon ultrafiltration unit under 3 bars nitrogen pressure and then loaded on a Sephadex G-100 gel filtration column (2.5 x 100 cm) and eluted with buffer A. (e) The fractions of interest were concentrated to 10 mL by ultrafiltration as described above and then loaded on a Ultrogel AcA54 gel filtration column (2.5 x 100 cm) eluted with buffer A. The recombinant TFA α-amylase (pET-TFA plasmid) was produced and purified as described above except that the Sephadex G-100 step was omitted. PPA was from Roche.

Except where specified, enzyme concentration was determined spectrophotometrically at 280 nm using $A^{0.1\%}$ = 1.90 for AHA, 1.71 for DMA, 2.41 for PPA and 1.95 for TFA. Dynamic light scattering was performed on a DynaPro NanoStar instrument (Wyatt Technology Corporation) operated in batch mode at 20°C and fitted with a laser beam emitting at 658 nm. A globular protein model was used for mass estimation. The N-terminal amino acid sequence of DMA and TFA was determined by automated Edman degradation using a pulsed-liquid-phase protein sequencer Procise 494 (Applied Biosytems) fitted with an on-line phenylthiohydantoin analyzer. Mass determination was performed by ESI-Q-TOF mass spectrometry (Waters, Micromass) in 25% acetonitrile, 0.5% formic acid.

***Enzyme assays and Kinetics***

α-Amylase activity was recorded using 3.5 mM 4-nitrophenyl-α-D-maltoheptaoside-4,6-O-ethylidene (Et-G7-pNP) as substrate (Infinity™ Amylase kit, ThermoScientific) and by the dinitrosalicylic acid (DNS) method using 1% soluble starch as substrate [23]. Catalytic concentrations of enzymes were determined by the Bradford assay (Pierce).

The effects of pH on amylolytic activity was determined by the DNS method using a poly-buffer containing 25 mM Na acetate, 25 mM HEPES, 25 mM CHES, 25 mM MES and 20 mM NaCl between pH 3.5 –pH 10.5. Chloride-free α-amylase was prepared by extensive dialysis against 20 mM HEPES-NaOH, pH 7,2. The dissociation constants for $Cl^-$ were obtained from the saturation curves as described [23].

Thermodynamic activation parameters were calculated as described [34] using the equations:

$$\Delta G^{\#} = RT \text{ x } (\ln (k_B T/h) - \ln k_{cat}) \quad \text{(Eq. 1)}$$

$$\Delta H^{\#} = E_a - RT \quad \text{(Eq. 2)}$$

$$\Delta S^{\#} = (\Delta H^{\#} - \Delta G^{\#})/T \quad \text{(Eq. 3)}$$

where $k_B$ is the Bolzmann constant, $h$ the Planck constant, $E_a$ is the activation energy of the reaction and $R$ the gas constant.

***Differential scanning calorimetry***

Measurements were performed using a MicroCal VP-DSC instrument at a scan rate of 60 K $h^{-1}$ and under ~25 psi positive cell pressure. Samples (~2mg/ml) were dialyzed overnight against 30mM MOPS, 50mM NaCl, 1mM $CaCl_2$, pH 7.2. For DMA and TFA, both the sample and the reference buffer were brought to 1 M 3-(1-pyridinio)-1-propanesulfonate (*i.e.* a nondetergent sulfobetaine) as detailed [35]. After cell loading, the protein concentration was determined on the remaining sample by the bicinchoninic acid method (Pierce). Thermograms were analyzed according to a non-two-state model in which the melting point $T_m$, the calorimetric enthalpy $\Delta H_{cal}$ and the van't Hoff enthalpy $\Delta H_{eff}$ of individual transitions are fitted independently using the MicroCal Origin software (version 7). The magnitude and source of the errors in the $T_m$ and enthalpy values have been discussed elsewhere [36].

***Unfolding recorded by intrinsic fluorescence***

Heat-induced unfolding was recorded using an SML-Aminco Model 8100 spectrofluorometer (Spectronic Instruments) at an excitation wavelength of 280 nm and at an emission wavelength of 350 nm (AHA), 340 nm (DMA), 350 nm (PPA) or 336 nm (TFA). A scan rate of 60 K $h^{-1}$ was generated by a Lauda thermostat. GdmCl-induced unfolding was monitored at 20°C after overnight incubation of the samples at this temperature in 30 mM MOPS, 50 mM NaCl, 1 mM $CaCl_2$, pH 7.2 and increasing GdmCl concentrations on a Perkin-Elmer LS50B spectrofluorometer at protein concentration of ~0,1mg/ml [30]. The equilibrium condition was ascertained by recording unfolding as a function of time. Least-squares analysis of $\Delta G°$ values as a function of GdmCl concentrations allowed estimating the conformational stability in the absence of denaturant, $\Delta G°H_2O$, according to:

$$\Delta G° = \Delta G°H_2O - m\,[\text{GdmCl}] \qquad \text{(Eq. 4)}$$

***Circular dichroism***

Circular dichroism spectra of the native proteins were recorded using a Jasco J-810 spectropolarimeter under constant nitrogen flow. Spectra in the far UV were recorded at 20 °C in a 0.2 cm cell at a protein concentration of ~50 µg/ml in 5 mM MOPS, 50 mM NaCl, 1 mM $CaCl_2$, pH 7.2. Spectra were averaged over five scans and corrected for the buffer signal. Heat-induced unfolding was recorded under constant nitrogen flow at 222 nm in 30 mM MOPS, 50 mM NaCl, 1 mM $CaCl_2$, pH 7.2 at a scan rate of 60 K $h^{-1}$. Protein concentration was ~0,1 mg/ml for all proteins. GdmCl-induced unfolding was recorded at 222 nm and 20 °C on the samples used for intrinsic fluorescence.

***GdmCl concentration determination***

A Refractometer ATAGO R5000 was used to record the refractive index of each sample in chemical unfolding studies and to calculate the $\Delta N$ value (difference in refractive index between the sample and

the buffer without GdmCl). This $\Delta N$ value allows determination of GdmCl concentration according to [37]:

$$[\text{GdmCl}] = 57.147(\Delta N) + 38.68(\Delta N)^2 - 91{,}60(\Delta N)^3 \quad \text{(Eq. 5)}$$

***Dynamic quenching of fluorescence***

The acrylamide-dependent quenching of intrinsic protein fluorescence was monitored as described [38,30]. The Stern-Volmer quenching constants $K_{SV}$ were calculated according to the relation:

$$F/F_0 = 1 + K_{SV}\ [Q] \quad \text{(Eq. 6)}$$

where F and $F_0$ are the fluorescence intensity in the presence and absence of molar concentration of the quencher Q, respectively.

# RESULTS AND DISCUSSION

***Production of the recombinant DMA and TFA***

The genes coding for DMA and for TFA possess a signal sequence incompatible with periplasmic export in *E. coli*. Accordingly, these sequences have been removed and replaced by the signal peptide of AHA. The production and purification procedures yielded about 50 mg of TFA and 250 mg of DMA per liter of culture. These proteins were found to be homogenous by SDS-PAGE and monodisperse by dynamic light scattering (Fig. 3). N-terminal amino acid sequencing of the purified proteins indicated proper cleavage of the signal peptide in DMA whereas the recombinant TFA displayed four additional residues (Ile-Ala-Thr-Ala) from the AHA signal peptide, originating from incorrect processing. Mass determination by ESI-Q-TOF mass spectrometry also revealed the lack of other post-translational modifications and a single homogenous population for both proteins.

***General parameters***

Table 1 summarizes some general properties of the investigated enzymes. TFA differs from its homologues by its larger size resulting from an additional C-terminal extension comprising a linker (residues 452 to 472) and a type 20 carbohydrate-binding module (residues 473 to 572) [39] rich in tryptophan residues (Fig. 4). The optimum pH for starch hydrolysis was found in the range pH 7.2-7.5 for these α-amylases.

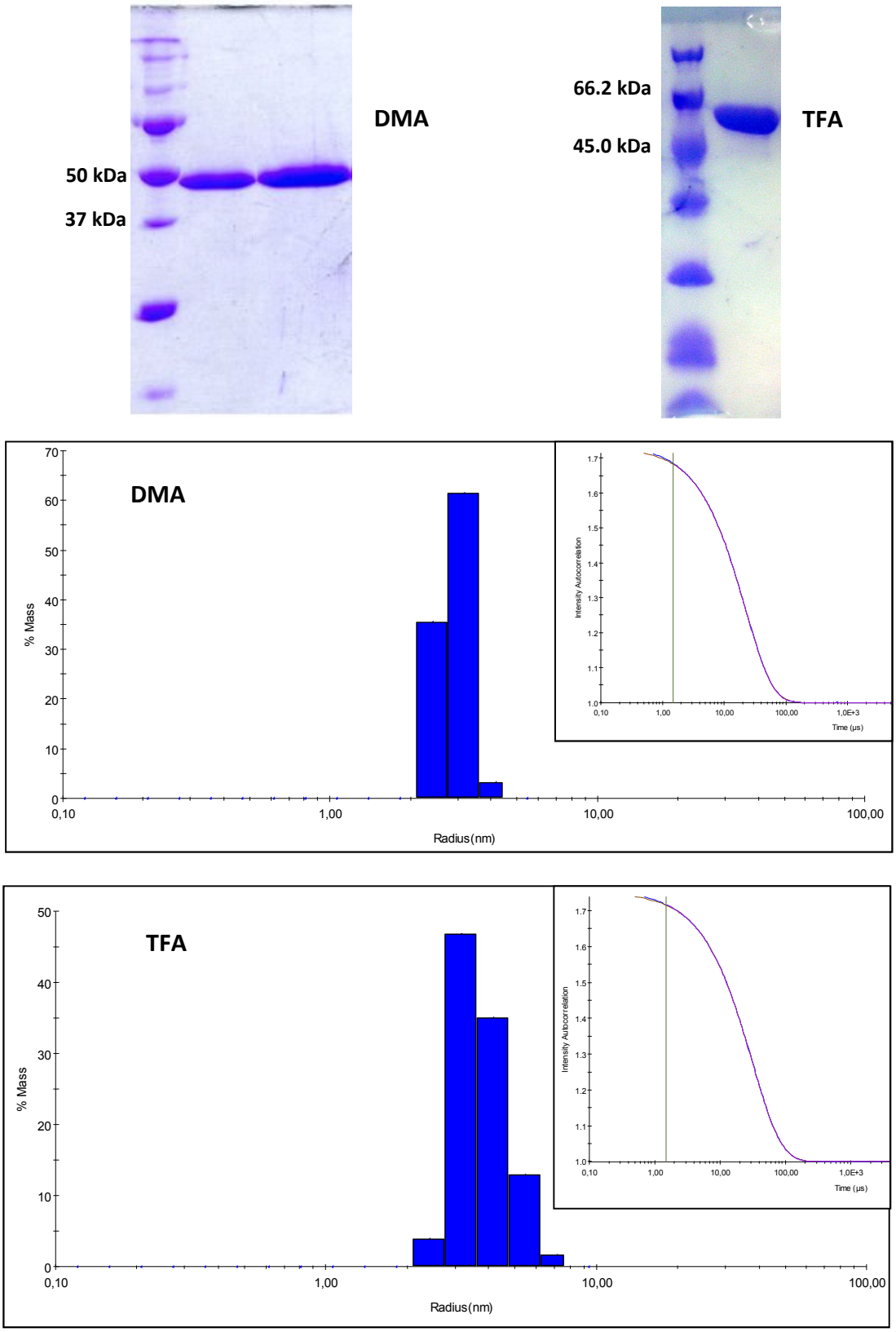


**Fig. 3.** Homogeneity of the newly purified α-amylases. Upper panel: SDS-PAGE of DMA and TFA samples. Lower panels: hydrodynamic radius distribution and autocorrelation function (inset) from dynamic light scattering. Mean radius and polydispersity were 3.1 nm and 14% for DMA, and 3.8 nm and 20% for TFA.

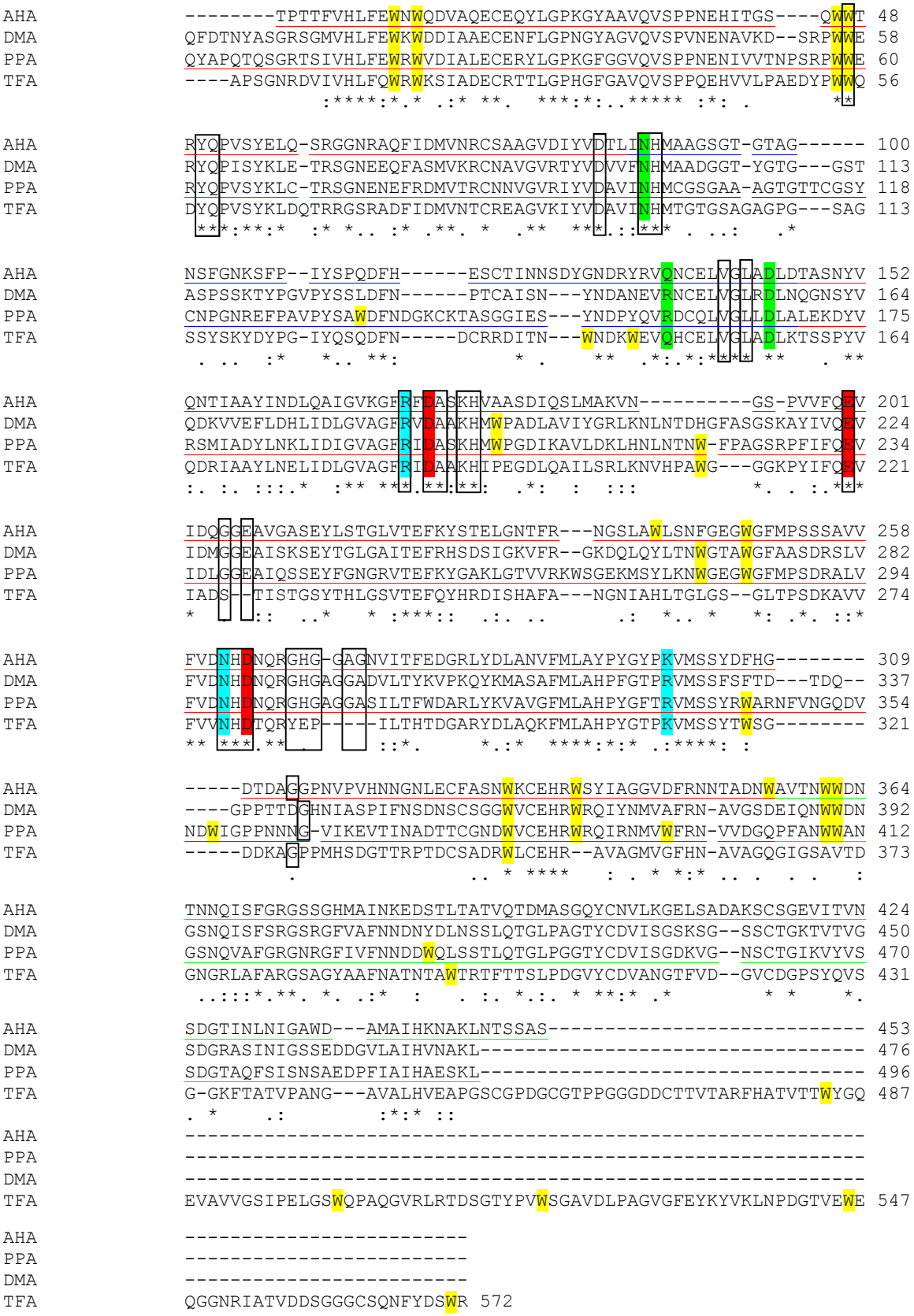


**Fig. 4.** Multiple sequence alignment by CLUSTALW2. Structural domains in AHA and PPA are underlined (domains A, B and C). Active site residues are boxed. Some important residues are indicated: catalytic residues (red), chloride binding site (blue), calcium binding site (green), and tryptophan residues (yellow).

**Table 1.** General properties of the investigated α-amylases

| Source | Abbr. | GenPept | CAZy subfam. | residues(n) | Mr (Da) | pI | PDB ID |
|---|---|---|---|---|---|---|---|
| Pseudoalteromonas haloplanktis | AHA | CAA41481.1 | GH13_xx[a] | 453 | 49343.1 | 4.82 | 1AQH |
| Drosophila melanogaster | DMA | CAA28238.1 | GH13_15 | 476 | 51899.2 | 5.38 | |
| Sus scrofa | PPA | AAF02828.1 | GH13_24 | 496 | 55598.3 | 6.55 | 1PPI |
| Thermobifida fusca (native) | TFA | AAZ55023.1 | GH13_32 | 572 | 61505.0 | 5.38 | |
| (recombinant) | | | | 576 | 61861.0 | 5.38 | |

[a] currently not classified

### *Chloride binding*

Both DMA and TFA were predicted to belong to the chloride-dependent α-amylase family on the basis of sequence alignments and conservation of the chloride ligands identified in available crystal structures [20,21]. This was ascertained by removing the chloride ions from the purified proteins by extensive dialysis and performing activation kinetics allowing the determination of the dissociation constants from saturation isotherms. As shown in Table 2, the animal-type DMA and PPA display a high affinity for chloride that can be related to the bidentate coordination by arginine, the main chloride ligand [23]. In this respect, replacement of this ligand by lysine (providing a monodentate coordination) in the bacterial-type AHA and TFA can account for their lower affinity (Fig. 5). The weak affinity of AHA has been also related to the flexible conformation of this psychrophilic enzyme [40,29] and it appears that the higher affinity of TFA (versus AHA) could be the result of a more stable and compact conformation of this thermophilic enzyme.

**Table 2.** Chloride binding by the investigated α-amylases

| α-amylases | Chloride ligands | | | Kd (mM)[a] |
|---|---|---|---|---|
| AHA | $172Arg^{NH2}$ | $262Asn^{ND2}$ | $300Lys^{NZ}$ | $6.70 \pm 0.22$[b] |
| DMA | $184Arg^{NH2}$ | $286Asn^{ND2}$ | $325Arg^{NH1\text{-}NH2}$ | $0.22 \pm 0.01$ |
| PPA | $195Arg^{NH2}$ | $298Asn^{ND2}$ | $337Arg^{NH1\text{-}NH2}$ | $0.29 \pm 0.01$[c] |
| TFA | $184Arg^{NH2}$ | $278Asn^{ND2}$ | $312Lys^{NZ}$ | $1.22 \pm 0.02$ |

[a] data at 25°C except for TFA (40°C)
[b] data similar to [40]
[c] data from [57]

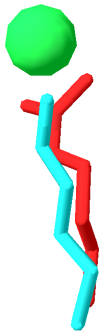

**Fig. 5.** Coordination of the chloride ion in α-amylases. Superimposition of the crystal structures of AHA (1AQH) and of PPA (1PPI) showing the main ligand of the chloride ion (green sphere). In AHA (blue) lysine provides monodentate coordination whereas in PPA (red) arginine provides bidentate coordination (adapted from [30])

***Temperature dependence of activity and conformation***

Fig. 6a depicts the thermodependence of activity, using starch as substrate, of the four investigated enzymes. The psychrophilic AHA retains a high relative activity at low temperature in order to maintain catalysis in the cold, whereas the thermophilic TFA is almost inactive at low temperatures, as generally observed [41]. There is a clear shift of the temperature range for efficient catalysis (left limb of the curves) and of the temperature for maximal activity (Table 3) with the environmental/physiological temperatures of the source organisms. When the turnover numbers are compared at the relevant temperature for the source organisms (Table 3), the $k_{cat}$ values exponentially increase from the psychrophilic to both mesophilic and the thermophilic enzymes (Fig. 7). This result somewhat contradicts the "corresponding states" hypothesis [42] suggesting that enzymes have evolved their functionality to reach similar activity at their respective environmental temperatures. In the case of the psychrophilic AHA, cold adaptations do not fully compensate activity when compared with both mesophilic α-amylases. As a matter of fact, microorganisms thriving at near-freezing temperatures grow much more slowly than their mesophilic counterpart at 37°C. On the other hand, the thermophilic enzyme benefits of the high temperature of its environment to boost its activity towards high $k_{cat}$ values. This can partly explain the powerful degrading capacity of *T. fusca* in hot environments [39]. The exponential increase of activity at relevant temperatures suggests that the thermal energy of the environment plays a crucial role in enzyme activity that is not averaged or normalized by adaptive mechanisms. However, similar comparisons in other homologous series are required before to conclude.

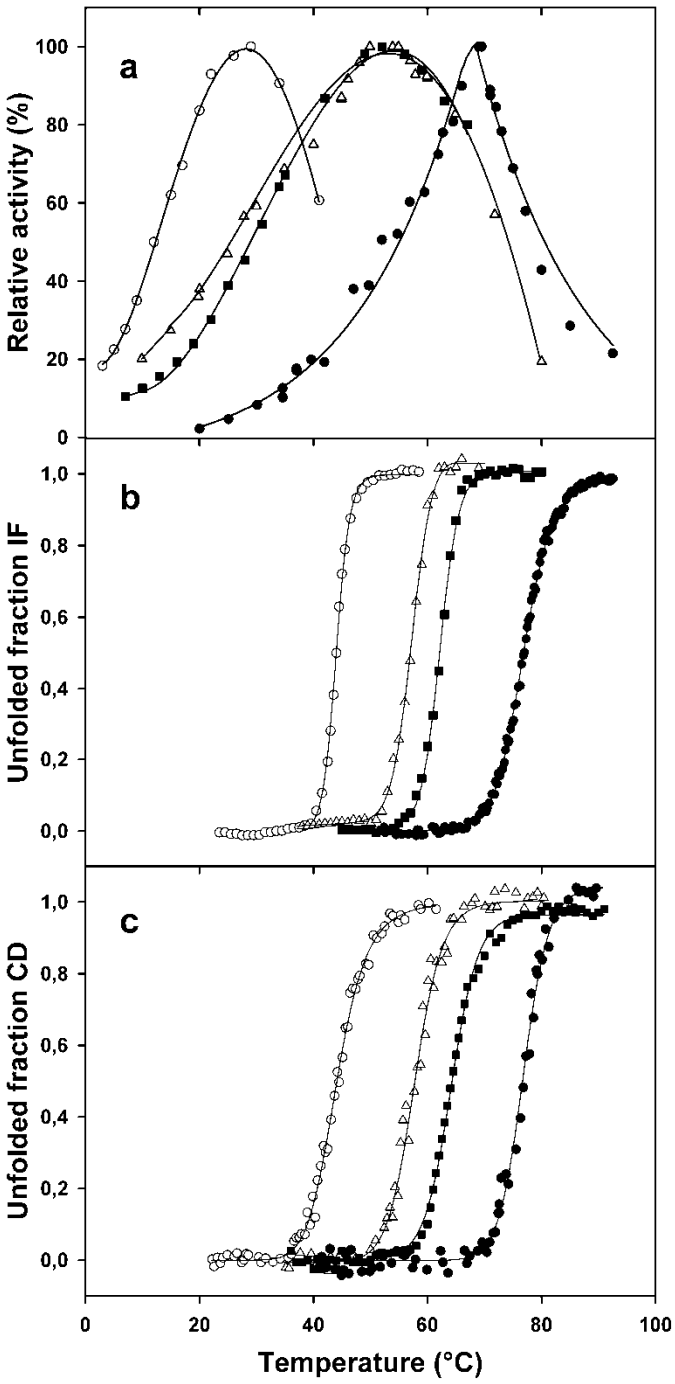


**Fig. 6.** Temperature dependence of activity (**a**) and heat-induced unfolding recorded by fluorescence (**b**) and circular dichroism (**c**). From left to right: the psychrophilic AHA (open circles), the ectothermic DMA (open triangles), the homeothermic PPA (closed squares) and the thermophilic TFA (closed circles). In panels a and b, data for AHA and PPA are from [32,38].

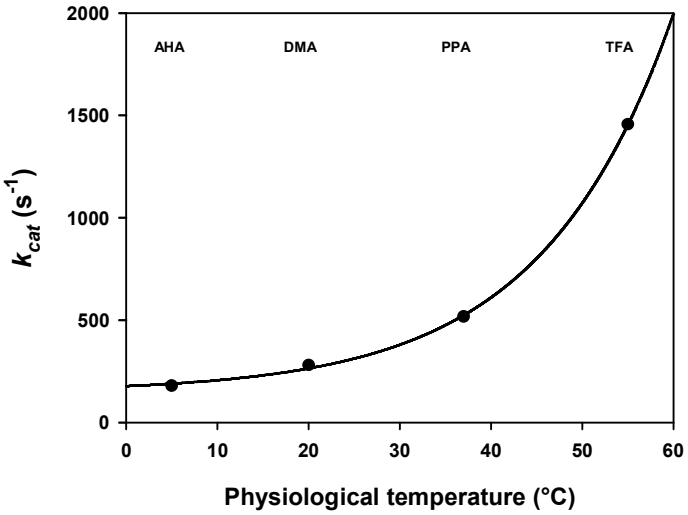


**Fig. 7.** Graphical representation of α-amylase activity at their environmental/physiological temperatures. Data from Table 3 in the main text. The solid line represents the fit of the data on an exponential growth.

Figures 6b and c display the heat-induced unfolding of the tertiary structures (as recorded by intrinsic fluorescence, IF) and of the secondary structures (as recorded by circular dichroism, CD). In all cases, these α-amylases unfold cooperatively, i.e. with simultaneous melting of both tertiary and secondary structures. The melting point $T_m$ of the structural conformation (Table 3) also increases with increasing environmental/physiological temperatures of the source organisms. Fig. 6 also indicates that the activity of both mesophilic enzymes and of the thermophilic α-amylase is heat-inactivated when their structure starts to melt, as judged by the correspondence between the maximal temperature for activity and the unfolding curves. This is in sharp contrast with the psychrophilic AHA which is heat-inactivated before any detectable structural change. It has been previously argued that a very flexible (and therefore heat-labile) active site is required for activity at low temperatures [11,31].

**Table 3.** Activity and stability of the investigated α-amylases

| α-amylases | Temperature of maximal activity | $k_{cat}$ at physiological temperature | | Melting temperature $T_m$ | |
|---|---|---|---|---|---|
| | | | | Tertiary structure | Secondary structures |
| | (°C) | ($s^{-1}$) | (°C) | (°C) | (°C) |
| AHA | 29 | 179 ± 9 | 5 | 44.1 | 44.1 |
| DMA | 54 | 280 ± 13 | 20 | 57.7 | 57.7 |
| PPA | 54 | 518 ± 22 | 37 | 65.0 | 65.0 |
| TFA | 72 | 1457 ± 37 | 55 | 76.8 | 76.9 |

***Thermodynamic parameters of activation***

The thermodynamic parameters of activation have been calculated from Arrhenius plots of the exponential rise of activity with temperature, providing the activation energy Ea, and are reported in Table 4. When the four enzymes are compared at an identical temperature, the $k_{cat}$ values clearly reflect the adaptive nature of activity that decreases from the psychrophilic to the thermophilic α-amylases, as also inferred from Fig. 6a. This is translated into increasing values of the Gibbs free energy of activation $\Delta G^{\#}$, which is an inverse function of $k_{cat}$ in the transition state formalism (Eq. 1). Amongst the activation parameters, the variation of activation enthalpy $\Delta H^{\#}$ appears to be the most instructive. Indeed, this parameter reflects two aspects. Firstly, it depicts the temperature dependence of the enzymatic reaction [43]: for a given variation of temperature, the activity of the psychrophilic enzyme is less modified than that of the thermophilic one. This ensures that a decrease in temperature will moderately reduce the activity of the psychrophilic enzyme therefore maintaining a high activity at low temperature, whereas an increase in temperature will sharply activate the thermophilic enzyme for maximal activity at high temperature. It should be noted that the ectothermic and homeothermic α -amylases display intermediate values in close relation with their physiological temperatures. Secondly, the $\Delta H^{\#}$ parameter is related to the number of enthalpically-driven weak interactions that have to be broken to reach the activated state [34]. It follows that the number of such interactions that are disrupted increases in the enzyme series, from a low number in the psychrophilic enzyme to a high number in the thermophilic α-amylase. It should be stresses that, in this respect, there is a striking correlation between the $\Delta H^{\#}$ parameter and the stability of the four enzymes which arises from increased numbers of stabilizing interactions. The entropic contribution $T\Delta S^{\#}$ to the free energy of activation is also worth commenting. In the case of the psychrophilic enzyme, the large and negative variation of activation entropy has been related to a transition from a flexible and mobile active site in the ground state, to a more ordered active site in the activated complex. This hypothesis was supported by experimental evidences using a transition state analog [38,30]. In Table 4, the progressive evolution of entropy in parallel with stability can be tentatively related to a progressively more stable free enzyme in the ground state. If calculated at the relevant environmental/physiological temperatures given in Table 3, all these activation parameters remain qualitatively similar (Table 5).

**Table 4.** Thermodynamic parameters of activation at 15°C.

| | $k_{cat}$ ($s^{-1}$) | $E_a$ (kcal $mol^{-1}$) | $\Delta G^{\#}$ (kcal $mol^{-1}$) | $\Delta H^{\#}$ (kcal $mol^{-1}$) | $T\Delta S^{\#}$ (kcal $mol^{-1}$) |
|---|---|---|---|---|---|
| AHA[a] | 392 ± 18 | 8.9 | 13.4 | 8.3 | -5.1 |
| DMA | 150 ± 6 | 10.9 | 14.0 | 10.3 | -3.6 |
| PPA[a] | 141 ± 4 | 12.0 | 14.0 | 11.5 | -2.5 |
| TFA | 42 ± 2 | 22.9 | 14.7 | 22.4 | 7.7 |

[a] data from [28]

**Table 5.** Thermodynamic parameters of activation at relevant environmental/physiological temperatures.

| | $T$ (°C) | $k_{cat}$ ($s^{-1}$) | $E_a$ (kcal $mol^{-1}$) | $\Delta G^{\#}$ (kcal $mol^{-1}$) | $\Delta H^{\#}$ (kcal $mol^{-1}$) | $T\Delta S^{\#}$ (kcal $mol^{-1}$) |
|---|---|---|---|---|---|---|
| AHA | 5 | 179 | 8.9 | 13.4 | 8.3 | -5.0 |
| DMA | 20 | 280 | 10.9 | 13.9 | 10.3 | -3.5 |
| PPA | 37 | 518 | 12.0 | 14.3 | 11.4 | -2.9 |
| TFA | 55 | 1457 | 22.9 | 14.5 | 22.2 | 7.7 |

***Substrate binding***

The kinetic parameters for hydrolysis of the chromogenic substrate Et-G7-pNP are reported in Table 6. It has been previously argued that a high activity at low or moderate temperature is gained at the expense of affinity for the substrate [29,41]. This allows a reduction of the activation free energy barrier (and therefore increased $k_{cat}$ values) by lowering the magnitude of the energy pit of the enzyme-substrate complex. This is supported in Table 6 by the simultaneous decrease of $k_{cat}$ and $K_m$ values, from AHA to DMA and PPA. Furthermore, the decrease of $K_m$ values suggests that the active site dynamics also decrease from AHA to DMA and PPA. By contrast, the affinity of TFA is weak and the low $k_{cat}/K_m$ ratio indicates that Et-G7-pNP is a poor substrate for the thermophilic enzyme. It should be mentioned that amongst the 24 residues forming the catalytic cleft [44] (strictly conserved in AHA, DMA and PPA), 6 are substituted in TFA (Fig. 4). These substitutions possibly account for the alteration in substrate binding by TFA. It should also be mentioned that TFA appears to be a maltotriose-forming α-amylase [45], therefore differing in product release.

**Table 6.** Kinetic parameters at 25°C for Et-G7-pNP hydrolysis

| | $k_{cat}$ ($s^{-1}$) | $K_m$ (μM) | $k_{cat}/K_m$ ($s^{-1}$ $\mu M^{-1}$) |
|---|---|---|---|
| AHA [a] | 675 ± 31 | 223 ± 15 | 3.0 |
| DMA | 364 ± 15 | 130 ± 8 | 2.8 |
| PPA [b] | 291 ± 8 | 65 ± 4 | 4.5 |
| TFA | 153 ± 4 | 260 ± 10 | 0.6 |

[a] data similar to [28]
[b] data from [28]

***Equilibrium unfolding in GdmCl***

The resistance towards chemical denaturation using GdmCl (guanidinium hydrochloride) was probed by equilibrium unfolding recorded by fluorescence and circular dichroism (Fig. 8, Table 7). Both methods indicate a single cooperative transition as well as a cooperative unfolding of secondary and tertiary structures in all enzymes. The GdmCl concentration for half denaturation ($C_{1/2}$ value in Table 7) increases from AHA to TFA, while the large $m$ value of AHA reflects its sharp cooperative

unfolding. Estimation of the conformational stability in the absence of denaturant ($\Delta G°H_2O$) in Table 7 shows that stability increases with the thermal regime of the source organism. However, the stability determined by GdmCl unfolding for PPA and TFA is very close (Fig. 8), in contrast with their thermal stability (Fig. 6). This indicates unusual differences between thermal denaturation and chemical unfolding in both proteins.

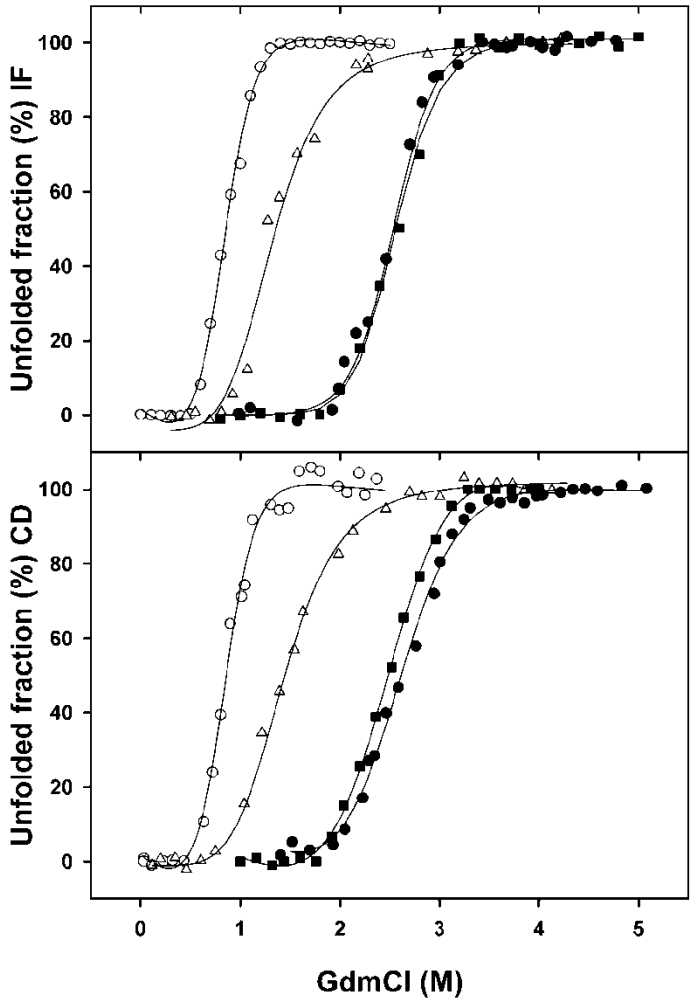


**Fig. 8.** Equilibrium unfolding in GdmCl recorded by intrinsic fluorescence (IF, upper panel) and circular dichroism (CD, lower panel). From left to right: the psychrophilic AHA (open circles), the ectothermic DMA (open triangles), the homeothermic PPA (closed squares) and the thermophilic TFA (closed circles). In the upper panel, data for PPA are from [38].

**Table 7.** Equilibrium unfolding parameters in GdmCl at 20°C recorded by intrinsic fluorescence (IF) and circular dichroism (CD)

| Protein | AHA | | DMA | | PPA | | TFA | |
|---|---|---|---|---|---|---|---|---|
| | IF | CD | IF | CD | IF [a] | CD | IF | CD |
| $C_{1/2}$ (M) | 0.82 | 0.83 | 1.34 | 1.45 | 2.5 | 2.48 | 2.54 | 2.59 |
| $m$ (kcal mol$^{-1}$ M$^{-1}$) | 4.32 | 4.37 | 2.43 | 2.73 | 2.7 | 2.75 | 2.96 | 2.75 |
| $\Delta G°H_2O$ (kcal mol$^{-1}$) | 3.66 | 3.87 | 3.80 | 3.94 | 6.9 | 6.82 | 7.39 | 7.14 |

[a] data from [38]

***Differential scanning microcalorimetry***

In order to gain deeper insights into stability of these α -amylases, thermal unfolding was recorded by differential scanning calorimetry (DSC). Both mesophilic and the thermophilic proteins required the addition of a nondetergent sulfobetaine to avoid heat-induced aggregation. The normalized thermograms are displayed in Fig. 9 and the related thermodynamic parameters are given in Table 8. The melting temperature $T_m$ (top of the main transition) increases from the psychrophilic AHA to the thermophilic TFA (Fig. 9) and closely corresponds to the values recorded by spectroscopic methods (Fig. 6, Table 3). Furthermore, the calorimetric enthalpy ($\Delta H_{cal}$, heat absorbed during unfolding calculated from the area under the transition) also increases from AHA to TFA (Table 8). This $\Delta H_{cal}$ value corresponds to the sum of all enthalpically-driven interactions that have to be broken for unfolding and precisely quantify the enthalpic stability of these α -amylases. Fig. 9 also shows that unfolding of both mesophilic and the thermophilic proteins is asymmetric and can be deconvoluted into two cooperative transitions that are not detected by spectroscopic methods. Accordingly, the cold-adapted AHA is uniformly unstable whereas the mesophilic and thermophilic proteins are characterized by the appearance of thermodynamic domains with increasing stability, in parallel to their thermal regime.

The thermophilic TFA differs by the occurrence of a small, very stable transition at 85°C. Two explanations can be proposed for this unusual transition. *i*) This domain can correspond to the unfolding of the additional C-terminal carbohydrate-binding module in TFA, although spectroscopic methods fail to detect such transition. *ii*) It has been shown that some thermophilic proteins retain residual structure in the unfolded state [46]. This residual structure reduces the entropy of the unfolded state and therefore increases the stability of the native state. The additional DSC transition in TFA can be regarded as the melting of such residual structure at high temperature.

**Table 8.** Thermodynamic parameters of stability recorded by microcalorimetry

| | | $T_m$ (°C) | $\Delta H_{cal}$ (kcal mol$^{-1}$) |
|---|---|---|---|
| AHA | | 44.0 | 214 |
| DMA | | 57.7 | 274 |
| PPA[a] | | 65.6 | 295 |
| TFA | (1)[b] | 74.0 | 415 |
| | (2) | 84.7 | 46 |

[a] data from [28]
[b] main (1) and minor (2) transitions in Fig.3.

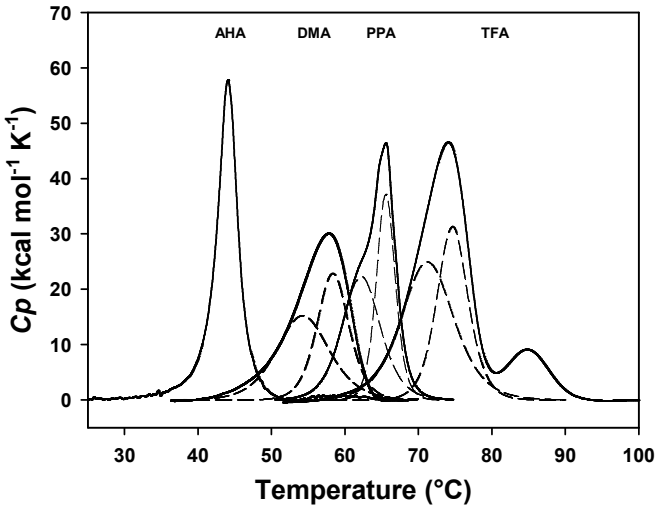


**Fig. 9.** Thermal unfolding of α-amylases recorded by differential scanning calorimetry. The individual thermograms are identified at the top of the transitions. Dashed lines are deconvolutions of the main transition into two cooperative units in mesophilic and thermophilic proteins. In TFA, note the additional transition melting around 85°C. Data for PPA are from [28].

***Stability curves***

On the basis of the microcalorimetric parameters (Table 7), the stability curves have been calculated according to the relation [47]:

$$\Delta G(T) = \Delta H_{cal}(1-T/T_m) + \Delta Cp(T-T_m) - T\Delta Cp\ ln\ (T/T_m) \qquad \text{(Eq. 7)}$$

In the present case, a $\Delta Cp$ value of 8.47 kcal mol$^{-1}$ K$^{-1}$ measured for various α -amylases [32] was used and the extra stability domain of TFA was excluded from calculations. These stability curves (Fig. 10) correspond to the work required to disrupt the native state at any temperature. The stability curve of AHA has been validated experimentally [32] whereas the curves for the other α -amylases are estimations due to the non-two-state unfolding of their structures (dashed in Fig. 9). By definition, the $\Delta G$ value is nil at the melting point $T_m$. It can be seen in Fig. 10 that the increasing stability of the α-

amylases is reached by uplifting the curves towards higher free energy values from AHA to TFA. The thermodynamic implications of these curves have been discussed elsewhere [41] and fit the present observations. For instance, the maximal stability of all α-amylases is reached near room temperature, possibly because the hydrophobic effect is optimal in this range [48]. From an evolutionary perspective, the adaptive variations in stability appear to be restrained by enthalpic stabilization ($\Delta H_{cal}$, $T_m$) as no significant alteration of the curve shape (minor displacement of maximal stability, no slope modification), except uplifting, are detected in Fig. 10.

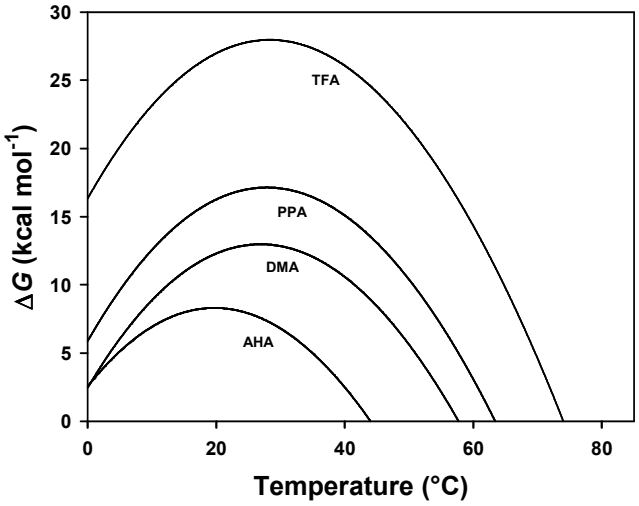


**Fig. 10.** Stability curves calculated from DSC data. The Gibbs free energy of unfolding corresponds to the work required to unfold the native state as a function of temperature. The increased stability of the α-amylases and of $T_m$ (at $\Delta G$=0) is essentially gained via uplifting the curves towards higher free energy values.

### *Dynamic fluorescence quenching*

The conformational flexibility of the α-amylases was probed by dynamic fluorescence quenching of aromatic residues [38,30]. Increased concentrations of a small quencher molecule (acrylamide) were used to probe the accessibility of tryptophan residues within the proteins. The decrease of fluorescence arising from diffusive collisions between acrylamide and tryptophans reflects the ability of acrylamide to penetrate the structure and provides an index of protein permeability. The difference between the slopes of Stern-Volmer plots at 30°C and 4°C illustrates the variations in protein structural permeability with an increase in temperature (Fig. 11). In the case of AHA, DMA and PPA, the recorded decrease in permeability correlates with the increase in stability. This reveals that when stability increases in this series, the proteins are characterized by progressively more compact conformation undergoing reduced micro-unfolding events of the native state and shorter native state fluctuations. However, TFA does not integrate the relation in the series (slope between DMA and PPA in Fig. 11). This could be related to its additional C-terminal domain rich in tryptophan residues (Fig. 4) that can interfere in this fluorescence-based experiment by the presence of solvent-exposed tryptophans (as expected in a carbohydrate binding module).Nevertheless, the thermostable α-amylase from *B. amyloliquefaciens* displayed very limited quenching under similar conditions [38], suggesting

that the flexibility-stability relationship can be extended to heat-stable proteins on the basis of fluorescence quenching.

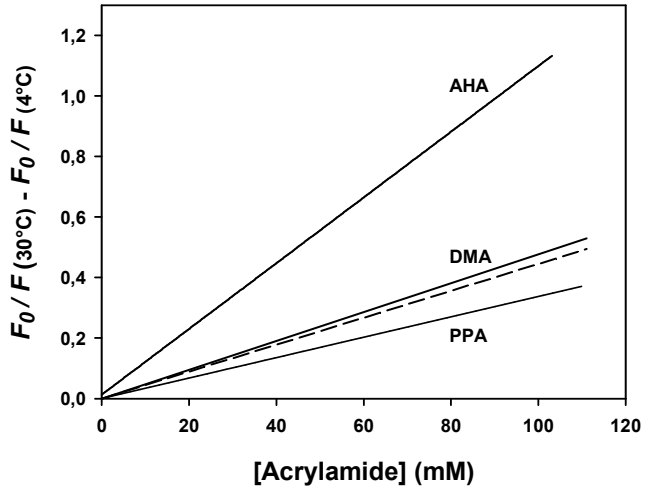


**Fig. 11.** Variation of fluorescence quenching by acrylamide between 4 and 30°C. Data for TFA are dashed and data for PPA are from [38]. The slope of the plots is proportional to the permeability of the proteins towards acrylamide.

# CONCLUSIONS

We report here a close correlation between thermal stability and the environmental/physiological temperature in mesophilic and extremophilic α-amylases. While the requirement for a high stability is obvious for the thermophilic protein, this correlation for all α-amylases cannot be fortuitous in regard of previous examples [42, 11, 16, 41]. It has been proposed that this correlation is the result of a genetic drift related to the lack of selective pressure for stable proteins at individual environmental temperatures [49]. More importantly, it has been also argued that protein dynamics has to be preserved at environmental temperatures in order to maintain a functional state. Furthermore, such dynamic properties are inversely linked with structural stability: the lower the mobility of the protein structure, the higher its stability [50-53], as also indicated here by fluorescence quenching. Such balance between stability, dynamics and activity clearly accounts for the continuum of the properties observed in the investigated α-amylases. The thermodependence of activity, the kinetic parameters and the activations parameters support these activity-stability trade-offs. In the case of the psychrophilic AHA, there is notably a strong selective pressure for a high activity at low and moderate temperatures. This selection should be less essential for mesophilic and the thermophilic α-amylases that benefit from thermally-induced activity: this can tentatively explain the exponential rise of $k_{cat}$ values at relevant temperature noted in the four α-amylases.

The enzyme functional properties are intimately governed by protein motions and conformational changes. In this respect, increasing attention is currently given to the pathways of adaptive protein evolution [54], the evolution of protein conformational changes [55] and to the mutational adjustments of conformational energy landscapes [56]. For instance, we have recently shown that mesophilic stability, activity and dynamics can be engineered in the psychrophilic AHA by introducing key adaptive substitutions [30]. The availability of the crystal structure of DMA and TFA will certainly further improve our understanding of temperature-driven adaptations of the enzyme function.

# ACKNOWLEDGMENTS

This work was supported by grants from the FRS-FNRS, Belgium (Fonds de la Recherche Fondamentale et Collective, contract number 2.4535.08) to G.F., the Belgian program of Interuniversity Attraction Poles initiated by the Federal Office for Scientific, Technical and Cultural Affaires (PAI n° P6/19) and from the Centre National de la Recherche Scientifique (France) to J.-L.D.L. AC was a FRIA fellow during this work.

# REFERENCES

1. J.W. Deming, Psychrophiles and polar regions, Curr. Opin. Microbiol. 5 (2002) 301-309.
2. K. Takai, K. Nakamura, T. Toki, U. Tsunogai, M. Miyazaki, J. Miyazaki, H. Hirayama, S. Nakagawa, T. Nunoura, K. Horikoshi, Cell proliferation at 122 degrees C and isotopically heavy CH4 production by a hyperthermophilic methanogen under high-pressure cultivation, Proc. Natl. Acad. Sci. U.S.A. 105 (2008) 10949-10954.
3. C. Gerday, N. Glansdorff, Physiology and Biochemistry of Extremophiles, ASM Press, Washington, D.C., 2007.
4. K. Horikoshi, G. Antranikian, A.T. Bull, F.T. Robb, K.O. Stetter (Eds.), Extremophiles Handbook, Springer Verlag, Tokyo, Berlin, Heidelberg, 2011.
5. B. Boussau, S. Blanquart, A. Necsulea, N. Lartillot, M. Gouy, Parallel adaptations to high temperatures in the Archaean eon, Nature 456 (2008) 942-945.
6. K.A. Maher, D.J. Stevenson, Impact frustration of the origin of life, Nature 331 (1988) 612-614.
7. M. Di Giulio, The universal ancestor and the ancestor of bacteria were hyperthermophiles, J. Mol. Evol. 57 (2003) 721-730.
8. M. Levy, S.L. Miller, The stability of the RNA bases: implications for the origin of life, Proc. Natl. Acad. Sci. U.S.A. 95 (1998) 7933-7938.
9. J. Attwater, A. Wochner, V.B. Pinheiro, A. Coulson, P. Holliger, Ice as a protocellular medium for RNA replication, Nat. Commun. 1 (2010) 76, doi:10.1038/ncomms1076.
10. C. Vieille, G.J. Zeikus, Hyperthermophilic enzymes: sources, uses, and molecular mechanisms for thermostability, Microbiol. Mol. Biol. Rev. 65 (2001) 1-43.
11. G. Feller, C. Gerday, Psychrophilic enzymes: hot topics in cold adaptation, Nat. Rev. Microbiol. 1 (2003) 200-208.
12. G.S. Bell, R.J. Russell, H. Connaris, D.W. Hough, M.J. Danson, G.L. Taylor, Stepwise adaptations of citrate synthase to survival at life's extremes. From psychrophile to hyperthermophile, Eur. J. Biochem. 269 (2002) 6250-6260.
13. D. Georlette, B. Damien, V. Blaise, E. Depiereux, V.N. Uversky, C. Gerday, G. Feller, Structural and functional adaptations to extreme temperatures in psychrophilic, mesophilic, and thermophilic DNA ligases, J. Biol. Chem. 278 (2003) 37015-37023.
14. E. Bae, G.N. Phillips, Jr., Structures and analysis of highly homologous psychrophilic, mesophilic, and thermophilic adenylate kinases, J. Biol. Chem. 279 (2004) 28202-28208.
15. A. Linden, M. Wilmanns, Adaptation of class-13 alpha-amylases to diverse living conditions, ChemBioChem 5 (2004) 231-239.
16. N. Coquelle, E. Fioravanti, M. Weik, F. Vellieux, D. Madern, Activity, stability and structural studies of lactate dehydrogenases adapted to extreme thermal environments, J. Mol. Biol. 374 (2007) 547-562.
17. B.L. Cantarel, P.M. Coutinho, C. Rancurel, T. Bernard, V. Lombard, B. Henrissat, The Carbohydrate-Active EnZymes database (CAZy): an expert resource for Glycogenomics, Nucleic Acids Res. 37 (2009) D233-238.
18. S. Janecek, alpha-Amylase family: molecular biology and evolution, Prog. Biophys. Mol. Biol. 67 (1997) 67-97.
19. S. Janecek, Sequence similarities and evolutionary relationships of microbial, plant and animal alpha-amylases, Eur. J. Biochem. 224 (1994) 519-524.
20. S. D'Amico, C. Gerday, G. Feller, Structural similarities and evolutionary relationships in chloride-dependent alpha-amylases, Gene 253 (2000) 95-105.
21. J.L. Da Lage, G. Feller, S. Janecek, Horizontal gene transfer from Eukarya to bacteria and domain shuffling: the alpha-amylase model, Cell. Mol. Life Sci. 61 (2004) 97-109.

22. J.L. Da Lage, E.G. Danchin, D. Casane, Where do animal alpha-amylases come from? An interkingdom trip, FEBS Lett. 581 (2007) 3927-3935.
23. G. Feller, O. Bussy, C. Houssier, C. Gerday, Structural and functional aspects of chloride binding to Alteromonas haloplanctis alpha-amylase, J. Biol. Chem. 271 (1996) 23836-23841.
24. M. Qian, H. Ajandouz el, F. Payan, V. Nahoum, Molecular basis of the effects of chloride ion on the acid-base catalyst in the mechanism of pancreatic alpha-amylase, Biochemistry 44 (2005) 3194-3201.
25. R. Maurus, A. Begum, L.K. Williams, J.R. Fredriksen, R. Zhang, S.G. Withers, G.D. Brayer, Alternative catalytic anions differentially modulate human alpha-amylase activity and specificity, Biochemistry 47 (2008) 3332-3344.
26. N. Aghajari, G. Feller, C. Gerday, R. Haser, Structures of the psychrophilic Alteromonas haloplanctis α-amylase give insights into cold adaptation at a molecular level, Structure 6 (1998) 1503-1516.
27. S. D'Amico, C. Gerday, G. Feller, Structural determinants of cold adaptation and stability in a large protein, J. Biol. Chem. 276 (2001) 25791-25796.
28. S. D'Amico, C. Gerday, G. Feller, Temperature adaptation of proteins: engineering mesophilic-like activity and stability in a cold-adapted alpha-amylase, J. Mol. Biol. 332 (2003) 981-988.
29. S. D'Amico, J.S. Sohier, G. Feller, Kinetics and energetics of ligand binding determined by microcalorimetry: insights into active site mobility in a psychrophilic alpha-amylase, J. Mol. Biol. 358 (2006) 1296-1304.
30. A. Cipolla, S. D'Amico, R. Barumandzadeh, A. Matagne, G. Feller, Stepwise adaptations to low temperature as revealed by multiple mutants of psychrophilic alpha-amylase from Antarctic Bacterium, J. Biol. Chem. 286 (2011) 38348-38355.
31. K.S. Siddiqui, R. Cavicchioli, Cold-adapted enzymes, Annu. Rev. Biochem. 75 (2006) 403-433.
32. G. Feller, D. d'Amico, C. Gerday, Thermodynamic stability of a cold-active α-amylase from the Antarctic bacterium Alteromonas haloplanctis, Biochemistry 38 (1999) 4613-4619.
33. M. Schramm, A. Loyter, Purification of alpha-amylases by precipitation of amylase-glycogen complexes, Methods Enzymol. 8 (1966) 533-537.
34. T. Lonhienne, C. Gerday, G. Feller, Psychrophilic enzymes: revisiting the thermodynamic parameters of activation may explain local flexibility, Biochim. Biophys. Acta 1543 (2000) 1-10.
35. S. D'Amico, G. Feller, A nondetergent sulfobetaine improves protein unfolding reversibility in microcalorimetric studies, Anal. Biochem. 385 (2009) 389-391.
36. A. Matouschek, J.M. Matthews, C.M. Johnson, A.R. Fersht, Extrapolation to water of kinetic and equilibrium data for the unfolding of barnase in urea solutions, Protein Eng. 7 (1994) 1089-1095.
37. C.N. Pace, Determination and analysis of urea and guanidine hydrochloride denaturation curves, Methods Enzymol. 131 (1986) 266-280.
38. S. D'Amico, J.C. Marx, C. Gerday, G. Feller, Activity-stability relationships in extremophilic enzymes, J. Biol. Chem. 278 (2003) 7891-7896.
39. A. Lykidis, K. Mavromatis, N. Ivanova, I. Anderson, M. Land, G. DiBartolo, M. Martinez, A. Lapidus, S. Lucas, A. Copeland, P. Richardson, D.B. Wilson, N. Kyrpides, Genome sequence and analysis of the soil cellulolytic actinomycete Thermobifida fusca YX, J. Bacteriol. 189 (2007) 2477-2486.
40. G. Feller, F. Payan, F. Theys, M. Qian, R. Haser, C. Gerday, Stability and structural analysis of α-amylase from the Antarctic psychrophile Alteromonas haloplanctis A23, Eur. J. Biochem. 222 (1994) 441-447.
41. G. Feller, Protein stability and enzyme activity at extreme biological temperatures, J. Phys.-Condens. Mat. 22 (2010) doi: 10.1088/0953-8984/1022/1032/323101.
42. G.N. Somero, Proteins and temperature, Annu. Rev. Physiol. 57 (1995) 43-68.
43. P.A. Fields, G.N. Somero, Hot spots in cold adaptation: Localized increases in conformational flexibility in lactate dehydrogenase A(4) orthologs of Antarctic notothenioid fishes, Proc. Natl. Acad. Sci. U.S.A. 95 (1998) 11476-11481.
44. N. Aghajari, M. Roth, R. Haser, Crystallographic evidence of a transglycosylation reaction: ternary complexes of a psychrophilic alpha-amylase, Biochemistry 41 (2002) 4273-4280.
45. C.H. Yang, W.H. Liu, Cloning and characterization of a maltotriose-producing alpha-amylase gene from Thermobifida fusca, J. Ind. Microbiol. Biotechnol. 34 (2007) 325-330.
46. S. Robic, M. Guzman-Casado, J.M. Sanchez-Ruiz, S. Marqusee, Role of residual structure in the unfolded state of a thermophilic protein, Proc. Natl. Acad.Sci. U.S.A. 100 (2003) 11345-11349.
47. P.L. Privalov, Stability of proteins: small globular proteins, Adv. Protein Chem. 33 (1979) 167-241.
48. S. Kumar, C.J. Tsai, R. Nussinov, Maximal stabilities of reversible two-state proteins, Biochemistry 41 (2002) 5359-5374.
49. P.L. Wintrode, F.H. Arnold, Temperature adaptation of enzymes: lessons from laboratory evolution, Adv. Protein Chem. 55 (2000) 161-225.

50. P.L. Privalov, Stability of proteins. Proteins which do not present a single cooperative system, Adv. Protein Chem. 35 (1982) 1-104.
51. P. Zavodszky, J. Kardos, A. Svingor, G.A. Petsko, Adjustment of conformational flexibility is a key event in the thermal adaptation of proteins, Proc. Natl. Acad. Sci. U.S.A. 95 (1998) 7406-7411.
52. M. Tehei, B. Franzetti, D. Madern, M. Ginzburg, B.Z. Ginzburg, M.T. Giudici-Orticoni, M. Bruschi, G. Zaccai, Adaptation to extreme environments: macromolecular dynamics in bacteria compared in vivo by neutron scattering, EMBO Rep. 5 (2004) 66-70.
53. M. Tehei, D. Madern, B. Franzetti, G. Zaccai, Neutron scattering reveals the dynamic basis of protein adaptation to extreme temperature, J. Biol. Chem. 280 (2005) 40974-40979.
54. J.D. Bloom, F.H. Arnold, In the light of directed evolution: pathways of adaptive protein evolution, Proc. Natl. Acad. Sci. U. S. A. 106 (2009) 9995-10000.
55. J. Jeon, H.J. Nam, Y.S. Choi, J.S. Yang, J. Hwang, S. Kim, Molecular evolution of protein conformational changes revealed by a network of evolutionarily coupled residues, Mol. Biol. Evol. 28 (2011)2675-2685.
56. J.P. Colletier, A. Aleksandrov, N. Coquelle, S. Mraihi, E. Mendoza-Barbera, M. Field, D. Madern, Sampling the conformational energy landscape of a hyperthermophilic protein by engineering key substitutions, Mol. Biol. Evol. (2012) doi:10.1093/molbev/mss015.
57. A. Levitzki, M.L. Steer, The allosteric activation of mammalian alpha-amylase by chloride, Eur. J. Biochem. 41 (1974) 171-180.

# Chapitre 4 : Conclusions et perspectives

Comme décrit dans le chapitre 2, les objectifs de cette thèse étaient d'améliorer notre compréhension des mécanismes moléculaires responsables de l'adaptation des protéines aux températures extrêmes. Pour se faire, nous avons étudié les mutants Mut5 et Mut5CC issus de la "mésophilisation" de l'α-amylase psychrophile AHA via l'ajout d'interactions faibles et de facteurs stabilisants présents chez l'α-amylase mésophile PPA. D'autre part, nous avons pu, grâce aux enzymes TFA et DMA, étudier l'adaptation aux températures dans le cas des α-amylases chlorure-dépendantes sur l'ensemble des températures physiologiques des organismes vivants (à l'exception des hyperthermophiles pour lesquels aucune α-amylase chlorure-dépendante n'a été découverte jusqu'à présent).

Au terme de la première section des résultats, nous avons pu conclure que la "mesophilisation" de l'enzyme psychrophile AHA, réalisée sur deux mutants multiples Mut5 et Mut5CC, démontre une réelle augmentation de la stabilité caractérisée par : la rigidité de la structure protéique observée en quenching de fluorescence, la stabilité thermique ($T_m$) et la résistance à la dénaturation chimique ($\Delta G°_{H20}$, $C_m$) ainsi que les cinétiques de dépliement/repliement ($k_f^{H_2O}$, $k_u^{H_2O}$ ). Cependant, suite à cette stabilisation, les deux mutants ont perdu l'optimalisation de l'activité à basse température présente chez AHA. Ceci renforce notre hypothèse relative aux mécanismes d'adaptation des protéines aux basses températures : la diminution d'interactions faibles et de facteurs stabilisants permet à l'enzyme psychrophile d'augmenter sa flexibilité. Cette flexibilité accrue est nécessaire à la catalyse à basse température et conduit à une activité élevée caractérisée par une plus faible affinité pour le substrat. L'une des observations les plus intéressantes est le fait que l'ajout des interactions faibles et du pont disulfure contribue à l'augmentation de la stabilité non pas par simple addition mais par synergie. Il en résulte un plus grand gain de stabilité lorsqu'on additionne le pont disulfure à Mut5, et donc aux interactions faibles, qu'à AHA seule comme le démontrent le $T_m$ et l'enthalpie calorimétrique ($\Delta H_{cal}$). En terme de caractérisation innovante de l'adaptation aux températures extrêmes, nous avons pu mettre en évidence que l'origine du gain de stabilité observé par les cinétiques de dépliement/repliement de Mut5 et Mut5CC est liée à une diminution de la cinétique de dépliement ($k_u^{H_2O}$) alors que les cinétiques de repliement restent inchangées ($k_f^{H_2O}$), ceci étant en parfaite adéquation avec les résultats obtenus par Perl *et al*. (1998) et Luke *et al.* (2007) pour les protéines thermophiles.

Dans la seconde section des résultats, nous avons mis en évidence l'étroite corrélation entre la stabilité thermique et la température physiologique et/ou de l'environnement pour les enzymes mésophiles et extremophiles. Les résultats obtenus démontrent le continuum des propriétés physico-chimique observées chez les enzymes étudiées. L'étude de l'activité des quatre α-amylases contredit l'hypothèse des états correspondants stipulant que les enzymes ont évolué pour acquérir une activité similaire à leurs températures environnementales respectives (Somero, 1995). En effet, dans notre cas,

la valeur de $k_{cat}$ augmente exponentiellement avec la température physiologique de chaque α-amylase. Ceci pourrait indiquer que l'énergie thermique de l'environnement a une influence sur l'activité enzymatique qui ne serait pas contrebalancée par les mécanismes adaptatifs. Par l'étude des paramètres thermodynamiques d'activation, nous montrons que l'effet de la température sur l'activité est moins important chez l'enzyme psychrophile que chez l'enzyme thermophile. Ainsi la diminution de température influencera moins l'activité de l'enzyme psychrophile conservant une activité élevée à basse température alors que chez l'amylase thermophile l'augmentation de température active rapidement l'enzyme qui présentera une activité maximale. D'autre part, il est maintenant démontré que sur base de la séquence en acide aminé d'une α-amylase, nous pouvons déterminer si elle est chlore-dépendante ou non, en témoignent les constantes d'affinité de DMA et TFA pour le chlore. Mais aussi, l'importance du résidu en position 300 (par rapport à la numérotation d'AHA). En effet, cette affinité par le chlore est régie par deux éléments : 1) le ligand qui détermine si la liaison est monodentée (une lysine chez AHA et TFA) ou bidentée (une arginine chez DMA et PPA) et 2) la flexibilité de la structure de la protéine (liée à la stabilité de la protéine).

Dans un futur proche, nous espérons pouvoir comparer les structures cristallographiques de ces quatre α-amylases que sont AHA, DMA, PPA et TFA de manière à corroborer les observations réalisées via la comparaison des structures mais aussi éventuellement mettre d'autres adaptations en évidence. De plus, nous pourrons affiner notre compréhension du site de fixation de l'ion chlorure dont la constante d'affinité semble être influencée par la flexibilité de la protéine.

En ce qui concerne la construction de mutants visant à élucider le rôle des interactions faibles dans les mécanismes d'adaptation des protéines, on notera les nouvelles avancées en termes de bioinformatique et de modélisation *in silico*. Papaleo *et* al. (2011) et Pasi *et* al. (2009) ont proposé bon nombre de mutations à étudier mais ont également confirmé le choix des mutants sélectionnés dans le premier article. D'autres, comme Vemparala *et al*. (2011), utilisent la bioinformatique pour étudier le rôle des boucles dans l'adaptation des protéines aux températures extrêmes. Ceci pourrait-être transposable à l'étude des α-amylases, la position et la longueur des boucles étant un facteur important dans l'adaptation thermique des protéines et principalement au niveau du mécanisme catalytique (voir 1.3.5 de la section I de l'Introduction).

Enfin, l'une des perspectives à long terme de ce type d'étude serait d'être en mesure de proposer aux industries de nouvelles protéines extremophiles et plus particulièrement psychrophiles : soit par la découverte de nouvelles enzymes issues de la prospection (ex : métagénomique) des zones froides de notre globe, soit en modifiant des enzymes existantes pour leur faire acquérir des propriétés précises d'enzymes psychrophiles. Ce dernier point ne peut être réalisé qu'à condition de connaitre les règles générales et souvent particulières (en fonction du type de protéine) de l'adaptation aux basses températures.

# Bibliographie

(Sont reprises uniquement les références du chapitre 1-*Section I* et du chapitre 4)

# BIBLIOGRAPHIE

Aghajari N., Feller G., Gerday C. and Haser R. Structural basis of α-amylase activation by chloride. Protein Sci. 2002. 11: 1435-1441.

Aghajari N., Feller G., Gerday C. and Haser R. Structures of the psychrophilic Alteromonas halopanctis α-amylase give insights into cold adaptation at a molecular level. Structure. 1998. 6: 1503-1516.

Aghajari N., Feller G., Gerday C. and Haser R. Crystal structures of the psychrophilic α-amylase from *Alteromonas haloplanctis* in its native form and complexed with an inhibitor. Protein Sci. 1998. 7: 564-572.

Bae E. and Phillips G. N. Roles of static and dynamic domains in stability and catalysis of adenylate kinase. Proc. Natl. Acad. Sci. U. S. A. 2006. 103: 2132-2137.

Baxter S., The pig's response to the thermal environment. In: Intensive pig production: environmental management and design. 1984. London: Granada Publishing, p. 35-54.

Bonamore A., Ilari A., Giangiacomo L., Bellelli A., Morea V., Boffi A. A novel thermostable hemoglobin from the actinobacterium Thermobifida fusca. FEBS J. 2005. 272: 4189-4201.

Brayer G.D., Luo Y. and Withers S.G. The structure of human pancreatic alpha-amylase at 1.8 Å resolution and comparisons with related enzymes. Protein Sci. 1995. 4: 1730-1742.

Buléon A., Colonna P., Planchot V. and Ball S. Starch granules: structure and biosynthesis. Int J Biol Macromol. 1998. 23: 85-112.

Buisson G., Duée E., Haser R. and Payan F. Three dimensional structure of porcine pancreatic alpha-amylase at 2.9Å resolution. Role of calcium in structure and activity. EMBO J. 1987. 6: 3909-3916.

Collins T., Meuwis M.A., Stals I., Claeyssens M., Feller G. and Gerday C. A novel family 8 xylanase, functional and physicochemical characterization. J. Biol. Chem. 2002. 277: 35133-35139.

Copeland L., Blazek J., Salman H. and Tang C.M. Form and functionality of starch. Food Hydrocolloids. 2009. 23: 1527-1534.

D'Amico S., Gerday C. and Feller G. Structural determinants of cold adaptation and stability in a large protein. J. Biol. Chem. 2001. 276: 25791-25796.

D'Amico S., Gerday C. and Feller G. Structural similarities and evolutionary relationships in chloride-dependent α-amylases. Genes. 2000, 253: 95-105.

D'Amico S., Gerday S. and Feller G. Dual effects of an extra disulfide bond on the activity and stability of a cold-adapted α-amylase J. Biol. Chem. 2002. 277: 46110-46115.

D'Amico S., Marx J-C., Gerday C. and Feller G. Activity-stability relationships in extremophilic enzymes. J. Biol. Chem. 2003a. 278: 7891-7896.

D'Amico S., Gerday C. and Feller G. Temperature adaptation of proteins: Engineering mesophilic enzymes. J. Mol. Biol. 2003b. 332: 981-988.

Da Lage J-L., Feller G and Janecek S. Horizontal gene transfer from Eukarya to Bacteria and domain shuffling: the α-amylase model, Cell. Mol. Life. Sci. 2004. 61: 97-109.

Davies G. & Henrissat B. Structures and mechanisms of Glycosyl hydrolases. Structure. 1995. 3: 853-859

Davies G.J., Wilson K.S. and Henrissat B., Nomenclature for sugar-binding subsites in glycosyl hydrolases. Biochem. J. 1997. 321: 557-559.

Feller G., Payan F., Theys F., Qian M., Haser R. and Gerday C. Stability and structural analysis of α-amylase from the antarctic psychrophile Alteromonas haloplanctis A23. Eur. J. Biochem. 1994. 222: 441 -447.

Feller G., D'Amico D. and Gerday C. Thermodynamic stability of cold-active α-amylase from Antarctic bacterium Alteromonas haloplanktis. Biochemistry. 1999. 38: 4613-4619.

Feller G., le Bussy O. and Gerday C. Expression of psychrophilic genes in mesophilic hosts: Assessment of the folding state of a recombinant α-amylase. Appl. Environ. Microbiol. 1998. 64: 1163-1165.

Feller G., Dehareng D. and Da Lage J-L. How to remain nonfolded and pliable: the linkers in modular α-amylases as a case of study. FEBS J. 2011. 278: 2333-2340.

Feller G., Lonhienne T., Deroanne C., Libioulle C., Van Beeumen J. and Gerday C. Purification, characterization, and nucleotide sequence of the thermolabile alpha-amylase from the antarctic psychrotroph Alteromonas haloplanctis A23, J. Biol. Chem. 1992. 267: 5217-5221.

Feller G., le Bussy O., Houssier C. and Gerday C. Structural and functional aspects of chloride binding to alteromonas haloplanctis α-amylase. J. Biol. Chem. 1996. 271: 23836-23841.

Fields P. A. and Somero G. N. Hot spots in cold adaptation: Localized increases in conformational flexibility in lactate dehydrogenase A(4) orthologs of Antarctic notothenioid fishes. Proc. Natl. Acad. Sci. U. S. A. 1998. 95: 11476-11481.

Garsoux G., Lamotte J., Gerday C. and Feller G. Kinetic and structural optimization to catalysis at low temperatures in a psychrophilic cellulase from the Antarctic bacterium Pseudoalteromonas haloplanktis. Biochem J. 2004. 384: 247-53.

Georlette D., Jonsson Z.O., Van Petegem F., Chessa J., Van Beeumen J., Hubscher U. and Gerday C. A DNA ligase from the psychrophile Pseudoalteromonas haloplanktis gives insights into the adaptation of proteins to low temperature. Eur. J. Biochem. 2000. 267: 3502-3512.

Hasegawa K., Kubota M. and Matsuura Y. Roles of catalytic residues in alpha-amylases as evidenced by the structures of the product-complexed mutants of a maltotetraose-forming amylase. Protein Eng. 1999. 12: 819-824.

Henrissat B. & Bairoch A. New families in the classification of Glycosyl hydrolases based on amino acid sequence similarities. Biochem J. 1993. 293: 781-788.

Henrissat B. & Davies G. Structural and sequence-based classification of glycoside hydrolases. Curr. Opin. Struc. Biol. 1997. 7: 637-644.

Henrissat B. A classification of Glycosyl hydrolases based on amino acid sequence similarities. Biochem. J. 1991. 280: 309-316.

Hoyoux A., Jennes I., Dubois P., Genicot S., Dubail F., François J-M., Baise E., Feller G. and Gerday C. Cold-adapted beta-galactosidase from the Antarctic psychrophile Pseudoalteromonas haloplanktis. Appl. Environ. Microbiol. 2001. 67: 1529-1535.

http://www.cazy.org/Home.html

Janecek S., Svensson B. and Henrissat B. Domain evolution in the α-amylase family. J. Mol. Evol. 1997. 45: 322-331.

Janecek S. New conserved amino acid region of α-amylases in the third loop of their (β/α)8-barrel domains. Biochem. J. 1992. 288: 1069-1070.

Janecek S. Sequence similarities and evolutionary relationships of microbial, plant and animal α-amylase. Eur. J. Biochem. 1994. 224: 519-524.

Kadziola A., Abe J., Svensson B. and Haser R. Crystal and molecular structure of barley α-amylase. J. Mol. Biol. 1994. 239: 104-121.

Kirk O., Borchert T.V. and Fuglsang C.C. Industrial enzyme applications. Curr. Opin. Biotechnol. 2002. 13: 345-351.

Koshland D.E. Stereochemistry and the mechanism of enzymatic reactions. Biol. Rev. Camb. Philos. Soc. 1953. 28: 416-436.

Levitzki A. & Steer M.L. The Allosteric Activation of Mammalian α-Amylase by Chloride, Eur. J. Biochem. 1974. 41: 171-80.

Long C.M., Virolle M.J., Chang S.Y., Chang S. and Bibb M.J. α-amylase gene of Streptomyces limosus : nucleotide sequence, expression motifs, and amino acid sequence homology to mammalian and invertebrate α-amylase. J. Bacteriol. 1987. 169: 5745-5754.

Luke K.A., Higgins C.L. and Wittung-Stafshede P. Thermodynamic stability and folding of proteins from hyperthermophilic organisms. Febs J. 2007. 274: 4023-4033.

MacGregor E.A. Janecek S. and Svensson B. Relationship of structure to specificity in the α-amylase family of enzymes. Biochim. Biophys. Acta. 2001. 1546: 1-20.

MacGregor EA. α-amylase structure and activity. J. Protein. Chem. 1988. 7: 399-415.

Machius M., Declerck N. and Huber R. Activation of Bacillus licheniformis alpha-amylase through a disorder-order transition of the substrate-binding site mediated by a calcium-sodium-calcium metal triad. Structure. 1998. 6: 281-92.

Maczkowiak F. & Da Lage J-L. Origin and evolution of the Amrel gene in the α-amylase multigene family of Diptera. Genetica. 2006. 128: 145-158.

Motyan J.A., Gyémant G., Harangi J. and Bagossi P. Computer –aided subsite mapping of α-amylases. Carbohydrate research. 2011. 346: 410-415.

Nelson D.L. & Cox M.M. Principles of Biochemistry: fourth edition. Ed. Freeman. 2005. Chapter 7. p.238-252.

Numao S., Maurus R., Sidhu G., Wang Y., Overall CM., Brayer GD. and Withers SG. Probing the role of chloride ion in the mechanism of human pancreatic α-amylase, Biochemistry. 2002. 41: 215-225.

Papaleo E., Pasi M., Tiberti M. and De Gioa L. Molecular Dynamics of mesophilic-like mutants of a cold-adapted enzyme : Insights into distal effects induced by the mutantions. PlosOne. 2011. 6 : 1-13

Pasi M., Riccardi L., Fantucci P., De Gioia L. and Papaleo E. Dynamic properties of a psychrophilic α-amylase in comparison with a mesophilic homologue. J. Phys. Chem. B. 2009. 113 : 13585-13595.

Payen & Persoz. « Mémoire sur la diastase, les principaux produits de ses réactions et leurs applications aux arts industriels », Annales de chimie et de physique, 2e série. 1833. 53: 73-92.

Perl D., Welker C., Schindler T., Schröder K., Marahiel M.A., Jaenicke R. and Schmid F.X. Conservation of rapid two-state folding in mesophilic, thermophilic and hyperthermophilic cold shock proteins. Nat. Struct. Biol. 1998. 5: 229-235.

Qian M., Haser R., Buisson G., Duee E. and Payan F. The active site center of a mammalian alpha-amylase. Structure of the complex of a pancreatic alpha-amylase with carbohydrate inhibitor refined to 2.2-Å resolution. Biochemistry. 1994. 33: 6284-6294.

Qian M., Haser R. and Payan F. Carbohydrate binding sites in a pancreatic α-amylase-substrate complex, derived from X-ray structure analysis at 2.1Å resolution. Protein Sci. 1995. 4: 747-755.

Ramasubbu N., Paloth V., Luo Y., Brayer G.D. and Levine M.J. Structure of human salivary alpha-amylase at 1.6 Å resolution: implications for its role in the oral cavity. Acta Crystallogr. D Biol. Crystallogr. 1996. 52: 435-446.

Somero G.N. Proteins and temperature. Annu. Rev. Physiol. 1995.57: 43-68.

Tanaka A. & Hoshino E. Secondary calcium-binding parameter of Bacillus amyloliquefaciens α-amylase obtained from inhibition kinetics. J. Biosci. Bioeng. 2003. 96: 262-267.

Uitdehaag J.C., Mosi R., Kalk K.H., van der Veen B.A., Dilkhuizen L., Withers S.G. and Dijkstra B.W. X-ray structures along the reaction pathway of cyclodextrin glycosyltransferase elucidate catalysis in the α-amylase family. Nat. Struct. Biol. 1999. 6: 432-436.

Van der Maarel M.J., van der Veen B., Uitdehaag J.C., Leemhuis H. and Dijkhuizen L. Properties and applicaitons of starch-converting enzymes of α-amylases family. J. Biotechnol. 2002. 94: 137-155.

Vemparala S., Mehrotra S. and Balaram H. Roel of loop dynamics in thermal stability of mesophilic and thermophilic *adenylosuccinate synthetase*: A molecular dynamics and normal mode analysis study. Biochim Biophys Acta. 2011. 1814: 630-637.

Závodszky P., Kardos J., Svingor and Petsko G. A. Adjustment of conformational flexibility is a key event in the thermal adaptation of proteins. Proc. Natl. Acad. Sci. U. S. A. 1998. 95: 7406-7411.

L'adaptation thermique des protéines extremophiles a été étudiée de manière à approfondir notre compréhension des mécanismes moléculaires qui en sont responsables. Dans ce but, deux études ont été initiées et ont été publiées.

La première est basée sur la "mésophilisation" de l'α-amylase psychrophile AHA, issue de la bactérie Antarctique *Pseudoalteromonas haloplanktis*. L'ajout d'interactions faibles et d'un pont disulfure présents chez son homologue mésophile PPA de *Sus scrofa* et absents chez AHA ont permis de construire deux mutants multiples stabilisés, Mut5 et Mut5CC. Ces quatre enzymes ont été étudiées sur base de leur stabilité, de leur activité et de la perméabilité de leur structure protéique. L'étude des cinétiques de renaturation/dénaturation d'AHA, Mut5 et Mut5CC a permis de déterminer l'origine cinétique du gain de stabilité liée à l'ajout d'interactions faibles et du pont disulfure chez AHA. Il en résulte que Mut5 et Mut5CC ont effectivement été stabilisés mais en contrepartie ils ont perdu l'optimalisation de l'activité à basse température observée chez AHA. De plus, la perméabilité de leur structure protéique s'est réduite, se rapprochant de celle de PPA. L'origine du gain de stabilité est liée à une diminution des cinétiques de dépliement sans modification des cinétiques de repliement. Non seulement ces résultats démontrent l'importance du rôle des interactions faibles dans l'adaptation thermique des protéines mais de plus, ils démontrent la synergie entre celles-ci.

La seconde étude a pu être développée par la découverte d'une α-amylase chlorure-dépendante thermophile TFA issue de l'actinomycète *Thermobifida fusca* et par la production de l'α-amylase chlorure-dépendante mésophile ectotherme DMA de *Drosophila melanogaster*. Ainsi avec AHA et PPA respectivement comme représentants psychrophile et mésophile homéotherme, nous pouvions couvrir l'ensemble des températures physiologiques/environnementales connues. Nous avons pu mettre en évidence le continuum des propriétés physico-chimiques observées (activité, stabilité, affinité pour le substrat…) mais aussi que l'énergie thermique de l'environnement influence grandement l'activité enzymatique qui ne serait pas contrebalancée par les mécanismes adaptatifs. L'influence de la température sur l'activité a mis en évidence la plus faible dépendance d'AHA par rapport à TFA.

Ces travaux ont permis d'améliorer notre compréhension des mécanismes moléculaires liés à l'adaptation thermique des protéines et du rôle joué par les interactions faibles dans cette adaptation. Ils ouvrent aussi la voie à de futures recherches visant à analyser par d'autres méthodes la flexibilité de la structure protéique et à cristalliser TFA pour étudier d'un point de vue structural le continuum des propriétés physico-chimiques mis en évidence au cours de ce travail.